COENCAPSULATION OF INSULIN-PRODUCING CELLS AND MESENCHYMAL STROMAL CELLS IN PEGDA HYDROGELS TO ENHANCE CHRONIC WOUND HEALING

by

AYESHA AIJAZ

A dissertation submitted to the

Graduate School-New Brunswick

and

The Graduate School of Biomedical Sciences

Rutgers, The State University of New Jersey

In partial fulfillment of the requirements

For the degree of

Doctor of Philosophy

Graduate Program in Biomedical Engineering

Written under the direction of

Ronke M. Olabisi

And approved by

_____

_____

_____

_____

New Brunswick, New Jersey

May 2017

ABSTRACT OF THE DISSERTATION

Coencapsulation of Insulin-Producing Cells and Mesenchymal Stromal Cells in PEGDA Hydrogels to Enhance Chronic Wound Healing

By AYESHA AIJAZ

Dissertation Director:

Ronke M. Olabisi

Wound healing is a hierarchical process of intracellular and intercellular signaling. Insulin is a potent chemoattractant and mitogen for cells involved in wound healing. Insulin's potential to promote keratinocyte growth and stimulate collagen synthesis in fibroblasts is well described. However, there currently lacks an appropriate delivery mechanism capable of continuously supplying a wound environment with insulin; current approaches require repeated applications of insulin, which increase the chances of infecting the wound. In addition to insulin, exogenous mesenchymal stromal cell or mesenchymal stem cell (MSC) application is a promising treatment strategy for chronic wounds, yet MSC therapies are still far from a clinical reality. MSCs have been shown to improve islet viability and function, regulate inflammation and secrete pro-wound healing factors. MSC-assisted wound healing is elicited through distinct pathways from insulin-assisted wound healing. In this dissertation, a potential synergistic effect of these two differing modes of wound healing was investigated.

Since topical insulin creams preclude using MSCs, here insulin-producing cells (IPCs) and MSCs were combined in a dual-cell therapy approach for wound healing. Polyethylene glycol diacrylate (PEGDA) was used to encapsulate IPCs and/or MSCs and results showed that the encapsulation did not alter insulin or MSC secretion profiles. It was hypothesized that MSCs would improve IPC viability and insulin secretion and that the combination of encapsulated IPCs and MSCs would release factors that synergistically accelerate wound repair at greater rates than either cell

used alone. The resulting coencapsulated IPC-MSC hydrogel system was applied to a diabetic mouse model of chronic wounds and provided prolonged release of insulin and soluble MSC factors without the need for reapplication.

The results showed that IPCs encapsulated within PEGDA hydrogels improved wound healing by 1.6 times, and remarkably IPC and MSC coencapsulation further accelerated wound closure 2.5 times faster, thus supporting the hypothesis. Results further showed increased release of insulin, vascular endothelial growth factor (VEGF), and transforming growth factor β1 (TGF-β1) when IPCs and MSCs were combined than when they were encapsulated singly. Since each of these factors support wound healing, it is unsurprising that wound healing proceeded faster in these groups. In addition, coencapsulated IPCs and MSCs stimulated Akt phosphorylation in myoblasts more than any other treatment group. The phosphatidylinositol 3-kinase (PI3K)-Akt pathway stimulates growth, proliferation, migration and secretion by keratinocytes, endothelial cells and fibroblasts and induces angiogenesis by promoting VEGF secretion. Thus, the PI3-AkT pathway was another pro-wound healing mechanism recruited by the IPC-MSC system. Wounds healed without intermediate scab or scar formation and histology showed mature skin features in IPC-MSC treated wounds. The system's ability to accelerate healing in chronic wounds with a single application has broad clinical and research implications.

DEDICATION

To my loving mother and father (late)

ACKNOWLEDGEMENTS

The journey towards completion of this dissertation has been a profound and memorable one which, could not have been possible without the many special people in my life. First and foremost, I am grateful to Dr. Ronke Olabisi for providing me the opportunity to pursue this work under her expertise. Dr. Olabisi has been a tremendous support throughout my five years at Rutgers University and I have benefited from her work, professional and career advice. I am grateful for her generous guidance, understanding and she been a source of endless motivation and confidence in me. Even apart from daily activities in the lab, Dr. Olabisi made sure I was doing well and felt at home while away from my family. All the recognitions that I have received for my work in these years would not have been possible without her support. She is the best supervisor anyone can ever ask for! I would like to thank Dr. Francois Berthiaume without whom the initial animal studies would not have been possible. His generous advice has been instrumental in guiding me through this dissertation and has been available whenever I needed quick answers. I also have to thank Dr. Joseph Freeman and Dr. Debabrata Banerjee for their encouragement and for taking out the time to mentor and advise me on this dissertation. No thesis is complete without the support of the academic department; I would like to thank Dr. David Shreiber, Dr. Noshir Langrana, Ms. Robin Yarborough and Mr. Lawrence Stromberg (Larry) for helping me successfully navigate through fellowships and administrative requirements. Tied to this, I am grateful to the Department of Biomedical Engineering for their funding support.

This is an excellent opportunity for me to acknowledge my sources of funding during these five years; United States Education Foundation in Pakistan (USEFP) and Institute of International Education (IIE) for giving me the initial thrust to pursue this graduate research and later Schlumberger Foundation for their generosity.

I have had an unparalleled experience at the Olabisi lab and I would like to thank all past and present members, especially Corina White and Kristopher White for timely processing of supply orders for me. Thank you to Matthew Teryek for providing me a very responsible and effective

helping hand in the experiments, Luke Fritzky at the Digital Imaging and Histology Core at Rutgers-NJMS Cancer Center for his expertise in histological sectioning and staining, and the Lab Animal Services at Rutgers University for their help during animal studies.

Last but my most dependable, unconditional and amazing support system; my fiancé, my mother and my brother for always being there for me regardless of the time of the day and for your endless motivation, understanding and confidence in me. Because of you I have been able to live my passion and dream. This dissertation would have very unlikely reached completion without them. Thanks for making me your priority.

TABLE OF CONTENTS

LIST OF ILLUSTRATIONS

LIST OF ABBREVIATIONS

α-SMA	alpha-Smooth Muscle Actin
µs AtT-20ins	Microencapsulated AtT-20ins
µs RIN-m	Microencapsulated RIN-M
BM	Bone Marrow
CM	Conditioned media
DPBS	Dulbecco's Phosphate Buffered Saline
DFU	Diabetic Foot Ulcer
EGF	Epidermal Growth Factor
EGFR	Epidermal Growth Factor Receptor
EPO	Erythropoietin
ECM	Extracellular Matrix
ERK	Extracellular Signal Regulated Kinases
FDA	Food and Drug Administration
FGF	Fibroblast Growth Factor
GSK	Glycogen Synthase Kinase 3
G-CSF	Granulocyte-Colony Stimulating Factor
GM-CSF	Granulocyte-Macrophage Colony Stimulating Factor
Grb2	Growth Factor Receptor-Bound Protein 2
H & E	Hematoxylin and Eosin
HCD	High Cell Density
HGF	Hepatocyte Growth Factor
HUVEC	Human Umbilical Vein Endothelial Cells
IR	Insulin Receptor
IRS	Insulin Receptor Substrate
IGF-1	Insulin-like Growth Factor-1
IPC	Insulin-Producing Cell
IFN	Interferon
IL	Interleukin
IL-1RA	Interleukin-1 Receptor Antagonist
ICD	Intermediate Cell Density
KGF	Keratinocyte Growth Factor
KHB	Krebs Henseleit Buffer
LPS	Lipopolysaccharides
LCD	Low Cell Density
MCP	Macrophage Chemoattractant Protein
MIP	Macrophage Inflammatory Protein
MMP	Matrixmetalloproteinases
MSC	Mesenchymal Stem Cell
MAPK	Mitogen-Activated Protein Kinases
NOS	Nitric Oxide Synthase
NOD	Non-Obese Diabetic
PI3K	Phosphatidylinositol 3-Kinase
PASR	Picric Acid Sirius Red
PBS	Phosphate Buffered Saline
PDGF	Platelet-Derived Growth Factor
PLGA	Poly(Lactic-Co-Glycolic Acid)
PEG	Polyethylene Glycol
PEGDA	Polyethylene Glycol Diacrylate
POD	Postoperative Days

RGD	Arginine Glycine Aspartic Acid
s-TNF-R1	Soluble Tumor Necrosis Factor Receptor-1
SOS	Son-of-Sevenless
SH2	Src Homology-2
SDF-1	Stromal Cell-Derived Factor-1
TGF-α	Transforming Growth Factor-α
TGF-β	Transforming Growth Factor-β
TIMP-1	Tissue Inhibitor of Metalloproteinases-1
TNF	Tumor Necrosis Factor
VEGF	Vascular Endothelial Growth Factor

CHAPTER 1: INTRODUCTION

Note: Portions of this chapter have been published in: 'A. Aijaz et al., **Hydrogel microencapsulated insulin-secreting cells increase keratinocyte migration, epidermal thickness, collagen fiber density, and wound closure in a diabetic mouse model of wound healing.** Tissue Eng Part A. 2015 Nov;21(21-22):2723-32. doi: 10.1089/ten.TEA.2015.0069', and represent the original work of the candidate.

Chronic or non-healing wounds suffer from chronic wound inflammation, abundant neutrophil and macrophage infiltration, delayed cell proliferation, reduced collagen synthesis and decreased angiogenesis [1]. Chronic wounds are both biologically and biochemically complex, characterized by altered growth factor and cytokine expression [2] and presence of proteases and reactive oxygen species in the wound, thus requiring concerted therapeutic strategies. According to the American Diabetes Association, chronic wounds affect more than 6.5 million people in the United States, resulting in an annual toll of $25 billion on the health care system [5]. Diabetic foot ulcers are a devastating subset of chronic wounds that affect the diabetic population, with estimates as high as 25 % of all diabetics developing a foot ulcer in their lifetimes [3, 4]. According to the Center for Disease Control Diabetes fact sheet, approximately 71,000 patients with diabetic foot ulcers (DFUs) undergo lower limb or digit amputation every year [13]. This number continues to grow due to an aging population and a sharp rise in diabetes and obesity [7]. Additionally, with an aging population the risk of developing a pressure ulcer due to immobility is increasing; annually 2.5 million pressure ulcers are treated in the US with yearly expenditures of $11 billion [7]. These chronic ulcers have a propensity to infection and are associated with prolonged hospital stays, immobility and a diminished quality of life [8, 9]. Therapeutic approaches such as local debridement, skin grafts, dermal scaffolds and growth factor treatments often yield less than satisfactory results due to the pro-inflammatory state of the wound [10]. This is described by a hostile extracellular microenvironment in which high levels of pro-inflammatory

cytokines and proteases are secreted by immune cells [14]. The presence of these proteolytic enzymes and an imbalance of their inhibitors leads to abnormal fragmentation of extracellular matrix (ECM) molecules in dermal scaffolds and skin grafts, cell senescence and apoptosis in skin grafts, and degradation of applied growth factors [14]. Thus, there is a pressing need to develop therapies that can regulate the pro-inflammatory wound environment. Insulin regulates the inflammatory state by regulating the hyperglycemic wound environment [11].

Current treatment approaches using topical insulin require repeated applications, increasing the chances of wound infection [12]. Mesenchymal stem cells (MSCs) secrete wound healing factors and have shown accelerated healing when applied to wounds [15-19]; however, MSCs migrate from target wounds [20, 21]. These challenges with using insulin and/or MSCs for wound healing have limited their widespread use. The work described in this dissertation overcomes these challenges by providing a bio-inert hydrogel barrier that prevents MSC migration and uses cells to deliver continuous insulin, thereby supplying a sustained dose of biological factors capable of promoting wound healing.

In chapter 2, a literature search is presented and relevant findings from previous studies are elucidated.

In chapter 3, a sustained-release insulin delivery system was developed in which insulin-producing cells (IPCs) were encapsulated in synthetic non-immunogenic and non-degradable polyethylene glycol diacrylate (PEGDA) hydrogel microspheres. Two IPC cell lines were employed, which differ in their response to glucose, for insulin release: RIN-m, which is a constant insulin producing β-cell line derived from a rat insulinoma and AtT-20ins, which is a cell line derived from a mouse sarcoma modified to express insulin cDNA such that the cell line increases insulin release in response to increasing glucose concentration in the microenvironment. In this chapter, the encapsulated cell viability and insulin secretion profiles were characterized, and compared to monolayer IPC controls to confirm that the microencapsulation procedure was

not detrimental to cell viability or insulin release. Bioactivity of the released insulin was confirmed by performing a scratch assay of keratinocyte migration *in vitro*.

In chapter 4, the performance of PEGDA-encapsulated RIN-m and AtT-20ins cells was investigated *in vivo* and compared to empty microsphere controls. The study was conducted in mice that are homozygous for diabetes spontaneous mutation in the leptin receptor. These mice become obese at 3-4 weeks of age and show elevations in blood sugar at 4-8 weeks. In this study 10-week old mice were used, which is an accepted diabetic mouse model for chronic wounds [22-24]. Cell-laden or empty hydrogel microspheres were applied to full-thickness excisional wounds created on the dorsa of diabetic mice and wound closure was followed for 35 days, after which mice were sacrificed and explants were processed for histology. The histological outcome was evaluated at the end point of the study and compared against controls.

In chapter 5, the limitations of the study described in chapter 3 and 4 were addressed. The hydrogel geometry was optimized, moving from hydrogel microspheres to hydrogels sheets for cell encapsulation. Cell viability and glucose-stimulated insulin release were re-validated for the new hydrogel geometry. At the end of this study, hydrogel sheet thickness was selected by assessing cell viability at multiple sheet thicknesses and multiple cell encapsulation densities. The sheet thickness selected here was used for subsequent studies in the following chapters.

In chapter 6, IPCs and MSCs were coencapsulated in hydrogel sheets. Employing MSCs served a dual purpose; (1) MSCs preserve IPC survival and improve their insulin secretory function, (2) MSCs themselves release soluble paracrine factors that accelerate wound healing. The goal of this chapter was to encapsulate IPCs and MSCs at multiple coencapsulation ratios and then to select the best ratio(s) that maximized insulin and MSC factor release. In this chapter, bioactivity of the secreted factors was also assessed by conducting the scratch assay for cell migration and Akt phosphorylation assay. The Akt phosphorylation assay served dual purposes; it tested a potential mechanism of the wound healing responses to the combined insulin and MSC factors stimulated and confirmed factor bioactivity. The studies conducted in this chapter also highlighted the

synergistic effect of insulin and MSC factors released from coencapsulation constructs by comparing them to single-cell encapsulation constructs. At the end of this chapter, the constructs that maximized insulin and/or MSC factor release and bioactivity were selected for *in vivo* studies in chapter 7.

In chapter 7, the wound healing responses of the chosen hydrogel constructs were evaluated *in vivo* by applying cell-hydrogel constructs to wounds on the dorsa of genetically diabetic mice. An animal study with two sacrificial time points (day 14 and day 28) is reported in this chapter. Mice (N=24 total; n=6/experimental group) were sacrificed on day 14 and wound tissue was collected to investigate the potential mechanism of accelerated wound healing during a time point when signaling pathways relevant to inflammation, proliferation, migration and angiogenesis are still active. Signaling molecules were elucidated by western blot and immunohistochemical analysis. To assess end-point histological outcomes, mice (N=12 total; n=3/experimental group) were sacrificed on day 28.

In chapter 8 of this dissertation, key findings are summarized, limitations in the study are acknowledged and future directions are mentioned.

REFERENCES

1. Sabine A. Eming, Thomas Krieg, Jeffrey M Davidson. Gene Therapy and Wound Healing. Clin Dermatol. 2007; 25(1): 79–92. doi: 10.1016/j.clindermatol.2006.09.011.
2. Shah JM, Omar E, Pai DR, Sood S. Cellular events and biomarkers of wound healing. Indian J Plast Surg. 2012 May;45(2):220-8. doi: 10.4103/0970-0358.101282.
3. Singh, N., Armstrong, D.G., and Lipsky, B.A. Preventing foot ulcers in patients with diabetes. JAMA 293, 217, 2005.
4. Amputee Coalition of America. National limb loss information fact sheet; diabetes and lower extremity amputations. 2008. Available at www.amputee-coalition.org/fact_sheets/diabetes_leamp.html. Accessed June 18, 2015.
5. American Diabetes Association, "Economic costs of diabetes in the U.S. in 2007", Diabetes Care, 2008; 31 (3):596–615.
6. Center for Disease Control and Prevention national Diabetes fact sheet. [Accessed 2/19/2013];National estimates on diabetes. 2007 http://www.cdc.gov/diabetes/pubs/pdf/ndfs_2007.pdf.
7. Sen, C.K., Gordillo, G.M., Roy, S., Kirsner, R., Lambert, L., Hunt, T.K., Gottrup, F., Gurtner, G.C., and Longaker, M.T. Human skin wounds: a major and snowballing threat to public health and the economy. Wound Repair Regen 17, 763, 2009.

8. Russo A, Steiner C, Spector W. Hospitalizations Related to Pressure Ulcers Among Adults 18 years and Older 2006. Rockville, MD: Agency for healthcare Research and Quality; 2008. http://www.hcup-us.ahrq.gov/reports/statbriefs/sb64.jsp.
9. Valensi P, Pariès J, Lormeau B, Attia S, Attali JR. Influence of nutrients on cardiac autonomic function in nondiabetic overweight subjects. Metabolism. 2005 Oct; 54(10):1290-6.
10. Olekson, M.A. Strategies for improving growth factor function in diabetic wounds. 2014. Available at https://rucore.libraries.rutgers.edu/rutgers-lib/45385/. Accessed June 16, 2015.
11. Chen, X., Liu, Y., and Zhang, X. Topical insulin application improves healing by regulating the wound inflammatory response. Wound Repair Regen 20, 425, 2012.
12. Lima MHM, Caricilli AM, de Abreu LL, Araújo EP, Pelegrinelli FF, Thirone ACP, Tsukumo DM, Pessoa AFM, dos Santos MF, de Moraes MA. Topical insulin accelerates wound healing in diabetes by enhancing the AKT and ERK pathways: a double-blind placebo-controlled clinical trial. PLoS One. 2012 7(5):e36974.
13. Barrientos S, Brem H, Stojadinovic O, Tomic-Canic M. Clinical application of growth factors and cytokines in wound healing. Wound Repair Regen. 2014 Sep-Oct;22(5):569-78. doi: 10.1111/wrr.12205.
14. Briquez PS, Hubbell JA, Martino MM. Extracellular Matrix-Inspired Growth Factor Delivery Systems for Skin Wound Healing. Advances in Wound Care. 2015;4(8):479-489. doi:10.1089/wound.2014.0603.
15. Badiavas EV, Abedi M, Butmarc J, Falanga V, Quesenberry P. Participation of bone marrow derived cells in cutaneous wound healing. J Cell Physiol. 2003; 196(2):245-50.
16. Badiavas EV, Falanga V. Treatment of chronic wounds with bone marrow-derived cells. Arch Dermatol. 2003; 139(4): 510-6.
17. Yamaguchi Y, Kubo T, Murakami T, Takahashi M, Hakamata Y, Kobayashi E, Yoshida S, Hosokawa K, Yoshikawa K, Itami S. Bone marrow cells differentiate into wound myofibroblasts and accelerate the healing of wounds with exposed bones when combined with an occlusive dressing. Br J Dermatol. 2005; 152(4): 616-22.
18. Liwen Chen, Edward E. Tredget, Philip Y. G. Wu, and Yaojiong Wu. Paracrine Factors of Mesenchymal Stem Cells Recruit Macrophages and Endothelial Lineage Cells and Enhance Wound Healing. PLoS ONE. 2008; 3(4): e1886.
19. Kinnaird T, Stabile E, Burnett MS, Shou M, Lee CW, et al. (2004) Local delivery of marrow-derived stromal cells augments collateral perfusion through paracrine mechanisms. Circulation 109: 1543–1549.
20. Ankrum J, Karp JM. Mesenchymal stem cell therapy: Two steps forward, one step back. Trends Mol Med. 2010 May;16(5):203-9. doi: 10.1016/j.molmed.2010.02.005.
21. Faulknor RA, Olekson MA, Nativ NI, Ghodbane M, Gray AJ, Berthiaume F. Mesenchymal stromal cells reverse hypoxia-mediated suppression of α-smooth muscle actin expression in human dermal fibroblasts. Biochem Biophys Res Commun. 2015.
22. suboi R, Shi CM, Rifkin DB, Ogawa H. A wound healing model using healing-impaired diabetic mice. J Dermatol 1992;19:673-5.
23. Klingbeil CK, Cesar LB, Fiddes JC. Basic fibroblast growth factor accelerates tissue repair in models of impaired wound healing. Prog Clin Biol Res 1991;365:443-58.
24. Werner S, Breeden M, Hübner G, et al. Induction of keratinocyte growth factor expression is reduced and delayed during wound healing in the genetically diabetic mouse. J Invest Dermatol 1994;103:473.

CHAPTER 2: LITERATURE REVIEW

2.1 SKIN HISTOLOGY

The skin is divided into three layers; epidermis, dermis and hypodermis, each composed of particular cell and tissue structures for functional specialization [1]. The epidermis is the outermost layer of skin and is the keratinized squamous epithelium. Epidermis predominantly contains keratinocytes along with a smaller proportion of melanocytes, Langerhans cells, Merkel cells and fibroblasts. Keratinocytes, the principal cell type of this layer, is responsible for distinct features during keratinocyte maturation that subdivide this layer into five strata; stratum germinativum, spinosum, granulosum, lucidum, and corneum (Figure 2.1) [2, 3]. The stratum germinativum or stratum basale contains a single cell layer of basal keratinocytes separated from the basement membrane by hemidesmosomes. These cells are considered the columnar stem cells of the epidermis and are responsible for continuous renewal of the layers of epidermis. Upon mitotic division, half of the daughter cells migrate to the outer layers where they mature in a process known as keratinization. The other half of the daughter cells divide continuously to replenish the cells in the basal layer. As these cells continue to actively divide and mature in the stratum spinosum, they transform from a columnar to polygonal morphology and are attached to one another by desmosomes. In this layer cells begin to synthesize keratin [4]. The stratum granulosum has a granular appearance due to the accumulation of basophilic keratohyalin granules, which contain lipids and provide the necessary water-proofing and prevention of fluid loss. Keratinocytes continue to differentiate in this layer and transform from polygonal and plump to a flatter polygonal morphology. The stratum lucidum is only present in regions where protection against frictional and shear forces is required, such as in the palms of hands and soles of feet. Cells within the stratum corneum are called corneocytes. These are dead cells containing mature keratin and provide the physical barrier to skin [5]. As new cells are formed in stratum granulosum, cells in the stratum corneum are pushed to the surface forming ‘squames’ which eventually slough off, a process known as desquamation [6].

Melanocytes are present in the stratum basale in a 1:10 ratio with keratinocytes. These are dendritic in morphology and contain melanosomes that are responsible for the production of skin pigment, melanin. Melanin protects keratinocytes against solar ultraviolet radiation [7]. Present in the stratum basale are Merkel cells. Merkel cells though relatively scarce in number, are believed to provide touch perception and discrimination of shapes and textures [8]. Langerhans cells are dendritic cells of the skin predominantly present in the stratum spinosum and papillary dermis. These cells engulf invading pathogens and mature into antigen presenting cells migrating via the lymphatic system to the local lymphoid tissue [9].

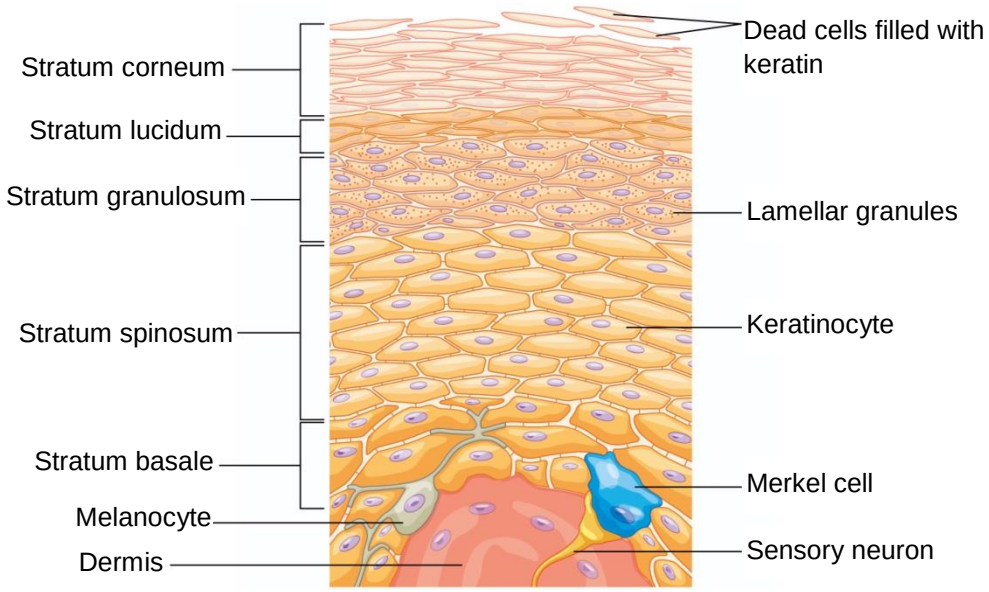

Fig. 2.1: Structure of the epidermal layer [208].

The dermis underlies the basement membrane and primarily functions in providing thermoregulation and supplies the avascular epidermis with nutrients. The nutrients diffuse through the intercellular channels that lie between the desmosomes. The dermis is characterized as a dense fibrous connective tissue and its predominant component collagen subdivides it into two regions; papillary dermis and the reticular layer [1]. The papillary dermis lies adjacent to the epidermis and consists of fine textured collagen. Reticular dermis lying underneath the papillary dermis is composed of an irregular network of collagen fibers and houses sweat and sebaceous

glands and hair follicles (Figure 2.2). Fibroblasts in the dermis produce collagen, elastin, and ground substance, providing structural support and elasticity to the skin [9]. The dermis transitions into the hypodermis, which is largely composed of loose connective tissue and adipocytes, while collagen and elastin fibers attach it to the dermis.

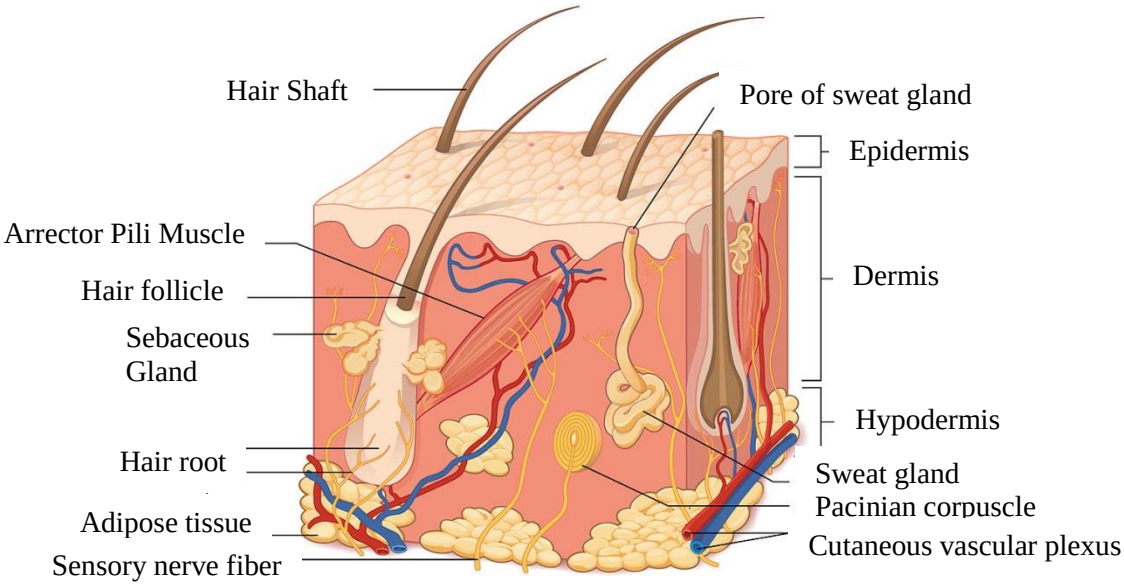

Fig. 2.2: Dermis and skin appendages [210].

Several structures are associated with skin, called skin appendages that help in thermoregulation, lubrication and other mechanical functions. Among these are sweat glands, sebaceous glands and hair follicles [2]. Sweat glands consist of a secretory portion lying deep in the dermis while it communicates with the surface via a duct through the epidermis. The sweat glands consist of cuboidal epithelial cells scattered among myoepithelial cells that contract to discharge sweat. Sweat glands are responsible for thermoregulation as sweat is secreted and evaporated as a regulator of body temperature. They are also involved in electrolyte balance [9]. Sebaceous glands consist of an outer layer of basal cells and multiple layers of sebocytes that are laden with lipids. Sebaceous glands mostly empty into the hair follicles [10].

2.2 DERMAL WOUNDS

A wound is described as a defect or discontinuity in the epithelium and a subsequent disruption of the integrity and protective function of skin. Several factors may be attributed to the occurrence of a wound, such as: a physical, chemical, or thermal insult to the skin, due to mechanical trauma, continuous pressure on the skin, or as a result of an underlying pathological condition. For the proper treatment of a wound, it is imperative that the wound type be categorized. Primarily, wounds are categorized as either acute or chronic. Acute wounds usually arise due to frictional forces on the skin such as abrasions and tears, surgical incisions, or penetrating injuries such as gunshots or sharp cuts. These wounds generally progress through the wound healing phases in a timely manner and heal completely. Wounds resulting from chemical or thermal insults are also classified as acute wounds; however, these wounds may or may not heal within the expected time frame depending on the degree of tissue damage.

2.2.1 Phases of Wound Healing

Wound healing occurs in a complex cascade of events or phases that overlap in both time and phase, namely: hemostasis, inflammation, proliferation, and remodeling. These phases of wound healing are characterized by a dynamic synchrony of cellular activities including phagocytosis, chemotaxis, cell proliferation, mitogenesis and collagen metabolism [11].

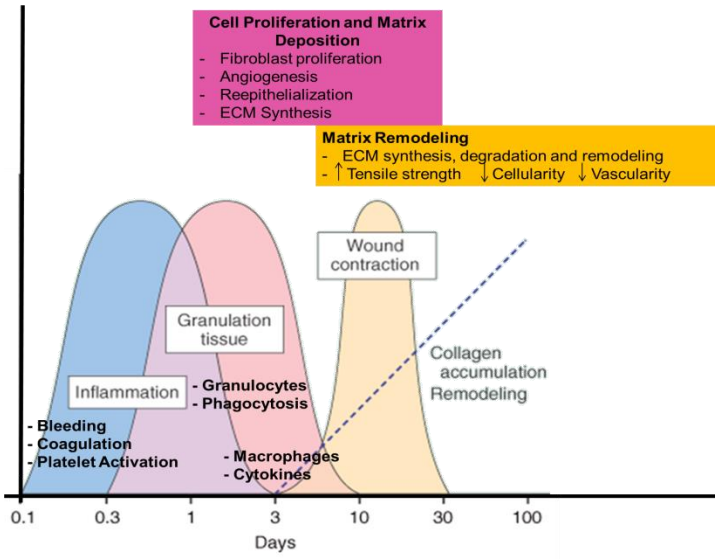

Fig. 2.3: Phases of wound healing. Modified from [209, 215].

Shortly after injury, hemostasis sets into play by intense vasoconstriction as a reflex to blood loss from severed vessels. The fibrillar collagen, fibronectin, and matrix proteins from the exposed extracellular matrix in the vessel wall activate the circulating platelets. Once activated, these platelets adhere and aggregate to form the platelet plug, thus triggering the initiation of an intrinsic coagulation cascade that transforms prothrombin to thrombin. Thrombin subsequently converts fibrinogen to fibrin leading to clot formation to achieve hemostasis [11-13]. Factors secreted by these platelets such as platelet-derived growth factor (PDGF), insulin-like growth factor-1 (IGF1), epidermal growth factor (EGF), transforming growth factor-β (TGFβ) and platelet factor-IV are key mediators of the healing cascade. These factors are responsible for attracting fibroblasts, endothelial cells and macrophages into the wound area while the clot provides the provisional matrix for cell migration. The hemostasis phase typically lasts 5-10 minutes followed by the vascular and cellular responses of the inflammatory phase [11, 13]. Platelets are also store houses of serotonin and histamine that increase capillary permeability, accumulation of lymphatic drainage, and fluid exudate into the extravascular space. This leads to the hallmarks of inflammatory phase; calor, dolor, rubor, and tumor. In response to the

chemoattractants released by the platelets, neutrophils and monocytes extravasate into the wound area where monocytes undergo phenotypic changes to become tissue macrophages. Within 24-48 hours after injury neutrophils begin to arrive at the wound site, eliciting the early inflammatory phase. They continue to infiltrate for a few days and clean up tissue debris and phagocytose foreign particles by releasing free oxygen radicals and lysosomal enzymes [11-13]. The prolonged presence (beyond 48 hours) of neutrophils at the site of injury signifies wound contamination and may lead to delays in wound healing [13]. Neutrophils that are rendered redundant after killing bacteria are phagocytosed by macrophages. Macrophages are key regulators of wound healing during the inflammatory phase. During the late inflammatory phase of wound healing, macrophages continue to phagocytose cellular and tissue debris and secrete growth factors such as PDGF, transforming growth factor-α (TGF-α), TGF-β, tumor necrosis factor (TNF) and fibroblast growth factor (FGF). Macrophages upon activation play an integral role in wound repair through secretion of these bioactive molecules [14] that affect extracellular matrix composition [15, 16] and influence proliferation and differentiation of keratinocytes, fibroblasts, and endothelial cells [17-19]. However, excess infiltration of macrophages into the wound area can lead to impaired wound healing and the wound may become chronic. The inflammatory phase sets the necessary framework for the proliferation phase that begins on day 3 post-injury and may continue until weeks 2-3. This phase is dominated by reepithelialization by keratinocytes, migration of fibroblasts to deposit new extracellular matrix, and formation of granulation tissue. The newly constructed ECM composed of fibronectin, hyaluronan, collagen, and proteoglycans supports cell adhesion and further ingrowth of cells. Reepithelialization is a requirement for successful wound healing. Within 24 hours of tissue injury, epidermal keratinocytes are mobilized from the free wound edges and epidermal appendages appendages [20] due to loss of contact inhibition and production of matrixmetalloproteinases (MMPs) [21]. Keratinocytes flatten and elongate and form a keratinocyte migration tongue by projecting lamellipodia to migrate as a sheet by “walking” on the extracellular matrix [22] and cover the

exposed area where they increase their mitotic activity. Once the advancing keratinocytes meet, their further migration is halted due to contact inhibition. Cellular growth and differentiation establishes the new stratified epithelium. This process of reepithelialization requires EGF, keratinocyte growth factor (KGF) and TGF-α. Following reepithelialization, the basement membrane anchors the basal keratinocytes to the underlying dermis. The interstitial matrix within ECM is later organized to form the basement membrane with an orderly arrangement of keratinocytes, endothelial cells and smooth muscle cells. Optimal healing of the injured tissue is signified by the presence of granulation tissue that appears to be formed by day 3-5 [13]. It is characterized histologically by the presence of proliferating fibroblasts and angiogenesis, indicated by newly formed capillaries in loose ECM sprouting from pre-existing vessels and by proteolytic degradation of the basement membrane. During angiogenesis, endothelial cells migrate to the wound site, proliferate and mature into capillary tubes. The metabolic needs of fibroblasts are fulfilled by the accompanying angiogenesis in response to biochemical stimuli from macrophages and platelets. Angiogenesis is essential for fibroblast migration and thus proper progression of wound healing. While the granulation tissue forms, fibroblasts also transform into specialized cells called myofibroblasts, which extend and retract to contract the wound along the lines of skin tension. Smooth muscle differentiation markers such as α-smooth muscle actin, smooth muscle myosin, and desmin are highly expressed during wound contraction, beginning on day 6 post injury and peaking around day 15 then progressively regressing shortly afterward. Changes in the composition of ECM are characteristic of the remodeling phase and occur simultaneously with the formation of granulation tissue. It has also been reported that wound tissue metabolism shifts from anaerobic metabolism during proliferation to aerobic metabolism during later phases, which favors collagen synthesis [23]. The tensile strength of the wound increases during this period due to continuous production of collagen. At approximately 3 weeks, homeostasis is reached where synthesis of collagen equals its degradation by specific metalloproteinases. As wound margins close, capillary outgrowth ceases, blood flow and

metabolic activity is reduced and the granulation tissue transforms into an avascular scar containing inactive fibroblasts, collagen and other ECM components.

2.2.2 Cytokines and Growth Factors in Wound Healing

A normal wound healing process undergoes a well-regulated sequence of events orchestrated by cells, growth factors and cytokines. Cytokines play an important role as mediators of host-injury response and as regulators of subsequent repair. Cytokines and growth factors are predominantly secreted by platelets and immune cells and act both locally at the site of injury and systemically to initiate reparative responses.

PDGF is released by degranulating platelets upon injury and plays a vital role during each stage of wound healing. PDGF stimulates mitogenesis and chemotaxis of neutrophils and macrophages during inflammatory phase, recruits pericytes and smooth muscle cells to improve structural integrity of blood vessels and promotes keratinocyte migration by stimulating production of IGF-1. In addition, PDGF also stimulates proliferation of fibroblasts, differentiation of fibroblasts to myofibroblasts, production of ECM and organization of the healing tissue [26, 27]. Cytokines such as interleukin (IL)-1α, IL-β, TNF-α and interferon [24] mediate the inflammatory phase in which immune cells infiltrate the wound to kill pathogens and phagocytose cellular debris. Macrophages are an important source of growth factors including granulocyte-macrophage colony stimulating factor (GM-CSF), TGF-α, TGF-β, basic FGF (bFGF), PDGF and VEGF during granulation tissue formation [25]. GM-CSF, a cytokine that exerts diverse biological effects during acute injury, has been shown to be an immune stimulator involved in local recruitment of inflammatory cells, epidermal proliferation, promotion of myofibroblast differentiation and wound contraction [28-38]. TGF-β, secreted by platelets, macrophages and fibroblasts, activates fibroblasts to secrete collagen which gives a structural framework to the newly formed stroma. VEGF has been known as a powerful angiogenic factor which stimulates endothelial cells to transmigrate through the basement membrane to the wound and form new blood vessels. Erythropoietin (EPO), a glycoproteic hormone, has been demonstrated to stimulate

angiogenesis in synergy with VEGF by stimulating endothelial cell mitosis, granulation tissue formation and dermal regeneration [39]. Delayed wound healing has partly been implicated to impaired VEGF expression.

2.2.3 Chronic Wounds

Normal wound healing is governed by the complex orchestrated cytokine milieu of the wound. Specific temporal and spatial expression of cytokines and growth factors in the wound ensure proper transition through the various phases of wound healing. These factors have both inhibitory and stimulatory effects. Wound healing is compromised in several medical conditions including diabetes, immobility, venous insufficiency, and continued chemotherapies. Chronic wounds, characterized by an inability to self-repair in a timely and orderly manner, demonstrate aberrant expression of the cytokines and growth factors integral to the wound healing process. Under these aberrant conditions, the dynamic synchrony of cellular activities including phagocytosis, chemotaxis, cell proliferation, mitogenesis, and matrix remodeling can be disrupted (Figure 2.4) [40]. The inflammatory phase is prolonged due to a rise in inflammatory cytokines (such as IL1, IL6 and TNFα) [41], and altered ratio of M1 (pro-inflammatory) to M2 (anti-inflammatory and healing) macrophages [195]. The prolonged inflammatory phase also increases levels of MMPs and reactive oxygen species, which degrade the ECM. Moreover, chronic wounds enter prolonged hypoxia due to vascular disruption and insufficient angiogenesis, contributing to the dysregulated cellular functions of keratinocytes and fibroblasts [42]. Each of these events is a contributing factor that leads to chronic wounds, thus concerted therapeutic strategies are required to tackle them.

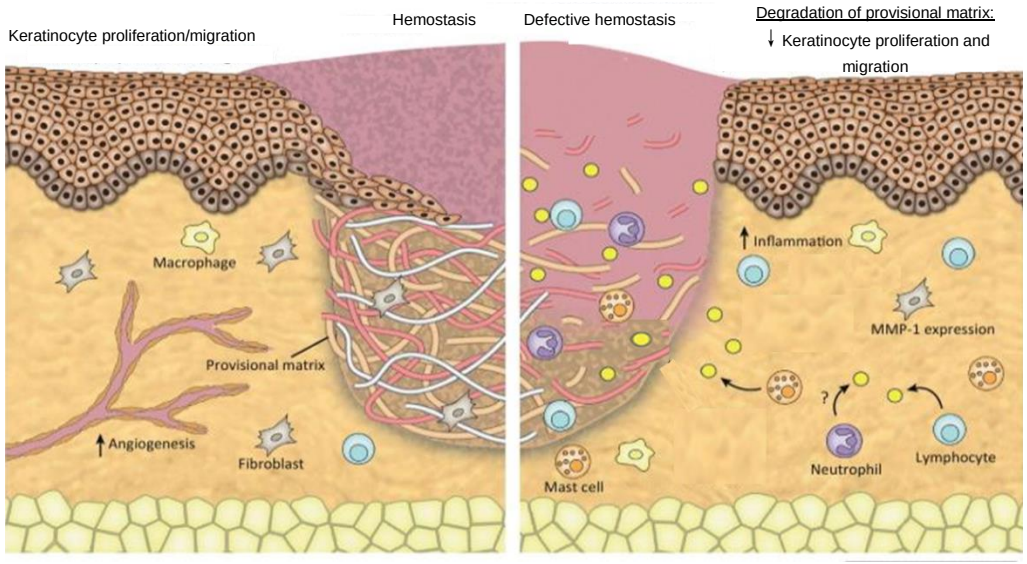

Fig. 2.4: Comparison of healthy and chronic wound. Reprinted from 'Trends in Molecular Medicine, 18, Paul R. Hiebert, David J. Granville, Granzyme B in injury, inflammation, and repair', 732-741, 2012, with permission from Elsevier.

2.3 WOUND HEALING THERAPIES

Cytokine and growth factor therapies provide a promising tool for altering the wound microenvironment [43] that can minimize inflammation and augment the healing capacity. However, success of growth factor clinical trials is limited by the inefficient delivery and biological degradation in the hostile environment.

2.3.1 Growth Factor Therapies

Growth factors are signaling peptides that modulate wound healing and cellular activities by binding to cell surface receptors and inducing signal transduction pathways that are involved in cell migration, proliferation, differentiation and synthesis of extracellular matrix molecules. Several growth factors have been reported that participate in wound healing including EGF, PDGF, FGF, GMCSF, KGF and TGF-β1 [171, 172]. Of these only PDGF is approved by the Food and Drug Administration (FDA).

PDGF has shown significant improvement in healing and its B chain dimer, PDGF-BB is approved by FDA for application to wounds [44]. Autologous PDGF treatment in 49 patients suffering from chronic cutaneous wounds led to complete wound closure in ten and a half weeks [176]. Encouraging animal studies in which PDGF improved granulation tissue formation and increased wound tensile strength [174, 175] led to development of recombinant human PDGF (rh-PDGF). Robson et al. reported a double-blind placebo-controlled study using rh-PDGF in 20 patients with pressure ulcers. Treatment with 10 μg rh-PDGF improved reduced wound size by 21 % compared to 6.4 % in placebo controls [177]. Another randomized controlled trial that inducted 118 patients [178] with lower extremity diabetic neuropathic ulcers used a daily topical application of 22 mg of rh-PDGF per square centimeter of ulcer area and 48% of the patients underwent complete healing. However, these results may only have been significant compared to placebo controls because of a large difference in initial mean ulcer area; 90 cm^2 in placebo group vs. 55 cm^2 in rh-PDGF group. Becaplermin, marketed as Regranex© is rh-PDGF and carboxymethyl cellulose gel, demonstrated complete healing in chronic pressure ulcers [45]. In a double-blind randomized clinical trial, patients with diabetic ulcers receiving becaplermin gel demonstrated significant increases in wound closure by 3 weeks of treatment. Additionally, four multicenter, randomized, placebo-controlled studies evaluating daily topical application of rh-PDGF demonstrated success with diabetic ulcers [46]. These trials concluded that 100 μg/mL becaplermin applied once daily was effective in improving healing. However, treatment with becaplermin is expensive ($400/100 g), requires frequent dressing changes, and most alarmingly has been shown to increase the incidence of cancer with prolonged repeated use [179].

TGF-β has also been shown to accelerate wound healing in animal models. Effects of recombinant TGF-β2 on diabetic foot ulcers in a double-blind randomized placebo-controlled trial by Robson et al. demonstrated higher healing rates compared to placebo [182]. However, patients receiving standard wound care alone healed the best. A review by Khan et al. elucidated

that the small sample size in the study by Robson et al. might be a contributing factor for their insignificant results [183].

bFGF, the most extensively studied of the nine homologous polypeptides is approved for clinical use in Japan and has shown to reduce scar formation in acute incisional wounds [47]. In animal studies FGF has been shown to increase tensile strength when injected around lesions [184] and has reversed the healing defect in diabetic wounds [185, 186]. Unfortunately, FGF has not demonstrated convincing results in human clinical trials on diabetic ulcers. In one such trial, only three of the nine patients receiving FGF healed compared to five out of eight in the placebo group [187]. In contrast, King et al. saw encouraging results in treating leg ulcers [188].

KGF also belongs to the FGF family. A multi-center double-blind placebo-controlled study using two doses (20 μg and 60 μg) of recombinant KGF-2 (repifermin) was conducted on patients suffering from venous leg ulcers [192]. Patients received standard wound care for leg ulcers and topical repifermin twice weekly. Statistically significant results were achieved and reductions in the wound size were 56%, 75%, and 73 % in placebo, repifermin at 20 μg, and repifermin at 60 μg, respectively.

GM-CSF has fundamental importance in wound healing and it has been reported by Mann et al. that deficiency of GM-CSF delays wound repair and results in poor quality of newly formed tissue [173]. Recombinant human-GM-CSF (rh-GM-CSF) has demonstrated therapeutic efficacy in the healing of pressure ulcers and formation of firm granulation tissue [48]. A small sample-size study with 10 chronic leg ulcer patients was conducted by Barbolla-Escaboza et al. [180] using a single perilesional injection of rh-GM-CSF (300 μg) and 80% complete healing occurred within 4 weeks. In a study conducted by Da Costa et al. on patients with chronic venous ulcers, 50 % of the wounds injected perilesionally with rh-GMCSF (leucomax) healed by 8 weeks compared to 11 % treated with placebos [49]. In a another double-blind randomized and placebo-controlled study, 200-400 μg perilesion injections of rh-GM-GSF improved healing in patients

with chronic venous ulcers and prevented recurrence for at least 40 months [50]. These studies led to the recommendation that 400 μg is the optimal GM-CSF dose. Another trial with topical application of GM-CSF reported complete healing in 47 of 52 ulcers with a mean healing time of 19 weeks [181]. Investigations into the molecular basis of the beneficial effects of GM-CSF treatment reveals that GM-CSF increases blood vessel density and VEGF in the wound bed with the inflammatory cell-derived VEGF possibly acting as a mediator of angiogenesis [51]. There have been other studies on sequential or combined cytokine therapies with GM-CSF/bFGF. Patients with pressure ulcers receiving bFGF daily for 35 days demonstrated the most significant reduction in wound volume, followed by patients treated sequentially with GM-CSF for 10 days, and bFGF for 25 days [52]. In this study, patients receiving only GM-CSF did not show significant wound closure compared to placebo [52]. In addition to their efficacy treating pressure ulcers, subcutaneous injections of granulocyte-colony stimulating factor (G-CSF) (Filgrastim) eradicated pathogens and prevented the need for amputations in insulin-dependent patients with infected diabetic foot ulcers [53]. This result was attributed to the ability of G-CSF to augment the wound neutrophil response and increase superoxide production, which is compromised in diabetic foot ulcers [54].

EGF was the first growth factor to be studied in wound healing [183]. A double-blind randomized study [189] was conducted with 18 venous leg ulcer patients in the placebo group and 17 patients receiving 10 μg/mL recombinant human EGF (rh-EGF). Six of the seventeen rh-EGF patients demonstrated complete ulcer reepithelialization at 10 weeks. These patients had a mean 48 % reduction in the ulcer size. However, the results were not statistically significant, possibly because of the small sample size or the low EFG dose [183]. The same study showed that up to 40 μg of rh-EGF per day can be safely used [189]. EGF has shown more promising results in experimental animal wounds [190] and human acute wounds [191].

2.3.2 Insulin Therapies

The insulin signaling pathway is critical in diabetes as it is known to control glucose homeostasis; lesser known is its role in wound healing. Insulin plays a vital role in several cellular processes. It stimulates mitogenesis and inhibits apoptotic cell death in fibroblasts, neuronal cells and endothelial cells [205]. Insulin is essential for glucose utilization by fibroblasts to produce collagen. Insulin promotes glycogen and protein synthesis, activates and inactivates enzymes, and regulates gene expression and cell survival [206]. One of the key components of the insulin signaling pathway is the insulin receptor (IR). IR is a heterotetrameric transmembrane glycoprotein consisting of two alpha (α) and two beta (β) subunits held by disulphide bridges and therefore functions as a dimer [207]. The α-subunits constitute the extracellular domain where the insulin binding occurs, while the β-subunit contains extracellular, transmembrane, and cytosolic domains. It is the cytosolic domain that contains the ATP-binding site, tyrosine phosphokinase and tyrosine-autophosphorylation site [62]. Insulin binds to one of the two binding sites present on each αβ monomer, implying negative cooperativity i.e., the binding of a ligand to the receptor decreases affinity of the IR for a second ligand. One of the roles of the α-subunit is to inhibit kinase activity of the β-subunit in the absence of insulin, while the presence of insulin activates it: binding of insulin to the α-subunit leads to autophosphorylation of the receptor at the β-subunit and activation of its tyrosine kinase activity [62]. Once the IR is activated, it phosphorylates the insulin receptor substrate 1(IRS1) at tyrosine residues and generates phosphotyrosine residues, which bind to receptor tyrosine kinases of effector molecules containing the Src homology-2 (SH2) domain [62]. This leads to activation of several downstream signaling proteins such as PI3K, extracellular signal regulated kinases (ERK), RAS, and the Mitogen-activated protein kinases (MAPK) cascade [62].

Activation of PI3K occurs via binding of tyrosine-phosphorylated IRS1 protein to its SH2 domain, leading to subsequent activation of its downstream target Akt and its recruitment to the plasma

membrane. It is through Akt that PI3K mediates metabolic targets of insulin signaling. Phosphorylated Akt enters the cytoplasm where it phosphorylates and inactivates glycogen synthase kinase 3 (GSK3). GSK3 plays a role in inhibiting glycogen synthesis by phosphorylating its substrate glycogen synthase, a key enzyme in the final step of glycogen synthesis. The PI3K/Akt pathway is activated in an insulin-dependent manner and is implicated in wound healing. Insulin also prevents apoptotic cell death induced by inflammatory stimuli by counteracting the dephosphorylation of Akt by TNF-α and promotes angiogenesis by stimulating expression of VEGF via Akt signaling [63]. The insulin-induced PI3K pathway is also involved in stimulating production of nitric oxide synthase (eNOS) in endothelial cells and its phosphorylation by Akt increases its activity [63].

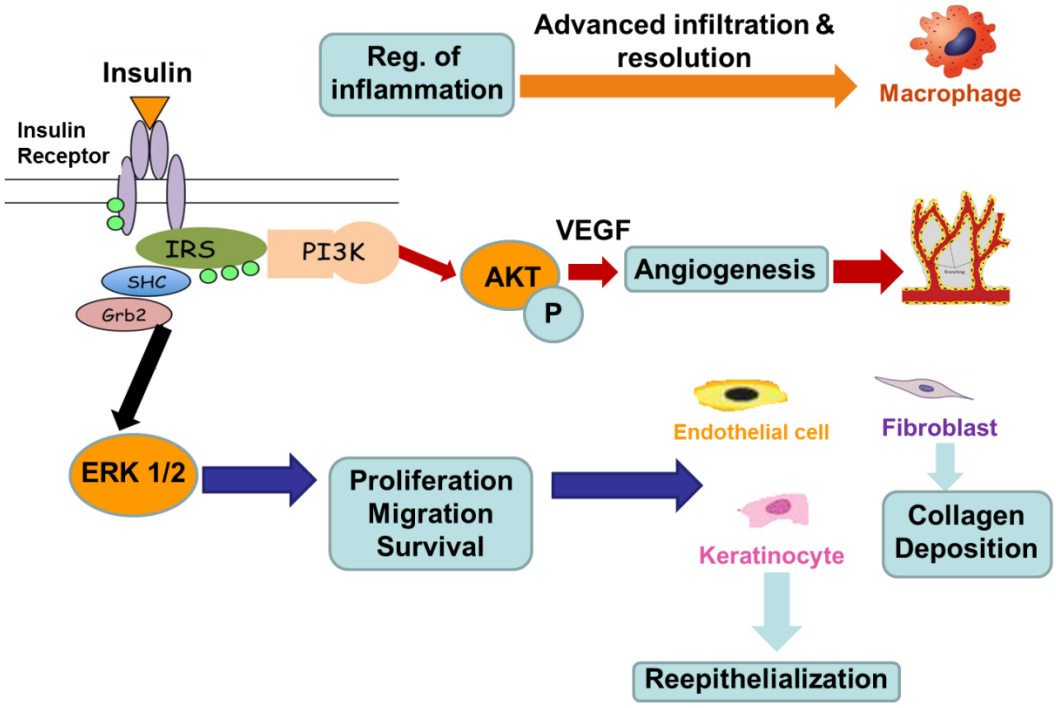

Fig. 2.5: Insulin regulated ERK1/2 and AKT signaling. Modified from [62].

Epidermal Growth Factor Receptor (EGFR) has also been shown to promote wound healing by inducing keratinocyte migration through activation of PI3K/Akt and ERK signaling [64]. Insulin plays an important role in EGFR signaling by inducing its phosphorylation; however, only insulin-induced ERK signaling and not insulin-induced PI3K signaling is dependent on EGFR.

This suggests that insulin induced keratinocyte migration is governed by both EGFR-dependent and EGFR-independent mechanisms [65].

Activation of the RAS-MAPK pathway is necessary for mitogenesis and occurs via adaptor molecule growth factor receptor-bound protein 2 (Grb2) containing the SH2 domain. Grb2 associates with son-of-sevenless (SOS) to bind to phosphotyrosine residues on IRS proteins, triggering a kinase cascade phosphorylating dual-specificity kinases MEK1 (MAPK and ERK kinase 1) to activate the pathway [66]. Moreover, activation of the RAS pathway leads to activation of MAP kinases and ERK, which are serine/threonine kinases. MAP and ERK kinases alter gene transcription and the cellular processes of cell growth, survival, and differentiation.

Several mechanisms have been delineated through which the activity of IR is regulated: by protein tyrosine phosphatases that dephosphorylate tyrosine residues; suppressors of cytokine signaling, which block the interaction of IR with IRS; or through receptor internalization and degradation that reduce its activity [66].

Lima et al. elucidated that the insulin signaling pathway plays an important role in wound healing and demonstrated that the expression of components of this pathway, particularly IRS, ERK and Akt is decreased in the wounded skin of diabetic subjects with a resulting increase in time to complete wound closure [202]. They further demonstrated that application of topical insulin normalizes and reverses this defective signal transduction and improves wound healing. The effects of insulin on epithelial cells, fibroblasts and endothelial cells have been studied extensively [75, 77, 78]. In a study employing corneal epithelial cells, Shanley et al. demonstrated that insulin promoted closure of *in vitro* monolayer scratches by activating the ERK1/2 and PI3K signaling [75]. Von Haam and Cappel showed that insulin increases fibroblast growth rates in *in vitro* cultures [77]. Hermann et al. elucidated the anti-apoptotic role of insulin in endothelial cells. They demonstrated that insulin prevents TNF-α induced apoptosis in human umbilical vein endothelial cells (HUVEC) by counteracting the dephosphorylation of Akt by TNF-α [78]. Proliferation and migration of endothelial cells is necessary for the formation of new blood

vessels. It is through the process of angiogenesis that required nutrients and oxygen is provided to the injured tissue and thereby accelerates wound healing. Liu et al. in their study demonstrated that insulin injection in the skin of mice stimulated angiogenesis, lead to longer and more branched blood vessels and were positive for α-smooth muscle actin. They also highlighted that this mechanism occurred independently of VEGF signaling albeit insulin stimulates secretion of VEGF by various cells types [79]. Joseph. in his 1930 study reported that insulin injection administered in non-diabetic patients with decubitus sores showed accelerated healing by day 10 [80]. Acceleration of wound closure following topical insulin administration has been reported in both diabetic and non-diabetic animals [197-202]. Insulin does so by increasing collagen deposition and serves as a chemoattractant and mitogen to cells necessary for wound healing [81]. *In vitro* studies on human skin fibroblasts have also shown increased collagen secretion in response to insulin [82]. Insulin therapy has shown efficacy in the healing of burn wounds. In a study by Madibally et al. in 2003, insulin administered subcutaneously after burn injury to rats diminished inflammation and increased collagen deposition [84]. One of the earliest studies conducted by Rosenthal et al in 1968 showed that rats treated with 8 units of topical protamine zinc insulin suspension demonstrated increased wound tensile strength on the seventh day [74]. Ulcerin, a zinc protamine insulin cream compound, was also used in an early study by Belfield et al. in 1969. The study was conducted to heal surgical wounds, bite wounds, lacerations or infected lesions in small animals and decubitus ulcers proteus ulcers and pressure sores in humans. The wounds were found to be infected with prolonged inflammation. After treatment with ulcerin, healing began from the wound periphery, insulin served as an auto-debridement agent and promoted cellular proliferation [85].

2.3.3 Cell Therapies

Cell therapies are a promising strategy to promote healing in both acute and chronic cutaneous wounds. Cell therapies provide several advantages over conventional negative pressure wound

therapy and hyperbaric oxygen therapy for chronic wounds, such as patient discomfort and pain. Also cell therapies circumvent the need for skin grafts and overcome the disadvantages of surgical procedures and donor site morbidity. In addition, cell therapies are advantageous for elderly and immobile patients who cannot tolerate the burden of skin grafting. However, applying cells as a suspension or in a spray without ECM or a carrier has inherent limitations; cell-only treatments do not benefit wound contraction [162]. In all, the goal of cell therapies as opposed to skin substitutes is to induce the host cells to migrate from the wound edges and reepithelialize the defect, and to trigger host fibroblasts in the wound bed to lay granulation tissue [162]. Fibroblasts, keratinocytes, stem cells, and platelet cell suspensions have been abundantly employed in various studies to promote wound closure. Keratinocytes have been used in cutaneous wound cell therapies since 1981 and have since then been used as autografts and allografts [163]. Like keratinocytes, fibroblasts are a representative treatment in diabetic foot ulcers [164-166]. Sheets of keratinocytes and fibroblasts over synthetic or natural polymers are being developed and characterized. Alternatively, platelets (as platelet-rich plasma) have been applied to supply chronic wounds with growth factors and promote healing [167, 168]. However in most cases autologous platelets are used, which is not recommended since generally patients with chronic wounds are immobile or suffer from systemic diseases or anemia, and thus drawing large blood volumes can have detrimental effects on hemodynamic stability [163]. However, single cell therapies do not compensate for all the growth factors presence in a healthy wound environment: for example, keratinocytes secrete several growth factors but lack the ability to rebuild the damaged ECM. Healthy wound healing is a complex mechanism requiring a cocktail of growth factors, cytokines, and cell interactions that cannot be effectively achieved with cells offering an epidermal and/or a dermal component only. Bone marrow-derived cells secrete factors that are required in all stages of wound healing and have the capacity to activate and accelerate the healing process. However, a study showed that only 4 % bone marrow-derived cells engraft as keratinocytes in the presence of injury [159]. Others have reported that stem cells respond to

these signals by tissues requiring repair and engrafting in those zones [160]. While in a chronic wound model, only 27 % bone marrow mesenchymal stem cells engrafted in the wound tissue [161].

Nevertheless, cells applied in a suspension are lost over time leading to engraftment failure and do not remain viable in the hostile chronic wound environment. Thus cell therapies require concerted efforts to prevent cell migration and provide a supporting matrix, scaffold or delivery vehicle. Polymers are excellent candidates for this application.

2.3.3.1 Encapsulated Cell Therapies

Hydrogels serve not only as delivery vehicles preventing cell migration and providing immunoisolation but also offering cells a microenvironment that preserves their viability and allows maintenance of their normal cellular functions. Cells require a three-dimensional scaffold that functions like the organ-interactive native ECM in order to maintain their characteristic phenotype and morphology. Apart from the repair and regeneration of diseased tissue, cell therapies are also being employed for controlled drug delivery [114]. Several natural and synthetic polymers have been explored in an attempt to provide cells with this critical need for an artificial ECM and the versatility to allow or prevent cell attachment.

Alginate, a widely used natural biomaterial, especially in wound dressings, is extracted as a polysaccharide from brown algae [112]. It has been utilized as a scaffold in regenerative medicine, as a delivery vehicle for drugs, and as a model extracellular matrix for cells [113]. Alginate is considered relatively bioinert and natively alginate gels do not promote cell attachment; however, coupling alginate with laminin [115], fibronection [116], collagen [117] or the fibronectin-derived adhesion peptide arginine glycine aspartic acid (RGD) [118] can mediate cell adhesion onto alginate substrates. Alginate forms a gel in the presence of calcium chloride and can be used to encapsulate or immobilize cells; however, the gelling reaction is reversible and the scaffold degrades *in vivo* when exposed to ions such as sodium [119-121]. Therefore, when permanent hydrogels are required, alginate is often coated with a polycation to increase its stability. The

most popular polycation is polylysine, which is unfortunately immunogenic [203, 204]. Alginate is approved by the U.S. Food and Drug Administration (FDA) and is used in commercially available wound dressings such as SeaSorb and Kaltostat [127]. Alginate has been widely characterized as a bio-occulusive moist wound dressing [133, 134]. It has been used for healing of split graft donor site wounds [135, 136]. Alginate has been used as a hydrogel matrix to form a bilayered structured in which keratinocytes are cultured over encapsulated fibroblasts [122]. In this approach autologous keratinocytes and fibroblasts were used, alginate degraded over time and fibroblast-secreted ECM replaced alginate over time and the construct integrated into the host wound. Though this seems to be an ideal strategy for healing dermal wounds, it is only successful when autologous cells are available. Moreover, such a strategy does not address the detrimental effects of inflammatory cytokines and MMPs on cell scaffolds placed in a chronic and diabetic wound environment. Tissue engineering approaches utilizing alginate employ it as dermal analogue intended to replace the lost ECM. Some studies have also shown that alginate gels applied to dermal wounds induce macrophages to produce elevated levels of TNFα, IL-6 and IL-1β [131, 132]. This may seem advantageous in induction of inflammation in recalcitrant wounds; however, it is strongly contraindicated in chronic wounds which are already arrested in the inflammatory phase.

Like alginate, fibrin has found applications in skin tissue engineering. Following injury, increases in local microvascular permeability allows the extravasation of fibrinogen and its subsequent conversion to fibrin by thrombin forms a fibrin gel at the wound site. Later, this is remodeled into mature collagenous tissue through migration and secretion by fibroblasts. Brown et al. confirmed this *in vitro* [137]. Fibrin has been attractive in wound healing applications as a dermal analogue [138] and an *in vitro* ECM model system [140], providing a 3D scaffold or encapsulation device for fibroblasts. A study by Cox et al. demonstrated that fibroblast migration, proliferation, and cytokine secretion in fibrin gels is dependent on the starting concentration of fibrinogen and thrombin [138]. Other studies reported culturing keratinocytes on fibrin as dermal equivalents and

developing composite bi-layered skin for wound coverage [139]. Fibrin polymer sprays have been used to deliver autologous MSCs to wound sites [130]. This MSC-fibrin polymerized gel adheres to wounds; however, fibrin degrades over time allowing migration of MSCs, thus requiring repeated applications. Since fibrin is a natural polymer that is rapidly degraded by enzymes present in the body, it is rationally only feasible in applications that require a degradable matrix with the end goal of integration of cells into the host.

In skin tissue engineering, collagen is used as a dermal substitute and as a hydrogel for cell encapsulation. However, collagen carries the risk of disease transmission and immune rejection [123, 124] because it is derived from animal sources. Also, studies have shown that collagen can inhibit the healing process by limiting the migration of endothelial cells, keratinocytes and macrophages into wounds [125, 126]. Another limitation of using collagen for cell encapsulation is maintaining suitable oxygen and nutrient access and concentration throughout the scaffold [141]. Chitosan-gelatin-hyaluronic acid composite hydrogels have also been explored for keratinocyte-fibroblast co-culture to construct artificial skin [128].

All the polymers mentioned thus far are utilized in the category of bioactive or biological polymers for dermal wounds, implying that they themselves take part in the wound healing process and become part of the wound tissue over time. Unlike natural polymers, synthetic materials provide greater mechanical strength and product consistency. Another concern with natural polymers is their reduced mechanical strength, which limits the ease of handling. Synthetic polymers such as polyethylene glycol (PEG) are non-reactive with biological tissues, non-adherent, non-irritant, and provide a cool surface thus reducing pain [142]. PEG is widely used as a cell scaffold and for cell encapsulation [146] and provides a “blank slate” that can be functionalized with biomolecules according to the application, allowing control over physical and biochemical properties. Mammalian cells encapsulated in PEG-based hydrogel microstructures remained viable for several days after encapsulation [158]. PEGDA, a PEG chain with two acrylate groups on either side, is well accepted and has been extensively used as a delivery

vehicle for pancreatic islets in diabetic applications [143-145]. In fact, subcutaneous implantation of PEGDA-encapsulated human islets in Type I diabetic patients have shown promising results with sustained islet function and no evidence of autoimmune reaction [144]. PEGDA encapsulation has permitted successful transplantation of xenogeneic pancreatic islet cells when porcine islets were implanted into diabetic rats; the animals achieved normoglycemia for up to a year [145]. Others have employed PEGDA for encapsulation of MSCs in differentiation studies [147-149]. Various types of fibroblasts such as human foreskin fibroblasts and pulmonary fibroblasts have been cultured on PEG hydrogels and the effect on cell culture and cell secretion has been elucidated [150]. Studies have demonstrated the effect on fibroblasts when modifying PEG substrates with varying matrix stiffnesses [151-154], growth factors [155, 156], and adhesion peptides [152].

2.3.3.2 Stem Cell Therapies

Several strategies have been explored that employ the use of growth factors and stem cells to accelerate wound repair in non-healing wounds. Bone marrow stromal cells or MSCs are multipotent non-haematopoeitic stem cells that have the ability to differentiate into osteogenic, chrondrogenic, and adipogenic lineages. MSCs are known for their immunomodulatory function, and production and secretion of a vast array of cytokines and growth factors that are involved in tissue repair and regeneration. MSCs express TGF-β1, EGF, VEGF, PDGF, KGF, FGF, IGF-1, EPO, stromal cell-derived factor-1 (SDF-1), soluble tumor necrosis factor receptor-1 (sTNF-R1) and hepatocyte growth factor (HGF); these growth factors are expressed constitutively or in the presence of pro-inflammatory factors and their expression is further increased under hypoxic conditions [55]. Liu et al. elucidated the role of MSC growth factors and demonstrated that the secretion of TGF-β1, FGF and VEGF from MSCs is stimulated and increased in a time-dependent manner in the presence of wound tissue fluid. PDGF, KGF, HGF and EGF are generally weakly expressed in normal tissue fluid but increased in the presence of pro-inflammatory signals such as lipopolysaccharides (LPS), TNF-α and IL-1 [55]. Several studies report that MSCs promote

healing in cutaneous wounds and chronic ulcers [56, 57], decrease the time to complete wound closure, differentiate into myofibroblasts to promote wound contraction, and participate in dermal rebuilding [58].

The presence of MSCs at the wound site has been separately shown to circumvent wound inflammation and promote wound repair. An effective wound healing response requires recruitment of a variety of cell types to the wound bed followed by subsequent survival and proliferation of these cells. MSCs recruit macrophages to the wound site by secreting the chemoattractant macrophage inflammatory protein (MIP) and macrophage chemoattractant protein (MCP) [59, 60]. In addition, MSCs have a chemoattractive and mitogenic effect on keratinocytes, endothelial progenitor cells, and endothelial cells [59]. MSCs promote angiogenesis and vascularization of the wound bed, which is necessary for the sustenance of the newly formed granulation tissue and survival of keratinocytes.

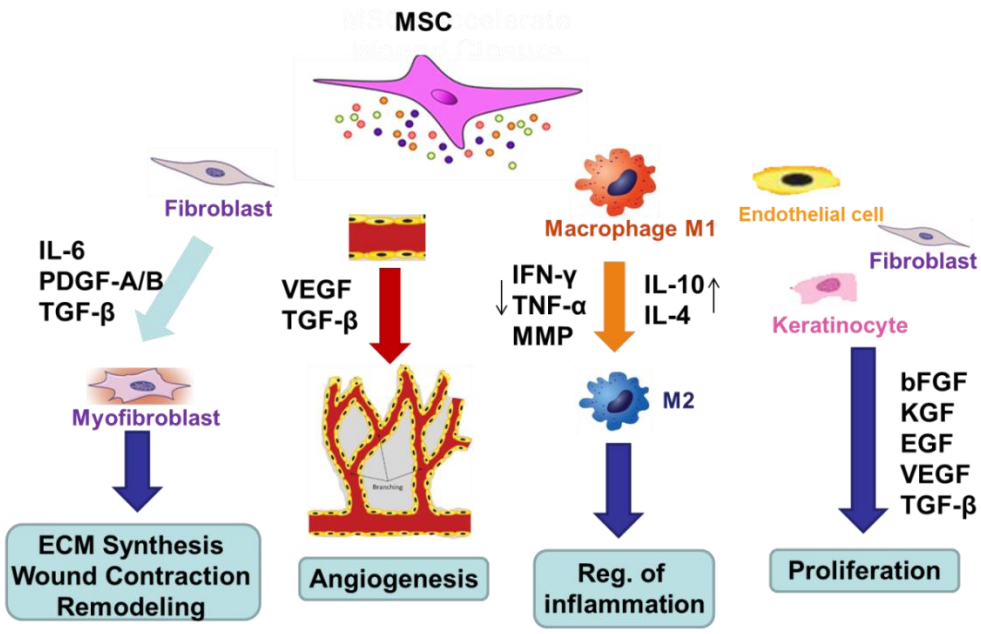

Fig. 2.6: MSC factors and their role in wound healing.

2.3.3.3 Insulin Producing Cell (IPC) Therapies

With the efficacy of insulin as a wound healing agent and the successful use of insulin producing cells (IPCs) as a cell therapy in diabetes, the logical next step would be to explore IPCs in wound

healing. However, with the exception of the work presented in subsequent chapters, no other groups have explored IPC therapies for wound healing. Nevertheless, many of the challenges delivering these cells remain the same, whether for wound healing or blood glucose regulation.

2.3.3.3.1 Acellular Strategies to Improve Islet Survival and Function

The use of islets for transplantation and regenerative medicine faces significant obstacles to achieve optimum therapeutic efficacy. The primary reasons for this include apoptosis due to hypoxic stress and decreased beta cell function. Islets are delicate cells to culture *in vitro* with approximately 60 % undergoing apoptosis following isolation [87]. Numerous strategies have been explored to improve islet culture conditions in order to promote survival and function. In a study conducted by Ling et al., fetal calf serum in combination with isobutylmethylxanthine increased cell survival to 78 %, partly due to the presence of low molecular weight constituents in the serum [88]. Peptide hormones such as glucagon, insulin-like growth factor-1, serum constituents such as ultroser, and metabolizable nutrients such as leucine and glutamine also promote beta cell survival for at least 9 days when added to culture media [88]. Achieving the optimum functional efficiency of islet transplantation requires a minimum number of days of islet culture *in vitro*. However, this results in a loss of viability and morphology of a substantial number of islets, resulting in a non-functional islet mass. Woods et al. investigated the potential of small intestinal submucosa for improving islet function *in vitro* [89]. They cultured human islets on membrane inserts coated with porcine-derived small intestinal submucosa and demonstrated that islets cultured employing this technique exhibited higher secretion indexes and improved morphology [89].

Rutzky et al. examined the effect of microgravity on islet culture [90]. The group demonstrated that culturing islets in modeled microgravity bioreactors improved pancreatic islet function and reduced immunogenicity, thereby promoting long term survival to achieve normoglycemia in diabetic allogenic recipients. They also reported that fewer islets were required to achieve euglycemia or normal blood glucose when cultured in microgravity prior to transplantation.

Ultrastructural analysis revealed a higher number of high-density hormone granules, development of multiple channels, and a decrease in tight junctional complexes, possibly for oxygen and nutrient transport or angiogenesis [90]. Murray et al. demonstrated that epithelial cells derived from the pancreas sustain islet function in rotational cultures [91].

In another attempt to maintain post transplantation pancreatic islet function, Miki et al. developed a pre-transplantation co-culture system with transduced human pancreatic islet-derived fibroblasts. The transduced islet-derived fibroblasts expressed α-smooth muscle actin, bFGF and type 1 collagen. Mouse, rat, and pig islets co-cultured with these transduced fibroblasts maintained their morphology, viability, and glucose responsive insulin secretion [92]. When transplanting islets, their morphology is critical. It has been shown that small islet aggregates perform better than large aggregates because of the efficient diffusion of oxygen and nutrients to the avascular islets, thus enhancing survival. Likewise, intra-islet architecture and interaction is required for normal insulin secretory function and responses to glucose in the environment.

2.3.3.3.2 MSC Co-Culture Strategies to Improve Islet Survival and Function

Soluble trophic factors such as vascular endothelial growth factor, hepatocyte growth factor, MMP-2, MMP-9, IL-6, and IL-10 have also been shown to improve islet survival and function [93-95]. Along these lines, Racham et al. demonstrated the effect of MSCs on islets in direct and indirect co-culture configurations [96]. Islet culture prior to transplantation is detrimental to survival of β-cells and produces inferior transplantation outcomes compared to fresh islet transplants. Racham et al. observed that the insulin content of co-cultured islets with MSCs in direct contact was similar to that of fresh islets and had a higher islet mass and number of insulin-positive β-cells as well as superior islet function *in vivo* compared to islet-alone cultures. MSCs have also been shown to promote intra-islet endothelial cell survival and engraftment of islet transplantation grafts [97-99]. However, pretransplantation culture of islets that had been in direct contact with MSCs demonstrated low endothelial cell and vascular density in grafts, which may

indicate that MSCs are also required at the graft site in order to promote graft revascularization [96].

MSCs contribute to maintenance of islet survival and preservation of glucose-induced insulin secretion by providing a suitable microenvironment that promotes islet longevity and function. MSCs regulate inflammatory cytokine production, specifically decreasing MCP-1 and TNF- α, and increase tissue inhibitor of metalloproteinases-1 (TIMP-1) and VEGF levels [100]. Islets cultured *in vitro* lose their structural integrity while in co-cultures where MSCs are directly in contact with islets, MSCs prevent islet fragmentation and maintain islet morphology by physically surrounding islets. In co-cultures where islets are separated from MSCs by a physical compartment such as a Transwell® system, islet morphology is preserved possibly through MSC-secreted soluble factors; however, the preservation is for a shorter duration, and islets begin to fragment and undergo apoptosis later on in culture.

Loss of a supportive microenvironment and damage to islets during the isolation procedures decrease islet longevity and function. Bone marrow (BM) or bone marrow cells (rich in MSCs) have been utilized to provide a favorable microenvironment and exploit their regenerative and reparative properties. Luo et al. reported preservation of islet morphology, insulin release and formation a pancreatic-like three dimensional tissue in 190 days of bone marrow cell and islet co-culture. The group also reported that beneficial effects on islet growth, longevity, and function were only achieved with bone marrow co-cultures, which provided a supportive milieu, and not with other cell sources including whole umbilical cord blood cells, mobilized peripheral blood cells, and isolated mobilized peripheral CD 34+ cells [101]. Luo et al. also demonstrated the interaction between BM cells and islets and reported that PKH26-marked BM cells migrate towards islets, the two cell types merge together and form an integrated tissue, while in the absence of BM cells, as culture proceeds, islets lose structure and begin to form monolayers [102]. Sorti et al. proposed that the possible mechanism of BM cells MSCs migration towards islets might be due to MSC cell surface markers CXCL12 and CX3CL1 [103]. MSCs are known to

migrate to sites in need of repair; it has been shown that MSCs are able to do so by secreting matrix-metalloproteases to degrade the extracellular matrix and promote migration of endothelial progenitor cells [104].

The same group also reported that a three week preculture of human islets with bone marrow improved islet viability, increased size, promoted vascularization, and achieved euglycemia in diabetic animals; the authors were able to detect human insulin in these animals. They demonstrated that achieving euglycemia in the animals was dependent on the transplants and removal of the islets on day 126 resulted in hyperglycemia [102]. Other studies have also reported that bone marrow co-culture reduces IL1β-mediated glucotoxicity of islets by reducing the release of the proinflammatory cytokine from resident islet macrophages. IL1β inhibits β-cell function and promotes FAS upregulation by activation NFkB to induce islet apoptosis and DNA fragmentation. IL1β also abolishes glucose-stimulated insulin release while IL-1Ra protects against glucose-induced β cell apoptosis and restores glucose stimulation of islets [105]. In addition to IL1β, paracrine factors such as HGF, IL-6, and TGF-β secreted from MSCs also protect from hypoxia and prevent apoptosis in islets.

Another study showed that MSCs display immunomodulatory functions. In this study, non-obese diabetic (NOD) or human type 1 diabetes mice were co-injected with MSCs and diabetogenic T cells. MSCs prevented beta-cell destruction and development of diabetes mellitus by reducing the capacity of diabetogenic T cells to infiltrate pancreatic islets and inducing regulatory T cells [106]. Similar to primary islets, maintenance of an unlimited *in vitro* replication potential and insulin secretion potential in insulinoma cell lines remains a challenge. Gartner et al. reported that long term persistence of *in vitro* insulinoma cell proliferation and the capacity to synthesize and secrete insulin depends on co-cultured fibroblasts and presence of trophic factors in culture media derived from other cell types [86].

2.3.3.3.3 Role of TGF-β in Islet Survival

TGF-β signaling plays a central role in islet biology where it is involved in immune modulation, differentiation, development, regulation of proliferation and apoptosis, glucose metabolism and regeneration of β-cells [107, 108]. Both TGF-β1 and EGF stimulate ERK 1/2 and PI3k in β-cells. TGF-β1 increases insulin release [109, 110] and proliferation of β-cells [109], dependent on TFG-β1 dose [109] and glucose concentration [109, 110]. TGF-β1 retains the structural integrity of islets in culture, maintains islet cell viability and prevents inflammatory-cytokines triggered apoptosis such as that in the presence of interferon (IFN)-γ and IL1β. The anti-apoptotic effect of TGF-β1 has also been confirmed in mouse insulinoma cell lines where TGF-β1 inhibited cleavage of caspase 3, 8 and 9 [107]. Islets isolated from transgenic TGF-β1 mice with high TGF-β1 mRNA expression and high TGF-β1 levels in the serum and in the secretions from islets showed bigger islets with enhanced insulin-positive β-cells and superior function even following cytokine assault [107]. Alternatively, transgenic mice lacking TGF-β signaling (dominant-negative TGF-β RII transgenic mice) exhibited significant increases in IL-1β, IL-2, TNF-α, and IFN−γ inflammatory cytokines, while only slight increases in anti-inflammatory cytokines IL-4 and IL-10 were observed compared to wild-type mice [111]. TGF-β is also an important regulator of MMPs and TIMPs.

2.4 SUMMARY

Repair of injured skin is vital for human survival and requires a coordinated response from hematopoietic cells, immune cells and resident cells of the skin. Studies, some of which were reported in this chapter, have improved our understanding of cutaneous wound healing and have guided us towards targeted therapeutic approaches to enhance repair. Despite the number of treatment modalities currently available, chronic wounds fail to heal in a timely manner. It is well established that growth factors influence the wound healing process by acting on the local wound environment and may serve as catalysts to improve healing in chronic wounds. However, TGF-β,

bFGF, KGF-2 (repifermin), GMCSF (leucomax), and EGF have not demonstrated convincing results in human trials, with the exception of PDGF (becaplermin). Becaplermin is FDA-approved for treatment of diabetic ulcers and improves healing in clinical trials; however, FDA placed a cancer risk warning on becaplermin in 2008, highlighting a potential drawback of direct growth factor-based therapeutics in wound healing. The use of a single growth factor has shown limited clinical efficacy because a single growth factor cannot augment the complex wound healing process. Like single growth factor delivery, treatments involving grafting a single cell type are insufficient and aid in either reepithelization with the use of keratinocytes or wound contraction when fibroblasts are used. Intuitively, MSC therapies provide a plausible solution as MSCs are a source of a multitude of growth factors that potentiate the entire wound healing process. Although clinical translation of MSC-based wound therapy is still in the early stages, the potential use of these cells holds great promise. In addition to the drawbacks of single growth factor and single cell transplantation therapies, as previously reviewed in this chapter, a major challenge in growth factor therapeutics and cell therapies is the protease-rich chronic wound environment onto which the growth factors or cells are administered. These proteases minimize the therapeutic benefit of these strategies as growth factors undergo rapid breakdown and clearance in this hostile wound environment, while cell therapies suffer from engraftment failure, loss of cell viability and/or morphology and fail to act physiologically. Cell entrapment in polymers such as alginate, fibrin and collagen have been explored for wound healing applications; however, these polymers are themselves immunogenic [203, 204], degrade in the proteolytic wound environment [40], allow entry of the harmful proteases [131, 132], or risk disease transmission [123, 124]. The protease-rich and chronic inflammatory wound environment can be circumvented by the application of insulin [212], a peptide hormone that regulates wound inflammation and decreases protease production by neutrophils. The wound healing mechanism of insulin is well known and has been traditionally delivered to cutaneous wounds as a topical ointment, which requires reapplication. Topical insulin administration precludes the use of cells

and insulin in a single therapy. In this thesis, the benefits of insulin were exploited and the need for reapplication was circumvented by using IPCs. PEGDA has demonstrated excellent compatibility for IPC encapsulation for diabetic applications and has shown success in human trials [144], while IPC and MSC co-culture has benefits to IPC performance. This knowledge has paved the way towards developing a cell therapy approach for wound healing whereby IPCs and MSCs are encapsulated in non-degradable PEDGA hydrogels. The hydrogels localize the cell secretome at the wound site, insulin and MSC factors execute their roles in promoting wound healing and the cells benefit from one another by inducing factor secretion and preserving cell viability. This thesis addresses some limitations of existing studies while exploiting their successes.

2.5 REFERENCES

1. Jeannie Khavkin and David A.F. Ellis. Aging Skin: Histology, Physiology, and Pathology. Facial Plastic Surgery Clinics of North America, 2011-05-01, Volume 19, Issue 2, Pages 229-234.
2. J. A. G. Rhodin, Histology: A Text and Atlas, Oxford University Press, New York, NY, USA, 1974.
3. Hill, M.A. 2017 Embryology Foundations - Histology Epithelia and Skin. Retrieved February 20, 2017, from https://embryology.med.unsw.edu.au/embryology/index.php/Foundations_-_Histology_Epithelia_and_Skin.
4. Bennet R.G.: Anatomy and physiology of the skin. In Papel I.D. (eds): Facial plastic reconstructive surgery, 2nd edition. New York: Thieme, 2002. pp. 3-14.
5. Madison K C. Barrier function of the skin: ‘‘la raison d’etre’’ of the epidermis.J Invest Dermatol 2003: 121: 231–242.
6. McGrath J.A., Eady R.A., and Pope F.M.: Anatomy and organization of human skin. In Burns T., Breathnach S., and Cox N. (eds): Rook’s textbook of dermatology, 7th edition. Malden (MA): Blackwell Publishing, 2004. pp. 1-53.
7. R. E. Boissy, “The melanocyte: its structure, function, and subpopulations in skin, eyes, and hair,” Dermatologic Clinics, vol. 6, no. 2, pp. 161–173, 1988.
8. Winkelman R.K.: The Merkel cell system and a comparison between it and the neurosecretory or APUD cell system. J Invest Dermatol 1977; 69: pp. 41-46.
9. Kanitakis J.: Anatomy, histology and immunohistochemistry of normal human skin. Eur J Dermatol 2002; 12: pp. 390-401.
10. Zouboulis C.C.: Acne and sebaceous gland function. Clin Dermatol 2004; 22: pp. 360-366.
11. Enoch S, Leaper DJ. Basic science of wound Healing’, SURGERY 23:2, , 1 February 2005, Pages 37-42.
12. Stadelmann WK, Digenis AG, Tobin GR. Physiology And Healing Dynamics Of Chronic Cutaneous Wounds. Am J Surg 176 (2a) August 24, 1998.

13. Li J, Chen J, Kirsner R. Pathophysiology of acute wound healing. Clin Dermatol. 2007 Jan-Feb;25(1):9-18.
14. Leibovich, S.J., and D.M. Wiseman. 1988. Macrophages, wound repair, and angiogenesis. Prog. Clin. Biol. Res. 266:131–145.
15. Porras-Reyes, B.H., H.C. Blair, J.J. Jeffrey, and T.A. Mustoe. 1991. Collagenase production at the border of granulation tissue in a healing wound: macrophage and mesenchymal collagenase production in vivo. Connect. Tissue Res. 27:63–71.
16. Fukasawa, M., J.D. Campeau, D.L. Yanagihara, K.E. Rodgers, and G.S. DiZerega. 1989. Mitogenic and protein synthetic activity of tissue repair cells: control by the postsurgical macrophage. J. Invest. Surg. 2:169–180.
17. Clark, R.A., R.D. Stone, D.Y.K. Leung, I. Silver, D.D. Hohn, and T.K. Hunt. 1976. Role of macrophages in wound healing. Surg. Forum. 27:16–18.
18. Polverini P.J., R.S. Cotran, M.A. Gimbrone, and E.R. Unanue. 1977. Activated macrophages induce vascular proliferation. Nature. 269:804–806.
19. Kovacs, E.J., and L.A. DiPietro. 1994. Cytokines and fibrous tissue production. FASEB J. 8:854–861.
20. Hunt TK. The physiology of wound healing. Ann Emerg Med 1988;17:1265–1273.
21. Saarialho-Kere UK, Kovacs SO, et al. Cell-matrix interactions modulate interstitial collagenase expression by human keratinocytes actively involved in wound healing. J Clin Invest 1993;92:2858–2866.
22. Rilla K, Lammi MJ, Sironen R, et al. Changed lamellipodial extension, adhesion plaques and migration in epidermal keratinocytes containing constitutively expressed sense and antisense hyaluronan synthase 2 (Has2) genes. J Cell Sci 2002;115:3633–3643.
23. Lampiaho, K., and Kulonen, E., 'Metabolic phases during the development of granulation tissue', Biochem. J. 105: 333,1967.
24. Schröder JM. Cytokine networks in the skin. J Invest Dermatol. 1995 Jul; 105(1 Suppl):20S-24S.
25. Leibovich SJ, Ross R. The role of the macrophage in wound repair. A study with hydrocortisone and antimacrophage serum. Am J Pathol. 1975 Jan; 78(1):71-100.
26. Lepisto J, Peltonen J, Vaha-Kreula M, et al. Selective modulation of collagen gene expression by different isoforms of platelet-derived growth factor in experimental wound healing. Cell Tissue Res 1996; 286: 449–455.
27. Eming SA, Yarmush ML, Krueger GG, et al. Regulation of the spatial organization of mesenchymal connective tissue: effects of cell-associated versus released isoforms of platelet-derived growth factor. Am J Pathol 1999; 154:281–289.
28. Rubbia-Brandt L, Sappino A, Gabbiani G. Locally applied GM-CSF induces the accumulation of alpha-smooth muscle actin containing myofibroblasts. Virchows Arch B Cell Pathol Incl Mol Pathol. 1991;60:73–82.
29. Yomen A, Cakir B, Culer S, Azal O, Corakci A. Effects of granulocyte colony stimulating factor in the treatment of diabetic foot infection. J Invest Dermatol. 1996;107:404–11.
30. Smith C, Allen M, Groves R, Barker J. Effect of granulocyte macrophage-colony stimulating factor on Langerhans cells in normal and healthy atopic subjects. Br J Dermatol. 1998;139:239–46.
31. Mann A, Breuhahan K, Schirmacher P, Blessing M. Keratinocyte-derived granulocyte-macrophage colony stimulating factor accelerates wound healing: stimulation of keratinocyte proliferation, granulation tissue formation and vascularization. J Invest Dermatol. 2001;117:1382–90.
32. Kaplan G, Walsh G, Guido L, Meyn R, Abalos R. Novel responses of human skin to intradermal recombinant granulocyte/macrophage-colony-stimulating factor: Langerhans cell recruitment, keratinocyte growth, and enhanced wound healing. J Exp Med. 1992;175:1717–28.

33. Schriber J, Negrin R, Chao N, Long G, Horning S, Blume K. The efficacy of granulocyte colony-stimulating factor following autologous bone marrow transplantation for non-Hodgkin's lymphoma with monoclonal antibody purged bone marrow. Leukemia. 1993;7:1491–95.
34. Fanin R, Baccarani M. Granulocyte-macrophage colony stimulating factor in acute non-lymphocytic leukemia. J Intern Med. 1994;236:487–93.
35. Carral A, de la Rubia J, Martin G, Martinex J, Sanz G, Jarque I. Factors influencing hematopoietic recovery after antilogous blood stem cell transplantation in patients with acute myeloblastic leukemia and with non-myeloid malignancies. Bone Marrow Transpl. 2002;29(10):825–32.
36. Visani G, Tosi P, Gamberi B, Cenacchi A, Mazzanti P, Stabilini C. Accelerated hemopoietic recovery after chemotherapy and autologous bone marrow transplantation in hematological malignancies using recombinant GM-CSF; preliminary results obtained in 14 cases. Hematologic. 1990;75:551–54.
37. Gorin N, Coieffier B, Haat M, Fouillard L, Kuentz M, Flesch M. Recombinant human granulocyte-macrophage colony stimulating factor after high dose chemotherapy and autologous bone marrow transplantation with unpurged and purged marrow in non-Hodgkin's lymphoma: A double blind placebo controlled trial. Blood. 1992;80:1149–57.
38. Jorgensen L, Argren M, Madsen S, Kallehave F, Vossoughi F, Rasmussen A. dose dependent impairment of collagen deposition of topical granulocyte macrophage colony stimulating factor in human experimental wounds. Ann Surg. 2002;236:684–92.
39. Galeano M, Altavilla D, Cucinotta D, Russo GT, Calò M, Bitto A, Marini H, Marini R, Adamo EB, Seminara P, Minutoli L, Torre V, Squadrito F. Recombinant human erythropoietin stimulates angiogenesis and wound healing in the genetically diabetic mouse. Diabetes. 2004 Sep;53(9):2509-17.
40. Sabine A. Eming, Thomas Krieg, Jeffrey M Davidson. Gene Therapy and Wound Healing. Clin Dermatol. 2007; 25(1): 79–92. doi: 10.1016/j.clindermatol.2006.09.011.
41. Shah JM, Omar E, Pai DR, Sood S. Cellular events and biomarkers of wound healing. Indian J Plast Surg. 2012 May;45(2):220-8. doi: 10.4103/0970-0358.101282.
42. S. Guo and L.A. DiPietro, 'Factors Affecting Wound Healing', J Dent Res. 2010 March; 89(3): 219–229.
43. Barrientos S, Brem H, Stojadinovic O, Tomic-Canic M. Clinical application of growth factors and cytokines in wound healing. Wound Repair Regen. 2014 Sep-Oct;22(5):569-78. doi: 10.1111/wrr.12205.
44. Gope R. The effect of epidermal growth factor & platelet-derived growth factors on wound healing process. Indian J Med Res. 2002 Nov; 116():201-6.
45. Rees RS, Robson MC, Smiell JM, Perry BH. Becaplermin gel in the treatment of pressure ulcers: a phase II randomized, double-blind, placebo-controlled study. Wound Repair Regen. 1999 May-Jun; 7(3):141-7.
46. Steed DL. Clinical evaluation of recombinant human platelet-derived growth factor for the treatment of lower extremity diabetic ulcers. Diabetic Ulcer Study Group. J Vasc Surg. 1995 Jan; 21(1):71-8; discussion 79-81.
47. Ono I, Akasaka Y, Kikuchi R, Sakemoto A, Kamiya T, Yamashita T, Jimbow K. Basic fibroblast growth factor reduces scar formation in acute incisional wounds. Wound Repair Regen. 2007 Sep-Oct; 15(5):617-23.
48. El Saghir NS, Bizri AR, Shabb NS, Husami TW, Salem Z, Shamseddine AI. Pressure ulcer accelerated healing with local injections of granulocyte macrophage-colony stimulating factor. J Infect. 1997 Sep; 35(2):179-82.
49. Da Costa RM, Ribeiro Jesus FM, Aniceto C, Mendes M. Randomized, double-blind, placebo-controlled, dose- ranging study of granulocyte-macrophage colony stimulating factor in patients with chronic venous leg ulcers. Wound Repair Regen. 1999 Jan-Feb; 7(1):17-25.

50. Jaschke E, Zabernigg A, Gattringer C. Recombinant human granulocyte-macrophage colony-stimulating factor applied locally in low doses enhances healing and prevents recurrence of chronic venous ulcers. Int J Dermatol. 1999 May; 38(5):380-6.
51. Cianfarani F, Tommasi R, Failla CM, Viviano MT, Annessi G, Papi M, Zambruno G, Odorisio T. Granulocyte/macrophage colony-stimulating factor treatment of human chronic ulcers promotes angiogenesis associated with de novo vascular endothelial growth factor transcription in the ulcer bed. Br J Dermatol. 2006 Jan; 154(1):34-41.
52. Robson MC, Hill DP, Smith PD, Wang X, Meyer-Siegler K, Ko F, VandeBerg JS, Payne WG, Ochs D, Robson LE. Sequential cytokine therapy for pressure ulcers: clinical and mechanistic response. Ann Surg. 2000 Apr; 231(4):600-11.
53. Gough A, Clapperton M, Rolando N, Foster AV, Philpott-Howard J, Edmonds ME. Randomised placebo-controlled trial of granulocyte-colony stimulating factor in diabetic foot infection. Lancet. 1997 Sep 20; 350(9081):855-9.
54. West NJ. Systemic antimicrobial treatment of foot infections in diabetic patients. Am J Health Syst Pharm. 1995 Jun 1; 52(11):1199-207; quiz 1239-40.
55. Liu Y, Dulchavsky DS, Gao X, Kwon D, Chopp M, Dulchavsky S, Gautam SC. Wound repair by bone marrow stromal cells through growth factor production. J Surg Res. 2006; 136(2): 336-41.
56. Badiavas EV, Abedi M, Butmarc J, Falanga V, Quesenberry P. Participation of bone marrow derived cells in cutaneous wound healing. J Cell Physiol. 2003; 196(2):245-50.
57. Badiavas EV, Falanga V. Treatment of chronic wounds with bone marrow-derived cells. Arch Dermatol. 2003; 139(4): 510-6.
58. Yamaguchi Y, Kubo T, Murakami T, Takahashi M, Hakamata Y, Kobayashi E, Yoshida S, Hosokawa K, Yoshikawa K, Itami S. Bone marrow cells differentiate into wound myofibroblasts and accelerate the healing of wounds with exposed bones when combined with an occlusive dressing. Br J Dermatol. 2005; 152(4): 616-22.
59. Liwen Chen, Edward E. Tredget, Philip Y. G. Wu, and Yaojiong Wu. Paracrine Factors of Mesenchymal Stem Cells Recruit Macrophages and Endothelial Lineage Cells and Enhance Wound Healing. PLoS ONE. 2008; 3(4): e1886.
60. Kinnaird T, Stabile E, Burnett MS, Shou M, Lee CW, et al. (2004) Local delivery of marrow-derived stromal cells augments collateral perfusion through paracrine mechanisms. Circulation 109: 1543–1549.
61. Singer AJ, Clark RA (1999) Cutaneous wound healing. N.Engl.J Med. 341: 738–746.
62. Lee J, Pilch PF. The insulin receptor: structure, function, and signaling. Am J Physiol. 1994 Feb;266(2 Pt 1):C319-34.
63. Hermann C1, Assmus B, Urbich C, Zeiher AM, Dimmeler S. Insulin-mediated stimulation of protein kinase Akt: A potent survival signaling cascade for endothelial cells. Arterioscler Thromb Vasc Biol. 2000 Feb;20(2):402-9.
64. Repertinger SK1, Campagnaro E, Fuhrman J, El-Abaseri T, Yuspa SH, Hansen LA. EGFR enhances early healing after cutaneous incisional wounding. J Invest Dermatol. 2004 Nov;123(5):982-9.
65. Lyu J, Lee KS, Joo CK. Transactivation of EGFR mediates insulin-stimulated ERK1/2 activation and enhanced cell migration in human corneal epithelial cells. Mol Vis. 2006 Nov 16;12:1403-10.
66. Taniguchi CM1, Emanuelli B, Kahn CR. Critical nodes in signalling pathways: insights into insulin action. Nat Rev Mol Cell Biol. 2006 Feb;7(2):85-96.
67. Thalhimer W, Insulin Treatment Of Postoperative (Nondiabetic) Acidosis. JAMA 81(5) 1923, 383-385.
68. Foster NB, Diabetic Coma. JAMA 84 (10) 1925, 719-722.
69. Rabinowitch I M. The Influence of Infection upon the Reaction of the Diabetic to Insulin Treatment. Canad. M. A. J., 26, 55I, 1932.

70. Rabinowitch, I. M. Simultaneous Respiratory Exchange and Blood Sugar Time Curves. Arch. Surg., 26, 696, I933.
71. Gurd FB, Postoperative Use of Insulin In The Nondiabetic, Ann Surg. 1937 Oct; 106(4): 761–769.
72. Goodson WH, Hunt TK. Wound-Healing In Experimental Diabetes-Mellitus - Importance Of Early Insulin Therapy, Surgical Forum. 29 (1978) 95-98.
73. Chen X1, Liu Y, Zhang X. Topical insulin application improves healing by regulating the wound inflammatory response. Wound Repair Regen. 2012 May-Jun;20(3):425-34. doi: 10.1111/j.1524-475X.2012.00792.x.
74. Rosenthal SP. Acceleration of primary wound healing by insulin. Arch Surg. 1968;96:53–55.
75. Shanley LJ1, McCaig CD, Forrester JV, Zhao M. Insulin, not leptin, promotes in vitro cell migration to heal monolayer wounds in human corneal epithelium. Invest Ophthalmol Vis Sci. 2004 Apr;45(4):1088-94.
76. Stuck, W., ' Effect of Insulin on the Healing of Experimental Fractures in the Rabbit', J. Bone Joint Surg. 14:109, 1932
77. E.Von Haam And L. Cappel 'Effect Of Hormones Upon Cells Grown Invitro 11.The Effect Of The Hormones From The Thyroid, Pancreas,And Adrenal Gland' , Am. J. Cancer 1940;39:354-359.
78. Hermann C1, Assmus B, Urbich C, Zeiher AM, Dimmeler S. Insulin-Mediated Stimulation of Protein Kinase Akt A Potent Survival Signaling Cascade for Endothelial Cells, Arterioscler Thromb Vasc Biol. 2000;20:402-409.
79. Liu Y, Petreaca M, Martins-Green M. Cell and molecular mechanisms of insulin-induced angiogenesis', J. Cell. Mol. Med. Vol 13, No 11-12, 2009 pp. 4492-4504
80. Joseph B. Insulin in the treatment of nondiabeticbed sores. Ann Surg. 1930; 92: 318–9.
81. Apikoglu-Rabus S1, Izzettin FV, Turan P, Ercan F. Effect of topical insulin on cutaneous wound healing in rats with or without acute diabetes', Clinical and Experimental Dermatology, 35, 180–185.
82. Villee, D. B., and Powers, M. L. Effect of glucose and insulin on collagen secretion by human skin fibroblasts in vitro. Nature 268(5616): 156, 1977.
83. Spanheimer RG1, Umpierrez GE, Stumpf V. Decreased collagen production in diabetic rats. Diabetes. 1988 Apr;37(4):371-6.
84. Madibally SV1, Solomon V, Mitchell RN, Van De Water L, Yarmush ML, Toner M. Influence of insulin therapy on burn wound healing in rats. J Surg Res. 2003 Feb;109(2):92-100.
85. Belfield WO, Golinsky S, Compton MD. The Use Of Insulin In Open-Wound Healing. Veterinary Medicine & Small Animal Clinician. 65 (1970) 455-460.
86. Gartner W, Koc F, Nabokikh A, Daneva T, Niederle B, Luger A, Wagner L. Long-term in vitro growth of human insulin-secreting insulinoma cells. Neuroendocrinology. 2006;83(2):123-30).
87. Noguchi H, Naziruddin B, Shimoda M, Fujita Y, Chujo D, Takita M, Peng H, Sugimoto K, Itoh T, Tamura Y, Olsen GS, Kobayashi N, Onaca N, Levy MF, Matsumoto S Transplant Proc. 2010 Jul-Aug; 42(6):2084-6).
88. Ling Z, Hannaert JC, Pipeleers D. Effect of nutrients, hormones and serum on survival of rat islet beta cells in culture. Diabetologia. 1994 Jan;37(1):15-21
89. Woods EJ1, Walsh CM, Sidner RA, Zieger MA, Lakey JR, Ricordi C, Critser JK. Improved in vitro function of islets using small intestinal submucosa. Transplant Proc. 2004 May;36(4):1175-7).
90. Rutzky LP, Bilinski S, Kloc M, Phan T, Zhang H, Katz SM, Stepkowski SM. Microgravity culture condition reduces immunogenicity and improves function of pancreatic islets1. Transplantation. 2002 Jul 15;74(1):13-21

91. Murray HE, Paget MB, Bailey CJ, Downing R. Sustained insulin secretory response in human islets co-cultured with pancreatic duct-derived epithelial cells within a rotational cell culture system. Diabetologia. 2009;52:477 – 85).
92. Miki A, Narushima M, Okitsu T, Takeno Y, Soto-Gutierrez A, Rivas-Carrillo JD, Navarro-Alvarez N, Chen Y, Tanaka K, Noguchi H, Matsumoto S, Kohara M,Lakey JR, Kobayashi E, Tanaka N, Kobayashi N. Maintenance of mouse, rat, and pig pancreatic islet functions by co-culture with human islet-derived fibroblasts. Cell Transplant. 2006;15(4):325-34).
93. K.S. Park, Y.S. Kim, J.H. Kim, B. Choi, S.H. Kim, A.H. Tan, et al. Trophic molecules derived from human mesenchymal stem cells enhance survival, function, and angiogenesis of isolated islets after transplantation. Transplantation, 89 (2010), pp. 509–517)
94. V. Sordi, R. Melzi, A. Mercalli, R. Formicola, C. Doglioni, F. Tiboni, et al. Mesenchymal cells appearing in pancreatic tissue culture are bone marrow-derived stem cells with the capacity to improve transplanted islet function Stem Cells, 28 (2010), pp. 140–151)
95. Human mesenchymal stem cells protect human islets from pro-inflammatory cytokines. Yeung TY1, Seeberger KL, Kin T, Adesida A, Jomha N, Shapiro AM, Korbutt GS. PLoS One. 2012; 7(5): e38189).
96. Cytotherapy. 2013 Apr;15(4):449-59. doi: 10.1016/j.jcyt.2012.11.008. Epub 2013 Jan 12. Pre-culturing islets with mesenchymal stromal cells using a direct contact configuration is beneficial for transplantation outcome in diabetic mice. Rackham CL1, Dhadda PK, Chagastelles PC, Simpson SJ, Dattani AA, Bowe JE, Jones PM, King AJ
97. T. Ito, S. Itakura, I. Todorov, J. Rawson, S. Asari, J. Shintaku, et al.Mesenchymal stem cell and islet co-transplantation promotes graft revascularization and function. Transplantation, 89 (2010), pp. 1438–1445)
98. D.M. Berman, M.A. Willman, D. Han, G. Kleiner, N.M. Kenyon, O. Cabrera, et al. Mesenchymal stem cells enhance allogeneic islet engraftment in nonhuman primates. diabetes, 59 (2010), pp. 2558–2568).
99. M. Figliuzzi, R. Cornolti, N. Perico, C. Rota, M. Morigi, G. Remuzzi, et al. Bone marrow–derived mesenchymal stem cells improve islet graft function in diabetic rats. Transplant Proc, 41 (2009), pp. 1797–1800).
100. Jung EJ, Kim SC, Wee YM, Kim YH, Choi MY, Jeong SH,Jiyeon L, Lim DG, Han DJ. Bone marrow-derived mesenchymal stromal cells support rat pancreatic islet survival and insulin secretory function in vitro. Cytotherapy; 13(1), 2011, 19-29.
101. Luo L, Badiavas E, Luo JZ, and Abby M. Allogeneic Bone Marrow Supports Human Islet β Cell Survival and Function Over Six Months. Biochem Biophys Res Commun. 2007 Oct 5; 361(4): 859–864).
102. Luo JZ, Xiong F, Al-Homsi AS, Ricordi C, Luo L. Allogeneic bone marrow co-cultured with human islets significantly improves islet survival and function in vivo. Transplantation. 2013 Mar 27;95(6):801-9. doi: 10.1097/TP.0b013e31828235c7).
103. Sordi V, Malosio ML, Marchesi F, Mercalli A, Melzi R, Giordano T, Belmonte N, Ferrari G, Leone BE, Bertuzzi F, Zerbini G, Allavena P, Bonifacio E, Piemonti L. Bone marrow mesenchymal stem cells express a restricted set of functionally active chemokine receptors capable of promoting migration to pancreatic islets. Blood. 2005 Jul 15; 106(2):419-27).
104. Johansson U, Rasmusson I, Niclou SP, Forslund N, Gustavsson L, Nilsson B, Korsgren O, Magnusson PU. Formation of composite endothelial cell-mesenchymal stem cell islets: a novel approach to promote islet revascularization. Diabetes. 2008 Sep; 57(9):2393-401).
105. Maedler K1, Sergeev P, Ris F, Oberholzer J, Joller-Jemelka HI, Spinas GA, Kaiser N, Halban PA, Donath MY. Glucose-induced beta cell production of IL-1beta contributes to glucotoxicity in human pancreatic islets. J Clin Invest. 2002 Sep;110(6):851-60).
106. Madec, A.M.; Mallone, R.; Afonso, G.; Abou Mrad, E.; Mesnier, A.; Eljaafari, A. & Thivolet, C. (2009). Mesenchymal stem cells protect NOD mice from diabetes by inducing regulatory T cells, Diabetologia, (Jul 2009), Vol.52, No.7, pp.1391-9).

107. Han B, Qi S, Hu B, Luo H, Wu J. TGF-beta i promotes islet beta-cell function and regeneration. J Immunol. 2011 May 15;186(10):5833-44. doi: 10.4049/jimmunol.1002303. Epub 2011 Apr 6.
108. Shalev A1, Pise-Masison CA, Radonovich M, Hoffmann SC, Hirshberg B, Brady JN, Harlan DM. Oligonucleotide microarray analysis of intact human pancreatic islets: identification of glucose-responsive genes and a highly regulated TGFbeta signaling pathway. Endocrinology. 2002 Sep;143(9):3695-8.
109. Xiao X, Wiersch J, El-Gohary Y, Guo P, Prasadan K, Paredes J, Welsh C, Shiota C, Gittes GK. TGFβ receptor signaling is essential for inflammation-induced but not β-cell workload-induced β-cell proliferation. Diabetes. 2013 Apr;62(4):1217-26. doi: 10.2337/db12-1428. Epub 2012 Dec 17.
110. Totsuka Y, Tabuchi M, Kojima I, Eto Y, Shibai H, Ogata E. Stimulation of insulin secretion by transforming growth factor-beta. Biochem Biophys Res Commun. 1989 Feb 15;158(3):1060-5.
111. Ki-Baik Hahm, Young-Hyuck Im, Cecile Lee,1 W. Tony Parks, Yung-Jue Bang, Jeffrey E. Green, and Seong-Jin Kim. Loss of TGF-β signaling contributes to autoimmune pancreatitis. J Clin Invest. 2000 Apr 15; 105(8): 1057–1065. doi: 10.1172/JCI8337.
112. Hunt, N.C. & Grover, L.M. Biotechnol Lett (2010) 32: 733. doi:10.1007/s10529-010-0221-0.
113. Augst AD, Kong HJ, Mooney DJ (2006) Alginate hydrogels as biomaterials. Macromol Biosci 6:623–633.
114. Chen RR, Mooney DJ. Polymeric growth factor delivery strategies for tissue engineering. Pharm Res. 2003 Aug;20(8):1103-12.
115. N. O. Dhoot, C. A. Tobias, I. Fischer, M. A. Wheatley, J. Biomed. Mater. Res. A 2004, 71, 191.
116. Mosahebi, M. Wiberg, G. Terenghi, Tissue Eng. 2003, 9, 209.
117. P. Prang, R. Muller, A. Eljaouhari, K. Heckmann, W. Kunz, T. Weber, C. Faber, M. Vroemen, U. Bogdahn, N. Weidner, Biomaterials 2006, Epub.
118. E. Ruoslahti, Ann. Rev. Cell Dev. Biol. 1996, 12, 697.
119. Hunt NC, Shelton RM, Grover LM. Reversible mitotic and metabolic inhibition following the encapsulation of fibroblasts in alginate hydrogels. Biomaterials. 2009 Nov;30(32):6435-43. doi: 10.1016/j.biomaterials.2009.08.014. Epub 2009 Aug 26.
120. J.A. Rowley, G. Madlambayan, D.J. Mooney. Alginate hydrogels as synthetic extracellular matrix materials. Biomaterials, 20 (1) (1999), pp. 45–53
121. A.M.F. Sun, M.F.A. Goosen, G. Oshea. Microencapsulated cells as hormone delivery systems. Crc Critical Reviews in Therapeutic Drug Carrier Systems, 4 (1) (1987), pp. 1–12.
122. Hunt NC, Shelton RM, Grover LM. An alginate hydrogel matrix for the localised delivery of a fibroblast/keratinocyte co-culture. Biotechnol. J. 2009, 4, 730–737
123. Eisenbud, D., Huang, N. F., Luke, S., Silberklang, M., Skinsubstitutes and wound healing: Current status and chal-lenges. Wounds Compend. Clin. Res. Pract. 2004, 16, 2–17.
124. MacNeil, S., Progress and opportunities for tissue engi-neered skin. Nature 2007, 445, 874–880.
125. Clark, R. A. F., Ghosh, K., Tonnesen, M. G., Tissue engineer-ing for cutaneous wounds. J. Invest. Dermatol. 2007, 127,1018–1029.
126. Welch, M. P., Odland, G. F., Clark, R. A. F., Temporal relation-ships of F-actin bundle formation, collagen and fibronectinmatrix assembly, and Fibronectin receptor expression towound contraction. J. Cell Biol. 1990, 110, 133–145.
127. Boateng, J. S., Matthews, K. H., Stevens, H. N. E., Eccleston, G. M. Wound healing dressings and drug delivery systems: A review. J. Pharm. Sci. 2008, 97, 2892–2923.
128. Liu H, Yin Y, Yao K. Construction of chitosan-gelatin-hyaluronic acid artificial skin in vitro. J Biomater Appl. 2007 Apr;21(4):413-30. Epub 2006 May 9.

129. Barminko, J., et al., Encapsulated mesenchymal stromal cells for in vivo transplantation. Biotechnol Bioeng, 2011. 108(11): p. 2747-58.
130. Falanga, V., et al., Autologous bone marrow-derived cultured mesenchymal stem cells delivered in a fibrin spray accelerate healing in murine and human cutaneous wounds. Tissue Eng, 2007. 13(6): p. 1299-312.
131. M.A. Otterlei, A. Sundan, G. Skjak-Braek, L. Ryan, O. Smidsrod, T. Espevik. Similar mechanisms of action of defined polysaccharides. lipopolysaccharides: characterization of binding and tumor necrosis factor alpha induction. Infect Immun, 61 (1993), pp. 1917–1925
132. Thomas A, Harding KG, Moore K. Alginates from wound dressings activate human macrophages to secrete tumour necrosis factor-alpha. Biomaterials. 2000 Sep;21(17):1797-802.
133. Seymour, J. Alginate Dressings in Surgery and Wound Management. Nurs. Times Oct 29–Nov 4 1997, 93 (44), 49–52. 9.
134. Piacquadio, D.; Nelson, D.B. Alginates. A "new" dressing alternative. J. Dermatol. Surg. Oncol. Nov 1992, 18 (11), 992–995.
135. O'Donoqhue, J.M.; O'Sullivan, S.T.; Beausang, E.S. Calcium Alginate Dressings Promote Healing of Split Skin Graft Donor Sites. Acta Chir. Plast. 1997, 39 (2), 53–55.
136. Disa, J.J.; Alizadeh, K.; Smith, J.W.; Hu, Q.; Cordeiro, P.G. Evaluation of a combined calcium sodium alginate and bio-occlusive membrane dressing in the management of split-thickness skin graft donor sites. Ann. Plast. Surg. Apr 2001, 46 (4), 405–408.
137. Brown LF, Lanir N, McDonagh J, Tognazzi K, Dvorak AM, Dvorak HF. Fibroblast migration in fibrin gel matrices. Am J Pathol. 1993 Jan;142(1):273-83.
138. Cox S, Cole M, Tawil B. Behavior of human dermal fibroblasts in three-dimensional fibrin clots: dependence on fibrinogen and thrombin concentration. Tissue Eng. 2004 May-Jun;10(5-6):942-54.
139. Meana A, Iglesias J, Del Rio M, Larcher F, Madrigal B, Fresno MF, Martin C, San Roman F, Tevar F. Large surface of cultured human epithelium obtained on a dermal matrix based on live fibroblast-containing fibrin gels. Burns. 1998 Nov;24(7):621-30.
140. Tuan TL, Song A, Chang S, Younai S, Nimni ME. In vitro fibroplasia: matrix contraction, cell growth, and collagen production of fibroblasts cultured in fibrin gels. Exp Cell Res. 1996 Feb 25;223(1):127-34.
141. Nazhat SN, Neel EA, Kidane A, Ahmed I, Hope C, Kershaw M, Lee PD, Stride E, Saffari N, Knowles JC, Brown RA. Controlled microchannelling in dense collagen scaffolds by soluble phosphate glass fibers. Biomacromolecules. 2007 Feb;8(2):543-51.
142. Boaateng JS, Matthews KH, Stevens HN, Eccleston GM. Wound healing dressings and drug delivery systems: a review. J Pharm Sci. 2008 Aug;97(8):2892-923.
143. Kepsutlu B, Nazli C, Bal T, Kizilel S. Design of bioartificial pancreas with functional micro/nano-based encapsulation of islets. Curr Pharm Biotechnol. 15(7), 590, 2014.
144. Schwartz S, Mulgrew P. A single-center phase I/II study of PEG-encapsulated islet allografts implanted in patients with type I diabetes (study NCT00260234). Available at: http://www.clinicaltrials.gov.
145. Cruise, G.M., Hegre, O.D., Lamberti, F.V., Hager, S.R., Hill, R., Scharp, D.S., and Hubbell, J.A. In vitro and in vivo performance of porcine islets encapsulated in interfacially photopolymerized poly(ethylene glycol) diacrylate membranes. Cell transplantation 8, 293, 1999.
146. Nicodemus, G. D., & Bryant, S. J. (2008). Cell encapsulation in biodegradable hydrogels for tissue engineering applications. Tissue Engineering Part B: Reviews, 14(2), 149-165.
147. Singh, A., & Elisseeff, J. (2010). Biomaterials for stem cell differentiation.Journal of Materials Chemistry, 20(40), 8832-8847.
148. Salinas, C. N., Cole, B. B., Kasko, A. M., & Anseth, K. S. (2007). Chondrogenic differentiation potential of human mesenchymal stem cells photoencapsulated within poly

(ethylene glycol)-arginine-glycine-aspartic acid-serine thiol-methacrylate mixedmode networks. Tissue engineering, 13(5), 1025-1034.
149. Nuttelman, C. R., Tripodi, M. C., & Anseth, K. S. (2005). Synthetic hydrogel niches that promote hMSC viability. Matrix biology, 24(3), 208-218.
150. Megan E. Smithmyer, Lisa A. Sawicki and April M. Kloxin. Hydrogel scaffolds as in vitro models to study fibroblast activation in wound healing and disease. Biomater. Sci., 2014, 2, 634-650
151. Chia HN, Vigen M, Kasko AM. Effect of substrate stiffness on pulmonary fibroblast activation by TGF-β. Acta Biomater. 2012 Jul;8(7):2602-11. doi: 10.1016/j.actbio.2012.03.027.
152. Wang, Huan; Haeger, Sarah M.; Kloxin, April M.; Leinwand, Leslie A.; Anseth, Kristi S. Redirecting valvular myofibroblasts into dormant fibroblasts through light-mediated reduction in substrate modulus. PLoS One (2012), 7(7), e39969.
153. Gould ST, Darling NJ, Anseth KS. Small peptide functionalized thiol-ene hydrogels as culture substrates for understanding valvular interstitial cell activation and de novo tissue deposition. Acta Biomater. 2012 Sep;8(9):3201-9. doi: 10.1016/j.actbio.2012.05.009.
154. Durst CA, Cuchiara MP, Mansfield EG, West JL, Grande-Allen KJ. Flexural characterization of cell encapsulated PEGDA hydrogels with applications for tissue engineered heart valves. Acta Biomater. 2011 Jun;7(6):2467-76. doi: 10.1016/j.actbio.2011.02.018.
155. Gobin AS, West JL. Effects of epidermal growth factor on fibroblast migration through biomimetic hydrogels. Biotechnol Prog. 2003 Nov-Dec;19(6):1781-5.
156. Sokic S, Papavasiliou G. FGF-1 and proteolytically mediated cleavage site presentation influence three-dimensional fibroblast invasion in biomimetic PEGDA hydrogels. Acta Biomater. 2012 Jul;8(6):2213-22. doi: 10.1016/j.actbio.2012.03.017.
157. Benton JA, Fairbanks BD, Anseth KS. Characterization of valvular interstitial cell function in three dimensional matrix metalloproteinase degradable PEG hydrogels. Biomaterials. 2009 Dec;30(34):6593-603. doi: 10.1016/j.biomaterials.2009.08.031.
158. Koh WG, Revzin A, Pishko MV. Poly(ethylene glycol) hydrogel microstructures encapsulating living cells. Langmuir. 2002 Apr 2;18(7):2459-62.
159. Borue X, Lee S, Grove J, Herzog EL, Harris R, Diflo T, Glusac E, Hyman K, Theise ND, Krause DS. Bone marrow-derived cells contribute to epithelial engraftment during wound healing. Am J Pathol. 2004; 165: 1767–1772.
160. Hatch HM, Zheng D, Jorgensen ML, Petersen BE. SDF-1alpha/CXCR4: a mechanism for hepatic oval cell activation and bone marrow stem cell recruitment to the injured liver of rats. Cloning Stem Cells. 2002; 4(4):339-51.
161. Wu, Y., Chen, L., Scott, P. G. and Tredget, E. E. (2007), Mesenchymal Stem Cells Enhance Wound Healing Through Differentiation and Angiogenesis. STEM CELLS, 25: 2648–2659. doi:10.1634/stemcells.2007-0226.
162. Yates CC, Whaley D, Wells A. Transplanted fibroblasts prevents dysfunctional repair in a murine CXCR3-deficient scarring model. Cell Transplant. 2012; 21(5):919-31.
163. Hi-Jin You and Seung-Kyu Han. Cell Therapy for Wound Healing. J Korean Med Sci. 2014 Mar; 29(3): 311–319.
164. el-Ghalbzouri A, Gibbs S, Lamme E, Van Blitterswijk CA, Ponec M. Effect of fibroblasts on epidermal regeneration. Br J Dermatol. 2002 Aug; 147(2):230-43.
165. You HJ, Han SK, Lee JW, Chang H. Treatment of diabetic foot ulcers using cultured allogeneic keratinocytes--a pilot study. Wound Repair Regen. 2012 Jul-Aug; 20(4):491-9.
166. Han SK, Choi KJ, Kim WK. Clinical application of fresh fibroblast allografts for the treatment of diabetic foot ulcers: a pilot study. Plast Reconstr Surg. 2004 Dec; 114(7):1783-9.
167. Han SK, Kim WK. Revisiting fresh fibroblast allograft as a treatment for diabetic foot ulcers. Plast Reconstr Surg. 2009;123:88e–89e.

168. Han SK, Kim HS, Kim WK. Efficacy and safety of fresh fibroblast allografts in the treatment of diabetic foot ulcers. Dermatol Surg. 2009;35:1342–1348.
169. Choi J, Minn KW, Chang H. The efficacy and safety of platelet-rich plasma and adipose-derived stem cells: an update. Arch Plast Surg. 2012 Nov; 39(6):585-92.
170. Shin HS, Oh HY. The Effect of Platelet-rich Plasma on Wounds of OLETF Rats Using Expression of Matrix Metalloproteinase-2 and -9 mRNA. Arch Plast Surg. 2012 Mar; 39(2):106-12.
171. Steenfos HH. 1994. Growth factors and wound healing Scand. J Plast Reconstr Surg 28:95–105.
172. Greenhalgh DG. 1996. The role of growth factors in wound healing. J Trauma Inj Infect Crit Care 41:159–167.
173. Mann A, Niekisch K, Schirmacher P, Blessing M. 2006. Granulocyte-macrophage colony-stimulating factor is essential for normal wound healing. J Investig Dermatol Symp Proc 11:87–92.
174. Pierce GF, Tarpley JE, Tseng J, Bready J, Kenney WC,Rudolph R, Robson M, Vanderberg J, Reid P.Detection of platelet-derived growth factor(PDGF)-AA in actively healing human woundstreated with recombinant PDGF-BB and absenceof PDGF in chronic nonhealing wounds. J ClinInvest 1995;96(3):1336—50.
175. Legrand EK. Preclinical promise of becaplermin (rh-PDGF-BB) in wound healing. Am J Surg 1998;176Suppl 2A:48S—54S.
176. Knighton DR, Ciresi KF, Fiegel VD, Austin LL, Butler EL. Classification and treatment of chronic non healing wounds. Ann Surg 1986;204(3): 322—3. 31
177. Robson MC, Phillips LG, Thompson A. A recombinant human platelet derived growth factor — BB in the treatment of chronic pressure ulcers. Ann Plast Surg 1992;29:193—201.
178. Steed DL. Clinical evaluation of recombinant platelet derived growth factor for the treatment of lower extremity diabetic ulcers. J Vasc Surg 1995;21:71—8.
179. Ziyadeh N, Fife D, Walker AM, Wilkinson GS, Seeger JD. A matched cohort study of the risk of cancer in users of becaplermin. Adv Skin Wound Care. 2011 Jan;24(1):31-9. doi: 10.1097/01.ASW.0000392922.30229.b3.
180. Barbolla-Escaboza JR, Maria-Aceves R, LopezHernandez MA, Collados-Larumbe MT. Recombinant human granulocyte-macrophagecolony stimulating factor as a treatment of chronic leg ulcers. Rev Invest Clin 1997;49(6):449—51.
181. Jaschke E, Zabernigg A, Gattringer C. Recombinant human granulocyte-macrophage-colony stimulating factor applied locally in low dose enhances healing and prevents recurrence of chronic venous ulcers. Int J Dermatol 1999;38(5):380—6.
182. Robson MC, Steed D, McPherson JM, Pratt BM. The use of transforming growth factor beta 2 in the treatment of chronic foot ulcers in diabetic patients. Abstract presented at the 3rd Joint Meeting of ETRS and Wound Healing Society; August 24—28 1999, Bordeaux.
183. Khan MN, Davies CG. Advances in the management of leg ulcers--the potential role of growth factors. Int Wound J. 2006 Jun;3(2):113-20.
184. McGee GS, Davidson JM, Buckley A, Sommer A, Woodward SC, Aquino AM, Barbour R, Demetriou AA. Recombinant basic fibroblast growth factor accelerates wound healing. J Surg Res 1988;45:145—53.
185. Hayward P, Hokanson J, Heggers J, Fiddes J, Klingbeil C, Goeger M, Robson M. Fibroblast growth factor reverses the bacterial retardation of wound contraction. Am J Surg 1992;163: 288—93.
186. Phillips LG, Abdullah KM, Geldner PD, Dobbins S, Ko F, Linares HA, Broemeling LD, Robson MC. Application of basic fibroblast growth factor may reverse diabetic wound healing impairment. Ann Plast Surg 1993;31:331—4.
187. Richard JL, Parer-Richard C, Daures JP, Clouet S, Vannereau D, Bringer J, Rodier M, Jacob C, Comte-Bardonnet M. Effect of topical fibroblast growth factor on the healing of chronic

diabetic neuropathic ulcer of the foot. A pilot, randomized, double-blind, placebo-controlled study. Diabetes Care 1995;18:64—9
188. King L, Norris D, Carter M, Herbert A, McAnaw M. Basic fibroblast growth factor in treatment of leg ulcers secondary to venous stasis and diabetes mellitus [abstract]. Wounds 1993;5:45.
189. Falanga V, Eaglstein WH, Bucalo B, Katz MH, Harris B, Carson P. Topical use of human recombinant epidermal growth factor in venous ulcers. J Dermatol Surg Oncol 1992;18:604—6.
190. Franklin JD, Lynch JB. Effects of topical applications of epidermal growth factor on wound healing. Plast Reconstr Surg 1979;64:766—70.
191. Brown GL, Nanney LB, Griffen J, Cramer AB, Yancey JM, Curtsinger LJ III,, Holtzin L, Schultz GS, Jurkiewicz MJ, Lynch JB. Enhancement of wound healing by topical treatment with epidermal growth factor. N Engl J Med 1989;321:76—9.
192. Robson MC, Phillips TJ, Falanga V, Odenheimer DJ, Parish LC, Jensen JL, Steed DL. Randomized trial of topically applied repifermin (recombinant human keratinocyte growth factor-2) to accelerate wound healing in venous ulcers. Wound Repair Regen 2001;9(5):347—52.
193. Sen, C.K., Gordillo, G.M., Roy, S., Kirsner, R., Lambert, L., Hunt, T.K., Gottrup, F., Gurtner, G.C., and Longaker, M.T. Human skin wounds: a major and snowballing threat to public health and the economy. Wound Repair Regen 17, 763, 2009.
194. Ganapathy Nalliappan, Venkataraman Siva Subramaniyan, Daniel Rajkumar, Aravind Ramraj Jayabalan, Kumarakrishnan Vilapakkam Bhikshewaran. Molecular biology of wound healing. Year : 2012 | Volume: 4 | Issue Number: 6 | Page: 334-337.
195. Leal, E. C., Carvalho, E., Tellechea, A., Kafanas, A., Tecilazich, F., Kearney, C., Veves, A. (2015). Substance P Promotes Wound Healing in Diabetes by Modulating Inflammation and Macrophage Phenotype. The American Journal of Pathology, 185(6), 1638–1648. http://doi.org/10.1016/j.ajpath.2015.02.011
196. American Diabetes Association. (2009). Diagnosis and Classification of Diabetes Mellitus . Diabetes Care, 32(Suppl 1), S62–S67. http://doi.org/10.2337/dc09-S062.
197. Greenway, S.E., Filler, L.E., and Greenway, F.L. Topical insulin in wound healing: a randomised, double-blind, placebo-controlled trial. J Wound Care 8, 526, 1999.
198. Madibally, S.V., Solomon, V., Mitchell, R.N., Van De Water, L., Yarmush, M.L., and Toner, M. Influence of insulin therapy on burn wound healing in rats. J Surg Res 109, 92, 2003.
199. Rezvani, O., Shabbak, E., Aslani, A., Bidar, R., Jafari, M., and Safarnezhad, S. A randomized, double-blind, placebo controlled trial to determine the effects of topical insulin on wound healing. Ostomy Wound Manage 55, 22, 2009.
200. Sen, C.K., Gordillo, G.M., Roy, S., Kirsner, R., Lambert, L., Hunt, T.K., Gottrup, F., Gurtner, G.C., and Longaker, M.T. Human skin wounds: a major and snowballing threat to public health and the economy. Wound Repair Regen 17, 763, 2009.
201. Procha´zka, V., Gumulec, J., Jaluvka, F., Salounova´, D., Jonszta, T., Czerny, D., Krajca, J., Urbanec, R., Klement, P., and Martinek, J. Cell therapy, a new standard in management of chronic critical limb ischemia and foot ulcer. Cell Transplant 19, 1413, 2010.
202. Lima MHM, Caricilli AM, de Abreu LL, Araújo EP, Pelegrinelli FF, Thirone ACP, Tsukumo DM, Pessoa AFM, dos Santos MF, de Moraes MA. Topical insulin accelerates wound healing in diabetes by enhancing the AKT and ERK pathways: a double-blind placebo-controlled clinical trial. PLoS One. 2012 7(5):e36974.
203. Gorka Orivea, Susan K. Tamb, José Luis Pedraza, Jean-Pierre Hallé. Biocompatibility of alginate – poly-L-lysine microcapsules for cell therapy. Biomaterials 27(20), 2006, Pages 3691–3700.

204. B.L. Strand, L. Ryan, P. In`t Veld, B. Kulseng, A.M. Rokstad, G. Skjåk-Bræk, et al. Poly L-lysine induces fibrosis on alginate microcapsuels via the induction of cytokines. Cell Transplant, 10 (2001), pp. 263–275.
205. Corinna Hermann, Birgit Assmus, Carmen Urbich, Andreas M. Zeiher and Stefanie Dimmeler. Insulin-Mediated Stimulation of Protein Kinase Akt. Arteriosclerosis, Thrombosis, and Vascular Biology. 2000;20:402-409.
206. Guo, S. (2014). Insulin Signaling, Resistance, and the Metabolic Syndrome: Insights from Mouse Models to Disease Mechanisms. The Journal of Endocrinology, 220(2), T1–T23. http://doi.org/10.1530/JOE-13-0327.
207. De Meyts P, Sajid W, Palsgaard J, et al. Insulin and IGF-I Receptor Structure and Binding Mechanism. In: Madame Curie Bioscience Database [Internet]. Austin (TX): Landes Bioscience; 2000-2013. Available from: https://www.ncbi.nlm.nih.gov/books/NBK6192/.
208. https://en.wikipedia.org/wiki/File:502_Layers_of_epidermis.jpg . Accessed on: 18 March 2017.
209. https://www.studyblue.com/notes/note/n/wound-healing/deck/8435474 . Accessed on: 19 March 2017.
210. https://commons.wikimedia.org/wiki/File:501_Structure_of_the_skin.jpg . Accessed on: 19 March 2017.
211. Reprinted from 'Trends in Molecular MEdicine, 18, Paul R. Hiebert, David J. Granville, Granzyme B in injury, inflammation, and repair', 732-741, 2012, with permission from Elsevier.
212. Abdollahi M, Ng TS, Rezaeizadeh A, Aamidor S, Twigg SM, Min D, McLennan SV. Insulin treatment prevents wounding associated changes in tissue and circulating neutrophil MMP-9 and NGAL in diabetic rats. PLoS One. 2017 Feb 9;12(2):e0170951. doi: 10.1371/journal.pone.0170951.
213. Lecube A, Pachón G, Petriz J, Hernández C, Simó R. Phagocytic Activity Is Impaired in Type 2 Diabetes Mellitus and Increases after Metabolic Improvement. Sesti G, ed. PLoS ONE. 2011;6(8):e23366.
214. Lachmandas E, Vrieling F, Wilson LG, et al. The Effect of Hyperglycaemia on In Vitro Cytokine Production and Macrophage Infection with Mycobacterium tuberculosis. Briken V, ed. PLoS ONE. 2015;10(2):e0117941. doi:10.1371/journal.pone.0117941.oi:10.1371/journal.pone.0023366.
215. https://www.fastbleep.com/medical-notes/surgery/8/278. Accessed on: 19 March 2017.

CHAPTER 3: ENCAPSULATION OF INSULIN-PRODUCING CELLS IN PEGDA MICROSPHERES

Note: Portions of this chapter have been published in: 'A. Aijaz et al., **Hydrogel microencapsulated insulin-secreting cells increase keratinocyte migration, epidermal thickness, collagen fiber density, and wound closure in a diabetic mouse model of wound healing.** Tissue Eng Part A. 2015 Nov;21(21-22):2723-32. doi: 10.1089/ten.TEA.2015.0069', and represent the original work of the candidate.

3.1 INTRODUCTION

The use of insulin for wound healing applications dates back to the 1920's. As described in the previous chapter, several *in vivo* and *in vitro* studies have demonstrated the beneficial effects of insulin on wound healing [1-4]. However, even with the reported benefits and acceleration of wound healing by insulin, one barrier to widespread use of topical insulin therapies is the lack of a delivery system that maintains a steady dose and does not require repeated exposure of the wound. Attempts have been made at sustained-release insulin delivery for wound healing applications in which crystalline insulin has been encapsulated within poly(lactic-co-glycolic acid) PLGA microspheres and embedded in alginate-PEG sponge dressing; however, the hydrolysis products of these polymers reduced bioactivity of the released insulin over time [6]. Though a reservoir of soluble insulin may seem to be a plausible solution, this may result in a potentially dangerous bolus release of insulin. Moreover, even reservoir systems would need frequent replenishing (every 2-3 days) since insulin contained in a reservoir loses effectiveness and potency over time. There have been applications which have successfully used cell therapies to achieve constant delivery of therapeutic products. IPCs encapsulated within a non-immunogenic barrier present a solution to overcome these limitations. Insulin secretory granules in IPCs serve as cellular factories where fresh insulin is produced and released for a therapeutic effect. PEGDA was chosen to encapsulate IPCs because it has previously shown success; in internal cell therapies

when cells were enclosed within PEGDA hydrogels that protected them from the host immune response, the viability and secretory characteristics of the encapsulated cells were prolonged [7-9]. In fact, pancreatic islet cells encapsulated within PEGDA injected into diabetic humans and animals have successfully returned them to normoglycemia without the tissue typing required when these cells are not encapsulated [7, 9].

In this chapter, insulinoma insulin-producing cells (RIN-m) or mouse anterior pituitary tumor cells that were transduced to produce insulin (AtT-20ins) were encapsulated within PEGDA hydrogel microspheres and characterized their viability and insulin secretion profiles. The bioactivity of their secreted insulin was assessed and the potential of the secreted insulin in promoting keratinocyte migration across *in vitro* scratches in monolayers was investigated. The present chapter focuses on *in vitro* assessment of these IPC-laden microspheres; following chapter describes their use for *in vivo* diabetic wound healing.

3.2 MATERIALS AND METHODS

3.2.1 Cell Culture

The constant insulin producing rat insulinoma beta cell line, RIN-m, and the glucose-stimulated insulin releasing mouse sarcoma line, GLUT-2 cDNA transfected AtT-20ins-(CGT6) cells, were purchased from American Type Culture Collection (ATCC, Manassas, VA) and propagated in RPMI-1640 medium (ATCC) or Dulbecco's modified Eagle's medium (Sigma, St. Louis, MO), respectively, supplemented with 10% fetal bovine serum (FBS; Sigma), 1% w/v penicillin-streptomycin (pen-strep; Sigma) in a humidified incubator at 37 °C/5% CO_2.

3.2.2 Microencapsulation

Cell-laden microspheres were formed as previously reported [10, 11]. Briefly, hydrogel precursor solution was formed by combining 0.1 g/mL 10 kDa PEGDA (10% w/v; Laysan Bio, Inc.) with (1.5% v/v) triethanolamine/HEPES-buffered saline (pH 7.4), 37 mM 1-vinyl-2-pyrrolidinone, 0.1

mM eosin Y, and RIN-m cells or AtT-20ins cells for a final concentration of 1.5×10^4 cells/μL. A hydrophobic photoinitiator solution containing 2,2-dimethoxy-2-phenyl acetophenone in 1-vinyl-2-pyrrolidinone (300 mg/mL) was combined in mineral oil (3 μL/mL; embryo tested, sterile filtered; Sigma). The cell-prepolymer suspension was added to the mineral oil solution, emulsified by vortexing for 4 seconds in ambient light, then for an additional 3 seconds under white light, then the vortex was stopped and the emulsion was exposed to white light for 20 seconds with a vortex pulse at 10 seconds. Crosslinked microspheres were isolated by addition of 1 mL complete media followed by centrifugation at 300 g for 5 minutes. The oil layer was removed by aspiration and pelleted microspheres were resuspended in media and placed in Transwells® (0.4 mm pore polycarbonate membrane Transwell® inserts; Corning, Inc., Lowell, MA) in a 12-well plate with 3 mL culture medium. Microencapsulated cells were maintained in a humidified incubator at 37 °C/5% CO_2. For glucose stimulation studies and cell migration studies, 3×10^6 IPCs were encapsulated and 1×10^6 IPCs were plated on 6-well tissue culture plates for comparisons. Since encapsulation efficiency was reproducibly 37%, 270 % more cells were encapsulated when comparing against monolayer cells to equalize cell numbers between microencapsulated cell groups and monolayer groups. Briefly, three 20 μl samples of microencapsulated cells from each group were placed in Transwells® in a 24-well plate with 1 mL of culture medium. Monolayer cells were trypsinized, counted with a hemocytometer and a serial dilution was used as a standard curve. CellTiter 96® AQueous One Solution Reagent (Promega Corporation, Madison, WI) at 200 μl was added into each well and plates were incubated for 3 hours in a humidified incubator at 37 °C/5% CO_2. The amount of soluble formazan produced by cellular reduction of the tetrazolium compound [3-(4,5-dimethylthiazol-2-yl)-5-(3-carboxymethoxyphenyl)-2-(4-sulfophenyl)-2H-tetrazolium, inner salt; MTS] was measured by reading the absorbance of the medium at 490 nm. Standard curves were used to calculate the number of live cells within microspheres, which in turn was used to determine the encapsulation efficiency.

3.2.3 Cell viability

Encapsulated cell viability was assessed on day 1, 3, 5, 7, 14, and 21 by incubating microsphere samples in media and 2 mM calcein acetoxymethyl ester and 4 mM ethidium homodimer (LIVE/DEAD Viability/Cytotoxicity Kit for mammalian cells; Life Technologies, Grand Island, NY) for 10 min at 37°C in a humidified, 5% CO_2 incubator then imaging the microencapsulated cells under an epifluorescent microscope (Zeiss Axiovert Observer Z1 Inverted Phase Contrast Fluorescent Microscope). Green fluorescent images for live cells and red fluorescent images for dead cells were separately processed on ImageJ software (Rasband, National Institutes of Health) to obtain cell counts.

3.2.4 Static Glucose Stimulation

Cells in monolayer or microspheres were maintained in complete culture medium at 37°C in a humidified, 5% CO2 incubator. After 48 hours, microencapsulated cells and monolayer cells were washed twice with Krebs Henseleit Buffer (KHB; BIOTANG Inc., Lexington, MA) containing 0.1 % bovine serum albumin (Sigma) and pre-incubated in KHB without glucose for 60 minutes. Glucose was then added to the KHB to obtain glucose concentrations of 0.67 mM, 1.67 mM, 2.8 mM, 5.56 mM, and 16.7 mM). Each concentration was used to perform static glucose incubations with each cell type for 2 hours. At the end of the stimulation period, the incubation buffer was collected from each well and stored at -20^{o}C until analysis. The insulin concentration of the samples was measured by enzyme linked immunosorbent assay (ELISA) kit (EMD Millipore, Billerica, MA).

3.2.5 Keratinocyte Scratch Assay

Human keratinocytes (HaCaT; Addex Bio, San Diego, CA) were propagated in DMEM (Sigma), supplemented with 10% FBS (Sigma), pen-strep (Sigma) in a humidified incubator at 37 °C/5%

CO_2. For scratch assays, 180,000 HaCaT cells/well were seeded onto 24 well plates (Greiner Bio-one; Monroe, NC). Cells were cultured for 48 hours to form a confluent monolayer at which time a single scratch of 175 µm ± 60 µm was produced in the center of the well with a 10 µl pipette tip. The wells were washed twice with Dulbecco's Phosphate Buffered Saline (DPBS; Sigma) to remove cell debris. HaCaT cells were then stimulated with conditioned-media (CM) from: (1) empty microspheres (control); (2) microencapsulated RIN-m cells on days 1, 7, or 21; (3) microencapsulated AtT-20ins cells on days 1, 7 or 21; (4) monolayer RIN-m cells on day 1; or (5) monolayer AtT-20ins cells on day 1. RIN-m and AtT-20ins cells were not maintained in monolayers beyond four days since the cells became over-confluent, resulting in cell death too great to collect insulin-conditioned media on days 7 and 21. HaCaT cell migration across scratches was imaged at 0, 4, and 24 hours using phase contrast microscopy and analyzed on NIH ImageJ software.

3.2.6 Statistical Analysis

All data were taken in triplicate and reported as mean ± standard deviation. Viability, insulin release and scratch closure were compared between the different treatment groups using a one-way analysis of variance (ANOVA). Pairwise comparisons were made between groups using Fisher's Least Significant Difference (LSD) post-hoc test. *p*-values less than 0.05 were considered significant. All analyses were performed using KaleidaGraph statistical software version 4.1.0, Synergy Software (Reading, PA).

3.3 RESULTS

3.3.1 Effect of microencapsulation on cell viability

The cell viability/cytotoxicity assay demonstrated the effect of microencapsulation on cell viability. Live cells within microspheres were identified based on intracellular enzymatic conversion of non-fluorescent calcein-AM to green fluorescent calcein while ethidium

homodimer-1 penetrated damaged membranes of dead cells and upon binding to nucleic acids fluoresced bright red (Figure 3.1). Microencapsulated RIN-m cell viability was 66.5 % ± 8.8 % on day 1 and dropped to 80 % of the initial encapsulated cell viability on day 7 (53.9 % ± 3.7 %) and then to 64 % of the initial viability post encapsulation on day 21 (42.6 % ± 7.7 %) (Figure 3.2). Microencapsulated AtT-20ins cells demonstrated higher cell viability at 70.6 % ± 8.23 % on day 1, which dropped to 82.5 % of the starting viability by day 7 (58.2 % ± 17.9 %) and 66 % of the initial viability on day 21 (46.6 % ± 9.9 %).

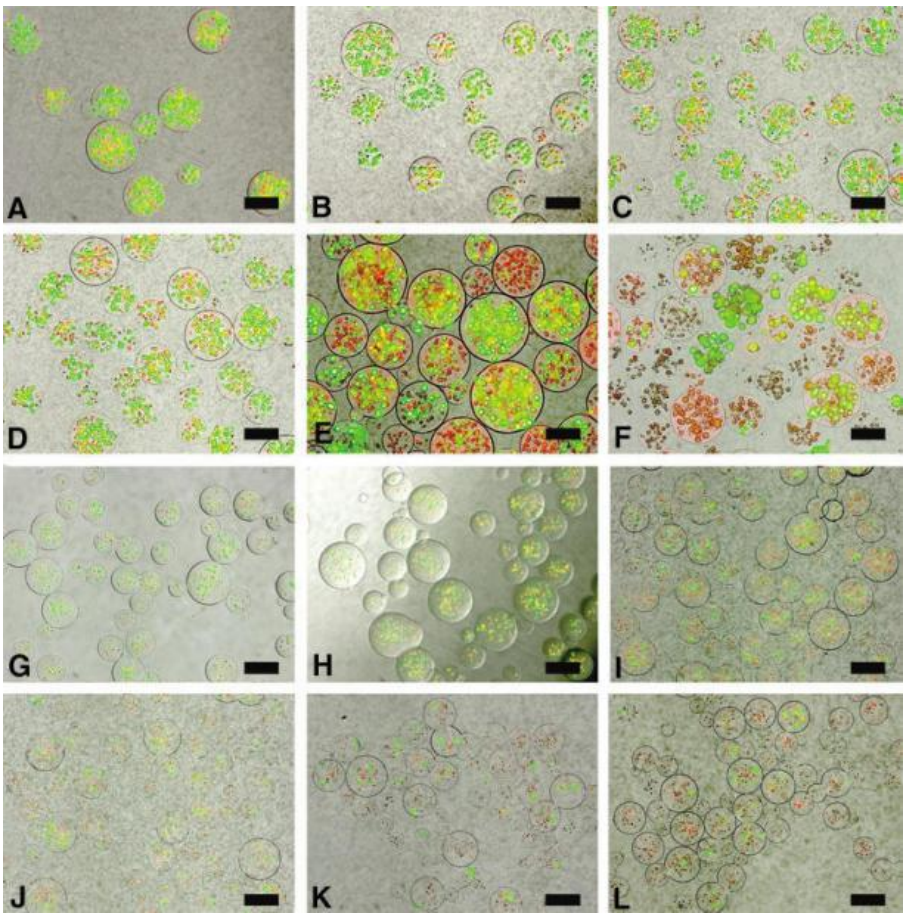

Fig. 3.1: Representative images of viability stains of microencapsulated AtT-20ins (A–F) and RIN-m (G–L) cells using a LIVE/DEAD® Viability/Cytotoxicity Kit for mammalian cells (Invitrogen, Molecular Probes, Eugene, OR). Stains of microencapsulated AtT-20ins cells on (A) day 1, (B) day 3, (C) day 5, (D) day 7, (E) day 14, and (F) day 21. Stains of microencapsulated

RIN-m cells on (G) day 1, (H) day 3, (I) day 5, (J) day 7, (K) day 14, and (L) day 21. Dead cells appear red and live cells appear green. Scale bars = 100 mm. Viability images from Aijaz et al.

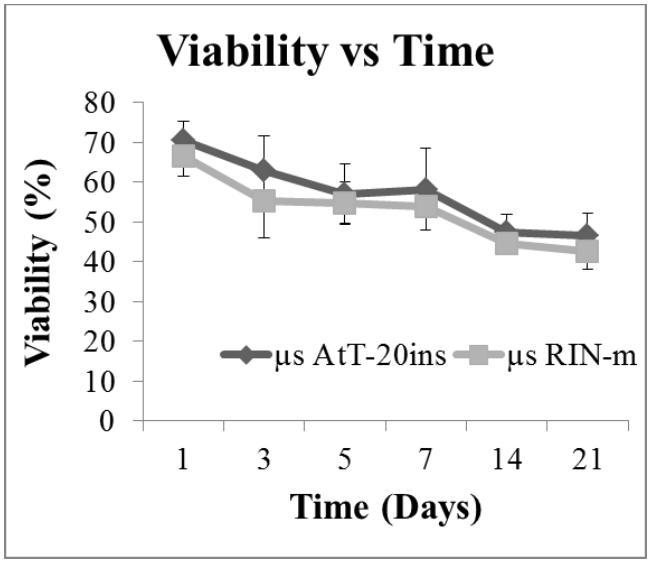

Fig. 3.2: Percentage viability curve of microencapsulated cells over time. Microencapsulated RIN-m (µs RIN-m) and AtT-20ins (µs AtT-20ins) cell viabilities were not statistically distinct at any time point. The viability of µs RIN-m cells on day 1 started at 66.5 % ± 8.8 %, while that of µs AtT-20ins cells started at 70.6 % ± 8.23 %. Viabilities of both cell types gradually decreased over time by approximately 20 % to 42.6 % ± 7.68 % (µs RIN-m) and 46.6 % ± 9.9 % (µs AtT-20ins) by day 21. Error bars show standard error of mean. Graph from Aijaz et al.

3.3.2 Insulin release kinetics

Both monolayer and microencapsulated RIN-m cells did not respond to glucose stimulation and maintained a constant insulin secretion profile when exposed to incremental concentrations of glucose and on average secreted 0.48 ± 0.03 ng/mL/hr and 0.35 ± 0.16 ng/mL/hr insulin, respectively (Figure 2A). AtT-20ins cells responded to glucose stimulation and demonstrated significant increases in insulin secretion at incremental glucose concentrations (Figure 3.3). Maximum increases in insulin release were observed at 5.56 mM glucose: for the monolayer, 0.53 ± 0.05 ng/mL/hr, for encapsulated cells, 0.66 ± 0.12 ng/mL/hr, which corresponded to

insulin increases of 3.9 and 3.6 fold greater than control (0 mM glucose) for monolayer and encapsulated cells, respectively. No significant difference in insulin release was observed between microencapsulated and monolayer cells.

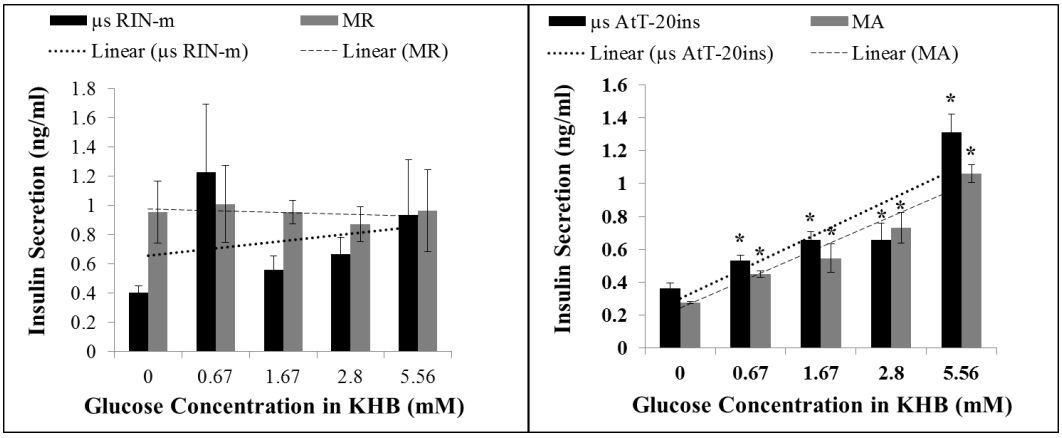

Fig. 3.3: Static glucose stimulation of (A) RIN-m and (B) AtT-20ins cells. Trend lines show that glucose secretion from AtT-20ins cells is increasing with increasing glucose. Trend lines fit to RIN-m cells are relatively flat, indicating no response to glucose stimulation. Asterisks show statistically significant differences ($p < 0.05$) in insulin secretion between incremental glucose concentrations versus control (0 mM). Error bars show standard error of mean. µs AtT-20ins: microencapsulated AtT-20ins cells, MA: monolayer AtT-20ins cells, µs RIN-m: microencapsulated RIN-m cells, MR: monolayer RIN-m cells. Graph from Aijaz et al.

3.3.3 Insulin Stimulated Cell Migration

Bioactivity of the insulin released from microencapsulated insulin-secreting cells was assessed by demonstrating their effect on keratinocyte migration. Keratinocytes were plated in a monolayer to simulate the epidermal layer of the skin and a defect (scratch assay) was created to simulate wound healing in vitro (Figure 3.4). CM containing insulin released from RIN-m microspheres sampled on day 1 demonstrated significantly increased rate of scratch closure compared to media from control empty microspheres ($p < 0.05$) (Figure 3.5). Rate of scratch closure was 29.5 ± 8.7 µm/hr and 6.9 ± 11.6 µm/hr for insulin sampled on day 1 from RIN-m microspheres and media

from empty microspheres, respectively. Rate of scratch closure for monolayer scratches stimulated with insulin from day 1 monolayer RIN-m cells was 22.9 ± 8.4 μm/hr, which was less than the closure observed in the microencapsulated group, but not significantly so. No significant difference in scratch closure rate was observed for keratinocyte monolayers treated with insulin-conditioned media sampled from RIN-m microspheres on day 1, day 7 or day 21. Similar results were observed for keratinocyte scratches treated with insulin-conditioned media from AtT-20ins microspheres. A significantly greater rate of scratch closure was observed in scratches stimulated with insulin released from day 1 AtT-20ins microspheres (19.8 ± 11.7 μm/hr) compared to scratches treated with insulin released from AtT-20ins monolayer cells (18.6 ± 9.5 μm/hr) or negative control empty microspheres (6.9 ± 11.6 μm/hr; Figure 3.5). Insulin-conditioned media sampled on day 7 from AtT-20ins microspheres also showed a significant scratch closure rate (19.2 ± 11.1 μm/hr) compared to control empty microspheres (6.9 ± 11.6 μm/hr). The rate of closure in scratches treated with insulin sampled on day 21 from AtT-20ins microspheres was not significantly different from the rate of closure in scratch wounds treated with media from empty microspheres. Empty microspheres served as insulin-free negative controls and failed to demonstrate any stimulation of cell migration across the scratches.

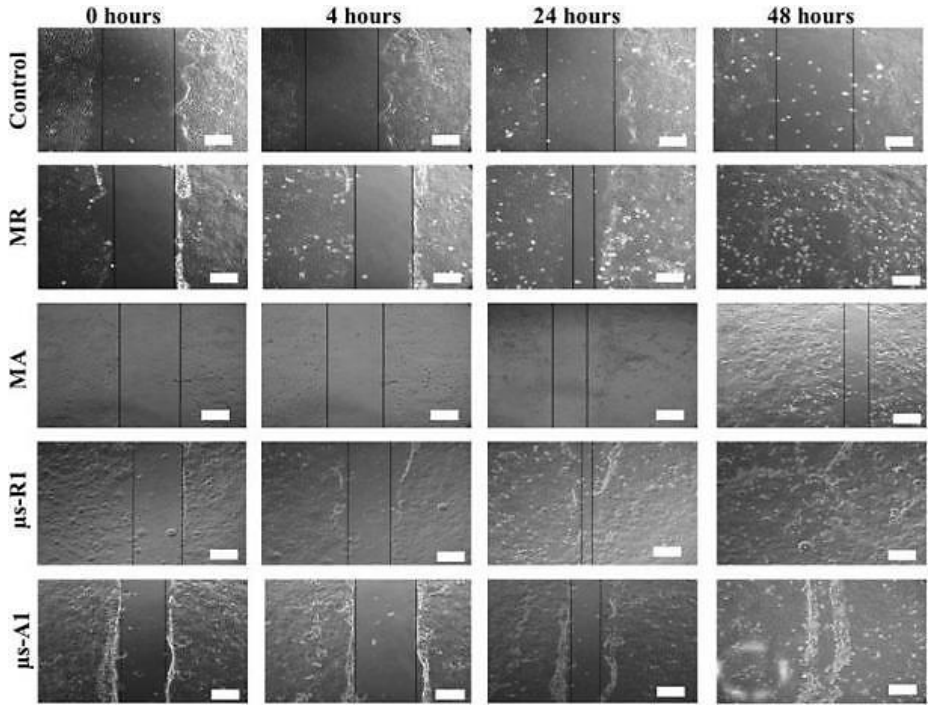

Fig 3.4: Representative bright-field images of scratches in monolayer keratinocytes at 0, 4, 24 and 48 h following stimulation by media from empty microspheres (control) and insulin containing CM from MR, MA, µs RIN-m cells on day 1 (µs-R1), and µs AtT-20ins cells on day 1 (µs-A1). Black lines depict scratch margins. Scale bars = 100 µm. Scratch images from Aijaz et al.

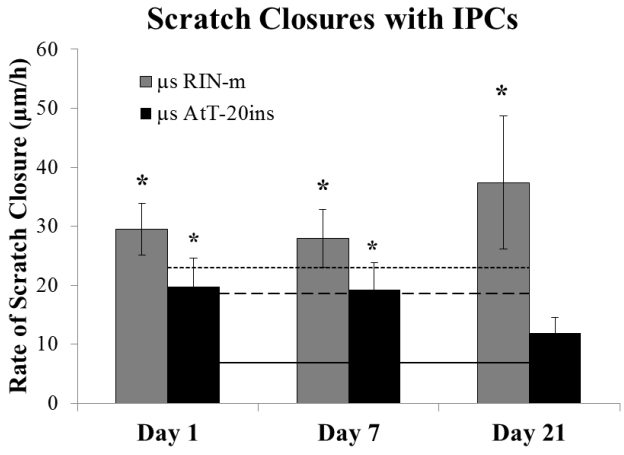

Fig. 3.5: Quantification of keratinocyte scratch assays of cell migration and insulin bioactivity.

Bars show experimental groups, solid line shows control closure rate, dashed line shows closure rate from monolayer AtT-20ins cells, dotted line shows closure rate from monolayer RIN-m cells. Asterisks show significant difference from control ($p<0.05$), error bars show standard error of mean. Both cell types accelerated scratch closure, though CM from RIN-m cells demonstrated a more profound effect on scratch closure than CM from AtT-20ins. Asterisks indicate statistically significant differences ($p<0.05$) between the indicated condition(s) and control. Error bars show standard error of mean. Modified from Aijaz et al.

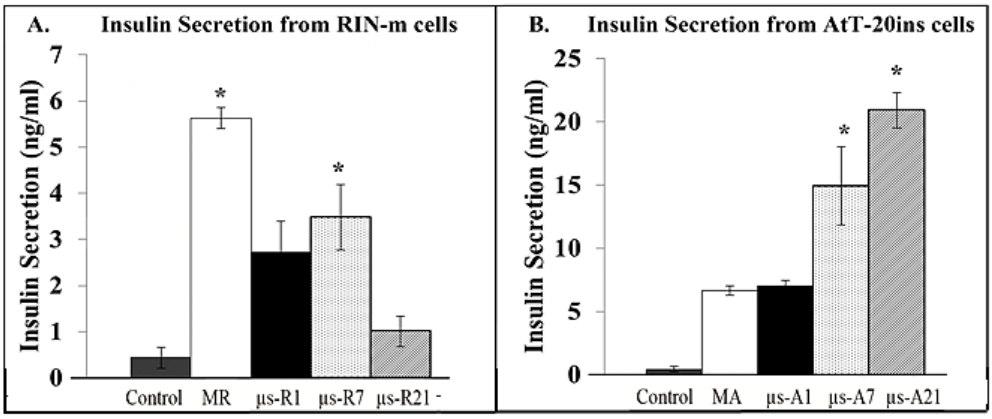

Fig. 3.6: Concentration of insulin in insulin-conditioned media sampled from (A) monolayer RIN-m cells (MR), microencapsulated RIN-m cells on day 1, 7, and 21 (µs-R1, µs-R7, and µs-R21, respectively), (B) monolayer AtT-20ins cells (MA), and microencapsulated AtT-20ins cells on day 1, 7 and 21 (µs-A1, µs-A7, and µs-A21). Empty microsphere (Control) served as insulin-free negative controls. Asterisks indicate statistically significant differences ($p<0.05$) between the indicated condition(s) and control. Error bars show standard error of mean.

3.4 DISCUSSION

Cell viability and cytotoxicity assays showed that the majority of cells survived the microencapsulation process. Data showed a gradual decline in viability over 21 days, which is expected since cells do not proliferate in these hydrogels. The total number of insulin-releasing

cells is more significant than the percentage of live cells, as demonstrated by the bioactivity and wound healing studies. Glucose stimulation studies demonstrated that the encapsulated cells maintained their insulin secretory characteristics and the microspheres' hydrogel mesh permitted free diffusion of insulin through the microspheres. The insulin molecule has a molecular weight of 5,808 Da and a molecular radius of 1.34 nm [12]. Free diffusion of insulin from microspheres as confirmed by our data was as expected since the 10% 10 kDa PEGDA hydrogels have a reported mesh size of 28 nm [13]. Thus, no statistically significant difference in insulin secretion was observed between monolayer insulin-secreting cells and microencapsulated insulin-secreting cells.

Once the release of insulin from the microspheres was confirmed, it was also important to determine whether the released insulin remained bioactive, which was accomplished by demonstrating that the released insulin was capable of stimulating a wound healing response. The keratinocyte scratch assay is an *in vitro* wound healing model and stimulation of HaCaT cell migration by insulin is an accepted indicator of insulin bioactivity over time and its ability to promote wound healing. Our microencapsulated RIN-m and AtT-20ins cells on average secrete 2.4 ± 0.2 ng/ml (0.4 nM) insulin and 14.3 ± 1.36 ng/ml (2.4 nM) insulin (Figure 3.6), respectively, which is comparable to the typical 10^{-7} M concentration of insulin used to stimulate keratinocyte migration [14, 15]. The bioactivity of insulin released from microspheres was maintained over time as indicated by its continued ability to accelerate scratch closure. Specifically, cell migration studies demonstrated that the insulin released from microencapsulated RIN-m cells remained bioactive for at least 21 days, which is sufficient time for a wound to completely heal. Rate of closure observed in scratches treated with insulin released from day 1, day 7 and day 21 RIN-m microspheres was not significantly different between groups but each group was significantly greater than the (control) empty microsphere group ($p<0.05$). Decreases in scratch closure rates were observed in scratches treated with insulin collected on day 21 from microencapsulated AtT-20ins cells compared to scratches treated with insulin collected on day 1. This reduction in rate of

scratch closure could be due to a loss of microspheres during media collection or decreased cell viability over time and therefore reduced concentration of insulin in the sample used to stimulate HaCaT cell migration.

3.5 CONCLUSION

The purpose of this chapter was to develop a system that provides a sustained and steady dose of insulin to regulate the hyperglycemic wound environment characteristic of diabetic and chronic wounds. PEGDA was used to immunoisolate and immobilize IPCs because it is bioinert, non-degradable and FDA-approved. Microencaspsulation within PEGDA preserved cell viability and insulin secretory characteristics of the entrapped ISCs, and the released bioactive insulin accelerated keratinocyte migration in scratch wounds in a single application. In the next chapter, the *in vivo* potential of these IPC-laden PEGDA hydrogel microspheres is described.

3.6 REFERENCES

1. Rosenthal SP. Acceleration of primary wound healing by insulin. Arch Surg. 96, 53, 1968.
2. Shanley LJ, McCaig CD, Forrester JV and Zhao M. Insulin, Not Leptin, Promotes In Vitro Cell Migration to Heal Monolayer Wounds in Human Corneal Epithelium. Invest Ophthalmol Vis Sci. 45(4), 1088, 2004
3. Chen X, Liu Y, Zhang X. Topical insulin application improves healing by regulating the wound inflammatory response. Wound Repair Regen. 20, 425, 2012.
4. Brem H. , J Clin Invest. 2007; 117(5):1219–1222.
5. Apikoglu-Rabus S, Izzettin FV, Turan P, Ercan F. Effect of topical insulin on cutaneous wound healing in rats with or without acute diabetes. Clin Exp Dermatol. 35(2), 180, 2010.
6. Hrynyk M, Martins-Green M, Barronc AE, Neufelda RJ. Sustained prolonged topical delivery of bioactive human insulin for potential treatment of cutaneous wounds. Int J Pharm 398 (2010) 146–154.
7. Kepsutlu B, Nazli C, Bal T, Kizilel S. Design of bioartificial pancreas with functional micro/nano-based encapsulation of islets. Curr Pharm Biotechnol. 15(7), 590, 2014.
8. Schwartz S, Mulgrew P. A single-center phase I/II study of PEG-encapsulated islet allografts implanted in patients with type I diabetes (study NCT00260234). Available at: http://www.clinicaltrials.gov.
9. Cruise, G.M., Hegre, O.D., Lamberti, F.V., Hager, S.R., Hill, R., Scharp, D.S., and Hubbell, J.A. In vitro and in vivo performance of porcine islets encapsulated in interfacially photopolymerized poly(ethylene glycol) diacrylate membranes. Cell transplantation 8, 293, 1999.
10. Olabisi RM, Lazard ZW, Franco CL, Hall MA, Kwon SK, Sevick-Muraca EM, Hipp JA, Davis AR, Olmsted-Davis EA, West JL. Hydrogel microsphere encapsulation of a cell-based

gene therapy system increases cell survival of injected cells, transgene expression, and bone volume in a model of heterotopic ossification. Tissue Eng Part A. 16(12), 3727, 2010.

11. Franco CL, Prince J, West JL. Development and optimization of a dual-photoinitiator, emulsion-based technique for rapid generation of cell-laden hydrogel microspheres. Acta Biomater. 7(9), 3267, 2011.
12. Lev Bromberg, Julia Rashba-Step, and Terrence Scott. Insulin Particle Formation in Supersaturated Aqueous Solutions of Poly(Ethylene Glycol). Biophys J. 89(5), 3424, 2005.
13. Liao, H., Munoz-Pinto, D., Qu, X., Hou, Y., Grunlan, M.A., and Hahn, M.S. Influence of hydrogel mechanical properties and mesh size on vocal fold fibroblast extracellular matrix production and phenotype. Acta Biomater. 4, 1161, 2008.
14. Liu Y, Petreaca M, Yao M, Martins-Green M. Cell and molecular mechanisms of keratinocyte function stimulated by insulin during wound healing. BMC Cell Biology 10:1, 2009
15. Benoliel AM, Kahn-Perles B, Imbert J, Verrando P. Insulin stimulates haptotactic migration of human epidermal keratinocytes through activation of NF-kappa B transcription factor. J Cell Sci. 110, 2089, 1997.

CHAPTER 4: HYDROGEL MICROENCAPSULATED INSULIN-PRODUCING CELLS INCREASE EPIDERMAL THICKNESS, COLLAGEN FIBER DENSITY, AND WOUND CLOSURE IN A DIABETIC MOUSE MODEL OF WOUND HEALING.

Note: Portions of this chapter have been published in: 'A. Aijaz et al., **Hydrogel microencapsulated insulin-secreting cells increase keratinocyte migration, epidermal thickness, collagen fiber density, and wound closure in a diabetic mouse model of wound healing.** Tissue Eng Part A. 2015 Nov;21(21-22):2723-32. doi: 10.1089/ten.TEA.2015.0069', and represent the original work of the candidate.

4.1 INTRODUCTION

Skin acts as a protective barrier against environmental toxins, provides thermoregulation and fluid homeostasis [1]. Any injury to the skin results in its loss of structural and functional integrity. Following injury, a wound healing cascade sets into play in three sequential phases that dynamically interact and overlap in time. The inflammatory response is the key to effective wound healing. If inflammation is not controlled and inflammatory cells persist in the wound site, it may lead to chronic inflammation. Chronic wounds have a hyperglycemic wound environment that causes immune cells to produce pro-inflammatory cytokines and impairs phagocytosis. In this environment, proteases such as MMPs rapidly degrade extracellular matrix components deposited by fibroblasts [2, 3]. The end result is decreased angiogenesis, reepithelialization, wound contraction, and reduced wound strength. Insulin has also been shown to regulate the wound inflammatory response even in non-diabetic animals by inducing advanced infiltration and resolution of macrophages [4]. Lima et al. reported attenuation of insulin signaling pathways in the skin of diabetic animals and an increase in the time to complete wound closure; topically applied insulin cream improved wound healing rates in these animals [5]. Greenway et al. treated diabetic and non-diabetic volunteers with topical insulin and demonstrated that insulin promoted healing 2.4 ± 0.8 days faster than the wounds treated with saline [6]. A double-blind placebo-

controlled clinical trial was conducted in which patients suffering from type 2 diabetes and who were taking subcutaneous insulin and oral anti-diabetic drugs presented with diabetic ulcers [5]. Remarkably, topical insulin application significantly improved wound healing in these patients. Thus, exogenous insulin administration can be effective in accelerating wound healing in both non-diabetic and diabetic patients and animals who may be on systemic insulin treatment [6-10]. Nevertheless, no external cell-based therapy involving insulin-secreting cells has yet been reported for treating chronic wounds.

In the previous chapter IPCs were encapsulated within PEDGA microspheres and the effect of the microencapsulation procedure on cell viability and bioactivity of the released insulin was assessed. This chapter describes the potential of microencapsulated constant insulin producing RIN-m cells and microencapsulated glucose dependent insulin-secreting AtT-20ins cells on wound closure in a diabetic mouse model. Our hypothesis was that microencapsulation in PEGDA hydrogels will provide a delivery system for sustained release of bioactive insulin at the wound site and the released insulin will promote wound closure potentially by counteracting the hyperglycemic wound environment.

4.2 MATERIALS AND METHODS

4.2.1 Cell Culture

Rat insulinoma beta cell line, RIN-m, and GLUT-2 cDNA transfected AtT-20ins-(CGT6) cells, were propagated in RPMI-1640 medium (ATCC) or Dulbecco's modified Eagle's medium (Sigma, St. Louis, MO), respectively, supplemented with 10% fetal bovine serum (FBS; Sigma) and 1% w/v penicillin-streptomycin (pen-strep; Sigma) in a humidified incubator at 37 °C/5% CO_2.

4.2.2 Microencapsulation

Cell-laden microspheres were formed as previously reported [16, 17]. Briefly, hydrogel precursor solution was formed by combining 0.1 g/mL 10 kDa PEGDA (10% w/v; Laysan Bio, Inc.) with (1.5% v/v) triethanolamine/HEPES-buffered saline (pH 7.4), 37 mM 1-vinyl-2-pyrrolidinone, 0.1 mM eosin Y, and RIN-m cells or AtT-20ins cells for a final concentration of 1.5×10^4 cells/μL. A hydrophobic photoinitiator solution containing 2,2-dimethoxy-2-phenyl acetophenone in 1-vinyl-2-pyrrolidinone (300 mg/mL) was combined in mineral oil (3 μL/mL, embryo tested, sterile filtered; Sigma). The cell-prepolymer suspension was added to the mineral oil solution, emulsified by vortexing for 4 seconds in ambient light, then for an additional 3 seconds under white light, then the vortex was stopped and the emulsion was exposed to white light for 20 seconds with a vortex pulse at 10 seconds. Crosslinked microspheres were isolated by addition of 1 mL complete media followed by centrifugation at 300 g for 5 minutes. The oil layer was removed by aspiration and pelleted microspheres were resuspended in media and placed in Transwells® (0.4 mm pore polycarbonate membrane Transwell® inserts; Corning, Inc., Lowell, MA) in a 12-well plate with 3 mL culture medium. Microencapsulated cells were maintained in a humidified incubator at 37 °C/5% CO_2 until animal studies.

4.2.3 Animal Studies

An animal study was performed to determine whether positive *in vitro* results could be translated to promising *in vivo* results. All procedures were performed in accordance with protocols approved by the Rutgers University Institutional Animal Care and Use Committee (IACUC). A 1 cm x 1 cm full thickness excisional wound was created on the dorsa of genetically diabetic male mice (BKS.Cg-m +/+ Leprdb/J; 10 weeks old, N=9 total; n=3/experimental group); Jackson Laboratories, Bar Harbor, ME). Microencapsulated RIN-m or AtT-20ins cells or empty microspheres were applied to wounds, which were then covered with Tegaderm™ and photographed at postoperative days (POD) 3, 7, 14, 21, 28, and 35 for gross appearance.

Tegaderm™ began to fail on POD 16, and therefore all microspheres were then removed. Wound area was measured by tracing the wound margins using ImageJ. Wound closure was calculated as percent area of original wound. Animals were sacrificed by CO_2 inhalation on POD 35 and wound tissue was collected for histology.

4.2.4 Histological Analysis

After sacrifice on POD 35, skin tissue was excised around the edges of the wounded area for histological analysis. Wound tissues were fixed in 10 % formalin for 24 hours at room temperature and then stored in 70 % ethanol at 4 ^{o}C until serial sectioning (5 μm thick) and staining with hematoxylin and eosin (H & E) or Picric Acid Sirius Red (PASR) at the Digital Imaging and Histology Core, Rutgers-NJMS Cancer Center. Tissue sections were stained with H & E for morphological analysis and PASR stain for collagen fiber density. Histological images were analyzed on ImageJ software to find epidermal and dermal thickness and collagen density. H & E-stained sections were analyzed in ImageJ to measure the thickness of epidermis and dermis using the Line Selection Tool. Lines were created across the thickness of the epidermal or dermal boundaries at five random locations in each H & E section and lengths were averaged. RGB images of PASR-stained sections were converted to gray scale by splitting the images into red, green and blue channels. For accurate visual determination of image threshold for collagen-stained areas, the red channel was selected as it yielded the best contrast between the stain and the background. The thresholded images were analyzed to measure percent area of collagen density [18].

4.2.5 Statistical Analysis

All data were taken in triplicate and reported as mean ± standard deviation. Dermal and epidermal thickness, collagen density, and wound closure were compared between the different treatment groups using a one-way analysis of variance (ANOVA). Pairwise comparisons were

made between groups using Fisher's Least Significant Difference (LSD) post-hoc test. *p*-values less than 0.05 were considered significant. All analyses were performed using KaleidaGraph statistical software version 4.1.0, Synergy Software (Reading, PA).

4.3 RESULTS

4.3.1 In vivo assessment of wound closure in diabetic mice

Gross examination showed an initial increase in wound area due to skin elasticity of the obese, diabetic mice. Animals treated with RIN-m microspheres showed statistically significant acceleration in wound closure by POD 7 (5.07 % ± 19.5 %) compared to AtT-20ins and control groups (Figure 4.1B). By POD 21 wound closures for RIN-m, AtT-20ins and control groups were 84.3 ± 13.62 %, 57.4 ± 36.2% and 72.98 ± 7.01%, respectively. Complete wound closure was achieved by POD 28 in all animals (n=3) treated with RIN-m microspheres while wound closures were 89.3 % ± 15.33 % and 94.39 % ± 2.06 % in AtT-20ins treated animals (n=3) and negative control animals (n=3), respectively. Large standard deviations in wound closures were observed in AtT-20ins treated animals. In this group complete wound closure was achieved in two animals by POD 35, while in the third animal wound closure was 82 %.

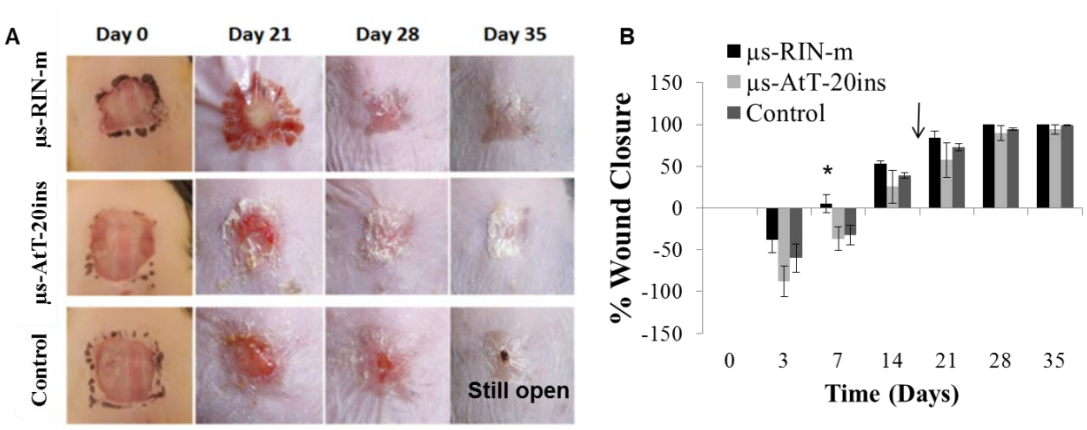

Fig. 4.1: Representative images and quantification of wound closure over time. **(**A**)** Gross appearance, **(**B**)** % wound closure. Images show wounds before Tegaderm™ application and after

its removal. Dark stains around the wound on Day 0 are from a skin marker to define the wound area. Arrow shows microsphere removal on POD 16. Asterisks indicate statistically significant differences ($p<0.05$) between microencapsulated cells vs. control. Error bars show standard error of mean. µs RIN-m: microencapsulated RIN-m cells, µs AtT-20ins: microencapsulated AtT-20ins cells. Scale bars = 1 cm. Taken from Aijaz et al.

4.3.2 Histological analysis

Microencapsulated insulin-secreting cells accelerated wound closure and H & E sections showed that the epidermis was 3-5 cells thick in both treatment groups while it was only 1-2 cells thick in the empty microsphere control group (Figure 4.2). Quantification of H & E sections revealed that the epidermis was significantly thicker in animals treated with RIN-m microspheres (42.7 µm ± 10.37 µm) and AtT-20ins microspheres (44.15 µm ± 10.26 µm) compared to the negative control animals (29.98 µm ± 7.96 µm; Figure 4.2G). No statistically significant difference was observed in dermal thickness between the treatment and control groups (Figure 4.2H); however, when the density of collagen fibers was analyzed in the PASR-stained sections, collagen fiber density (percent area) was significantly higher in RIN-m (83.74 % ± 2.7 %) and AtT-20ins (79.95 % ± 3.7 %) treatment groups compared to the control group (67.35 % ± 2.74 %; Figure 4.2H).

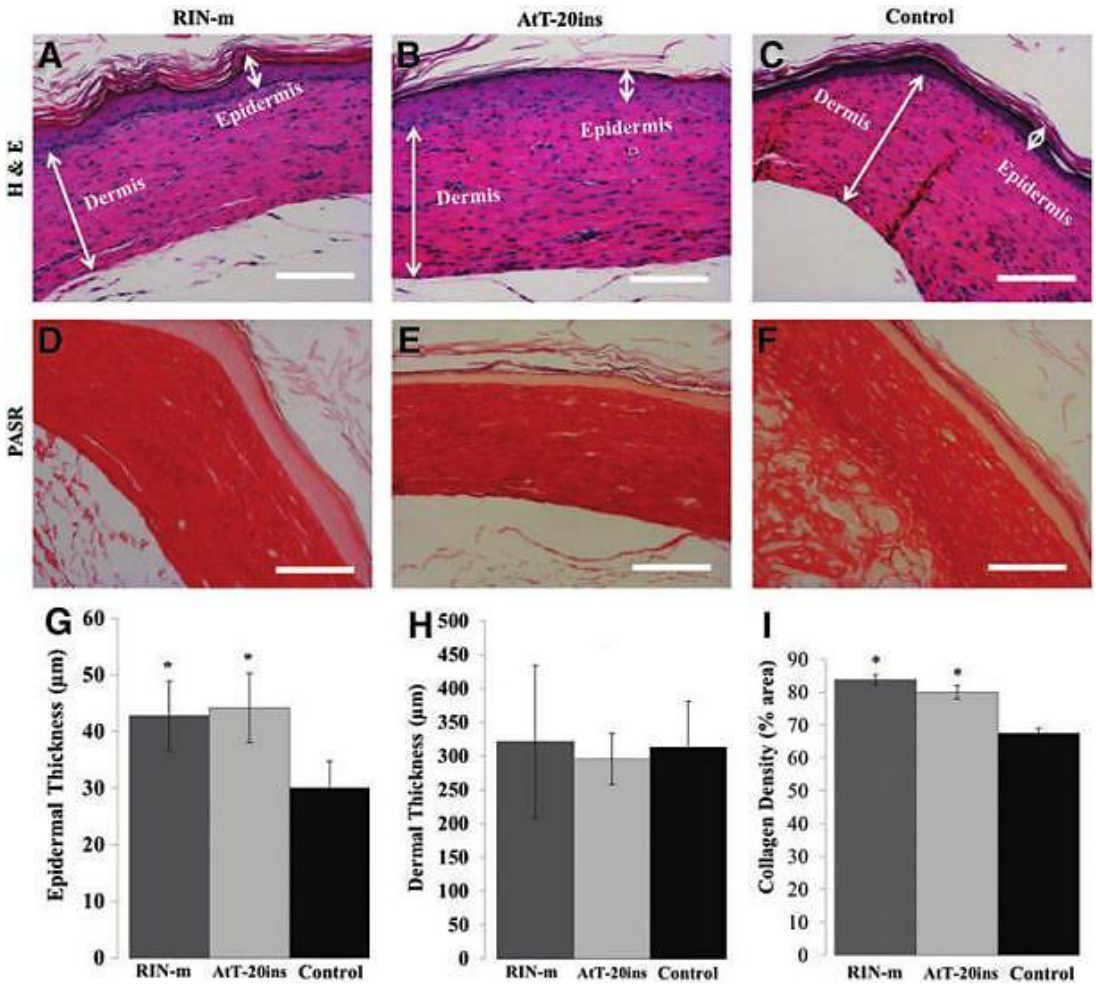

Fig. 4.2: Histological analysis of harvested wounds. H&E stained wound tissue sections of animals treated with: (A) RIN-m microspheres, (B) AtT-20ins microspheres, (C) empty microspheres (control). PASR-stained wound tissue sections of animals treated with: (D) RIN-m microspheres, (E) AtT-20ins microspheres, (F) empty microspheres (control). Quantification of **(**G**)** epidermal thickness, **(**H**)** Dermal thickness and **(I)** collagen fiber density. Although there is no statistical difference in dermal thickness between groups, epidermal thickness in treated wounds is statistically greater than control. Collagen fiber densities in treated groups are also statistically greater than control. Asterisks indicate statistically significant differences (p<0.05) between treated and control wounds. Error bars show standard error of mean. µs RIN-m: microencapsulated RIN-m cells, µs AtT-20ins: microencapsulated AtT-20ins cells. Scale bars = 50 µm. Taken from Aijaz et al.

4.4 DISCUSSION

Wound healing is a dynamic process that occurs in a well-orchestrated synchrony of events that overlap and are interdependent. Any biological or temporal defect may affect wound healing. Tight regulation and resolution of the inflammatory response as well as initiation of reepithelialization is critical to effective wound healing. Previous studies have reported that topical application of insulin accelerates wound healing by regulating the hyperglycemic wound environment and by promoting growth and proliferation of keratinocytes, fibroblasts and endothelial cells in both diabetic and non-diabetic patients. However, current approaches require repeated applications that increase the chances of infecting the wound with each opening of the wound dressing for every application. Cells that secret insulin into the wound area provide a solution to this problem. Here, a novel system that encapsulates constant or glucose-dependent insulin-secreting cells within synthetic hydrogels formed from PEGDA is presented. This approach maintains cell viability and insulin secretory characteristics of the cells while at the same providing a bioinert, non-immunogenic barrier. Moreover, insulin secretion is modulated in a sustained manner, eliminating the need for multiple applications as required in topical insulin ointments.

In non-diabetic mice, the relatively large 1 cm^2 full thickness excisional wound has been shown to take 25 days to heal [19]. In this chapter it was demonstrated that IPCs encapsulated within PEGDA hydrogels improve wound healing by 1.6 times faster than controls. In the diabetic mice in this study, the untreated wound takes over 35 days to heal, 40% longer. Thus, although the wounds show 94% closure, this closure is well past the normal time it should have taken. The percentage wound closure calculated for each group demonstrated a trend of accelerated closure in insulin treated animals prior to removal of microspheres on POD 16, after which negative control (empty microspheres) animals showed similar wound closure dynamics. Insulin is typically applied at 0.03 U in 20 µL saline to treat excisional wounds in mice which is equivalent to 52.05 ng/mL, while the study in this chapter reports accelerated wound healing at much lower

concentrations [20, 21]. Histology showed no evidence of immune reaction to empty PEGDA hydrogel microspheres or those containing insulin-secreting cells. The large standard deviation in percentage wound closure for microencapsulated AtT-20ins cells might be attributed to the fact that these cells grow in clusters, which may result in varying cell densities within microspheres between animals. This is due to the fact that our microencapsulation method is not 100 % efficient and more reproducibly encapsulates individual cells than clusters. In subsequent chapters this was rectified by encapsulating cells in thin sheets using molds and a method that does have 100 % encapsulation efficiency; however, based on the results presented in this chapter, subsequent studies proceeded with RIN-m cells, which demonstrated superior wound healing and do not grow in clusters. The healing attained with RIN-m cells suggest that the presence of insulin is sufficient for wound healing and does not need to be tailored to the glucose environment of the wound bed.

4.5 CONCLUSIONS

In this chapter, a system for accelerated wound healing in which insulin-secreting cells encapsulated into PEGDA hydrogel microspheres was evaluated. This permitted prolonged insulin release within the target site. Microsphere encapsulation prevented immune clearance and cell migration, keeping the microencapsulated cells in the desired location. Thus, the combination of insulin-releasing cells and PEGDA hydrogel microencapsulation provides a novel method for delivering a steady, constant dose of insulin to a wound. Future studies will explore dose responses, various hydrogel geometries, and insulin mediated induction of downstream signaling molecules. Our system is the first cell-based insulin treatment of its kind to speed wound closure, demonstrating that this system is a feasible method to accelerate wound healing and it may impact insulin-driven wound healing approaches to come.

4.6 REFERENCES

1. Church D, Elsayed S, Reid O, Winston B, Lindsay R. Burn wound infections. Clin Microbiol Rev. 19(2), 403, 2006.
2. McCarty SM, Cochrane CA, Clegg PD, Percival SL.The role of endogenous and exogenous enzymes in chronic wounds: a focus on the implications of aberrant levels of both host and bacterial proteases in wound healing. Wound Repair Regen. 20(2), 125, 2012
3. Apikoglu-Rabus S, Izzettin FV, Turan P, Ercan F. Effect of topical insulin on cutaneous wound healing in rats with or without acute diabetes. Clin Exp Dermatol. 35(2), 180, 2010.
4. Chen X, Liu Y, Zhang X. Topical insulin application improves healing by regulating the wound inflammatory response. Wound Repair Regen. 20, 425, 2012.
5. Lima MHM, Caricilli AM, de Abreu LL, Araújo EP, Pelegrinelli FF, Thirone ACP, Tsukumo DM, Pessoa AFM, dos Santos MF, de Moraes MA. Topical insulin accelerates wound healing in diabetes by enhancing the AKT and ERK pathways: a double-blind placebo-controlled clinical trial. PLoS One. 2012 7(5):e36974.
6. Greenway SE, Filler LE, Greenway FL. Topical insulin in wound healing: a randomised, double-blind, placebo-controlled trial. J Wound Care. 8(10), 526, 1999.
7. Madibally SV, Solomon V, Mitchell RN, Van De Water L, Yarmush ML, Toner M. Influence of insulin therapy on burn wound healing in rats. J Surg Res. 109(2), 92, 2003.
8. Rezvani O, Shabbak E, Aslani A, Bidar R, Jafari M, Safarnezhad S. A randomized, double-blind, placebo-controlled trial to determine the effects of topical insulin on wound healing. Ostomy Wound Manage. 55(8), 22, 2009.
9. Sen CK, Gordillo GM, Roy S, Kirsner R, Lambert L, Hunt TK, Gottrup F, Gurtner GC, Longaker MT. Human skin wounds: a major and snowballing threat to public health and the economy. Wound Repair Regen. 17(6), 763, 2009.
10. Procházka V, Gumulec J, Jaluvka F, Salounová D, Jonszta T, Czerny D, Krajca J, Urbanec R, Klement P, Martinek J. Cell therapy, a new standard in management of chronic critical limb ischemia and foot ulcer. Cell Transplant. 19(11), 1413, 2010.
11. Lev Bromberg, Julia Rashba-Step, and Terrence Scott. Insulin Particle Formation in Supersaturated Aqueous Solutions of Poly(Ethylene Glycol). Biophys J. 89(5), 3424, 2005.
12. Sen CK, Gordillo GM, Roy S, Kirsner R, Lambert L, Hunt TK, Gottrup F, Gurtner GC, Longaker MT. Human skin wounds: a major and snowballing threat to public health and the economy. Wound Repair Regen. 17(6), 763, 2009.
13. Procházka V, Gumulec J, Jaluvka F, Salounová D, Jonszta T, Czerny D, Krajca J, Urbanec R, Klement P, Martinek J. Cell therapy, a new standard in management of chronic critical limb ischemia and foot ulcer. Cell Transplant. 19(11), 1413, 2010.
14. Singh, N., Armstrong, D. G. and Lipsky, B. A. Preventing foot ulcers in patients with diabetes. Jama 293, 217, 2005.
15. Amputee Coalition of America. National limb loss information fact sheet; diabetes and lower extremity amputations. 2008 Available at http://www.amputee-coalition.org/fact_sheets/diabetes_leamp.html. Access Date: June 18, 2015.
16. Olabisi RM, Lazard ZW, Franco CL, Hall MA, Kwon SK, Sevick-Muraca EM, Hipp JA, Davis AR, Olmsted-Davis EA, West JL. Hydrogel microsphere encapsulation of a cell-based gene therapy system increases cell survival of injected cells, transgene expression, and bone volume in a model of heterotopic ossification. Tissue Eng Part A. 16(12), 3727, 2010.
17. Franco CL, Prince J, West JL. Development and optimization of a dual-photoinitiator, emulsion-based technique for rapid generation of cell-laden hydrogel microspheres. Acta Biomater. 7(9), 3267, 2011.
18. Hunter JM, Kwan J, Malek-Ahmadi M, Chera L. Maarouf, Tyler A. Kokjohn, Christine Belden, Marwan N. Sabbagh, Thomas G. Beach and Alex E. Roher. Morphological and

pathological evolution of the brain microcirculation in aging and alzheimer's disease. PLoS One 2012 16;7(5):e36893.
19. Sarkar A, Tatlidede S, Scherer SS, Orgill DP, and Berthiaume F. Combination of stromal cell-derived factor-1 and collagen–glycosaminoglycan scaffold delays contraction and accelerates reepithelialization of dermal wounds in wild-type mice. Wound Repair Regen. 19(1), 71, 2011.
20. Rabinowitch, I. M. Simultaneous Respiratory Exchange and Blood Sugar Time Curves. Arch. Surg., 26, 696, 1933.
21. Liu Y, Petreaca M, Yao M, Martins-Green M. Cell and molecular mechanisms of keratinocyte function stimulated by insulin during wound healing. BMC Cell Biology 10:1, 2009

CHAPTER 5: ENCAPSULATION OF INSULIN-PRODUCING CELLS IN PEGDA HYDROGEL SHEETS

Note: Portions of this chapter have been published in: 'A. Aijaz et al., **Hydrogel microencapsulated insulin-secreting cells increase keratinocyte migration, epidermal thickness, collagen fiber density, and wound closure in a diabetic mouse model of wound healing.** Tissue Eng Part A. 2015 Nov;21(21-22):2723-32. doi: 10.1089/ten.TEA.2015.0069', and represent the original work of the candidate.

5.1 INTRODUCTION

In the previous chapters a microencapsulation system that encapsulated insulin-producing cells within nondegradable PEGDA hydrogel microspheres was described. It was demonstrated that microencapsulation preserves cell viability, insulin secretory characteristics, and bioactivity of the released insulin. Application of IPC-laden PEGDA microspheres accelerated wound closure in diabetic mice and presented superior histological wound tissue outcomes. However, despite these successes, there were limitations with the IPC microencapsulation approach. The microencapsulation procedure employs a bulk polymerization method that results in varying cell densities within microspheres. This leads to a large standard deviation in results within each treatment group. Moreover, this microencapsulation method does not result in 100 % microencapsulation efficiency. Furthermore, during *in vivo* studies, the microspheres did not stay on the wound area beyond POD 16 and it was difficult to keep the microspheres in the region since the mice interfere with their bandages. In order to ensure 100 % encapsulation efficiency, IPCs were encapsulated within hydrogel sheets, as described in this chapter. Based on the promising *in vitro* and *in vivo* results with RIN-m IPCs which demonstrated superior wound healing, grow more rapidly, and are easier to encapsulate because they do not grow in clusters, RIN-m cells were selected for all subsequent studies.

Cell viability is affected by sheet thickness due to diffusion of waste and nutrients through the hydrogel, thus the goal of this chapter was to optimize the PEGDA hydrogel sheet thickness and choose one that demonstrates highest IPC viability for at least 21 days.

5.2 MATERIALS AND METHODS

5.2.1 Cell Culture

The constant insulin producing rat insulinoma beta RIN-m cell line was purchased from American Type Culture Collection (ATCC, Manassas, VA) and propagated in RPMI-1640 medium (ATCC) supplemented with 10% fetal bovine serum (FBS; Sigma) and 1% w/v penicillin-streptomycin (pen-strep; Sigma) in a humidified incubator at 37 °C/5% CO_2.

5.2.2 Cell Encapsulation

RIN-m cells (IPCs) were encapsulated within PEGDA hydrogel sheets by photopolymerizing cells suspended in a precursor solution formed by combining 0.1 g/mL 10 kDa PEGDA (10% w/v; Laysan Bio, Inc.) with (1.5% v/v) triethanolamine/ HEPES buffered saline (pH 7.4), 37mM 1-vinyl-2-pyrrolidinone, 0.1 mM eosin Y. The cell-prepolymer suspension (1×10^4 – $1x10^5$ cells/µL) was pipetted into 1 cm^2 custom made molds and exposed to white light for 20 seconds to achieve 300 µm, 400 µm or 500 µm thick cell-laden hydrogel sheets. Thus, IPC-laden hydrogels were encapsulated at low (LCD; 0.5 x 10^6 cells/sheet), intermediate (ICD; 2 x 10^6 cells/sheet) and high (HCD; 5 x 10^6 cells/sheet) cell densities were formed. Crosslinked hydrogels were gently lifted with blunt forceps and placed in Transwells (0.4 mm pore polycarbonate membrane Transwell® inserts; Corning, Inc., Lowell, MA) in a 12-well plate with 3 ml culture medium. Hydrogels were maintained in a humidified incubator at 37 °C/5% CO_2. IPCs or hMSCs were plated on 6-well tissue culture plates for monolayer comparisons.

5.2.3 Cell viability

The hydrogel sheet thickness was optimized by evaluating IPC viability encapsulated at low (LCD; 0.5 x 10^6 cells/sheet), intermediate (ICD; 2 x 10^6 cells/sheet) and high (HCD; 5 x 10^6 cells/sheet) cell densities in 300 µm - 500 µm thick sheets. Viable cells within the hydrogel sheets were identified based on intracellular enzymatic conversion of non-fluorescent calcein-AM to green fluorescent calcein while ethidium homodimer-1 penetrated damaged membranes of dead cells and upon binding to nucleic acids fluoresced bright red. Encapsulated cell viability was assessed on days 1, 7 and 21 by incubating hydrogels in media, 2 mM calcein acetoxymethyl ester, and 4 mM ethidium homodimer (LIVE/DEAD Viability/Cytotoxicity Kit for mammalian cells; Life Technologies, Grand Island, NY) at 37°C in a humidified, 5% CO_2 incubator. After 10 min, each hydrogel was imaged under an epifluorescent microscope (Zeiss Axiovert Observer Z1 Inverted Phase Contrast Fluorescent Microscope) and 10 - 15 optical slices at 28 µm intervals were taken in the z-plane at three diagonal positions (e.g., top left, center, and bottom right) in the x-y coordinates. Green fluorescent images for live cells and red fluorescent images for dead cells for each optical slice were separately processed on ImageJ software (Rasband, National Institutes of Health) to obtain cell counts.

5.2.4 Insulin Secretion profile

Glucose stimulation studies were conducted on cell laden hydrogel sheets to confirm that the diffusion of glucose and insulin is not impeded across the hydrogel sheet. Insulin secretion was assessed by ELISA following static stimulation at incremental glucose concentrations (1.67 mM, 2.8 mM and 5.56 mM) in KHB.

5.3 RESULTS

5.3.1 Assessment of encapsulated cell viability

Image slices taken in the z-plane at three positions in the x-y plane provide an objective evaluation of hypoxic centers in the hydrogel (Figure 5.1). Hydrogels of 400 µm thickness provided the best average viability at all cell densities for at least 21 days and was selected for all subsequent experiments. Percent viabilities in 400 µm were 82.6 ± 1.3 %, 85.3 ± 5.2 %, 81.5 ± 5.9 % on day 1 and 43.9 ± 4.2 %, 43.1 ± 1.7 %, 68.4 ± 7.7 % on day 21 for LCD, ICD, and HCD hydrogels, respectively (Figure 5.2).

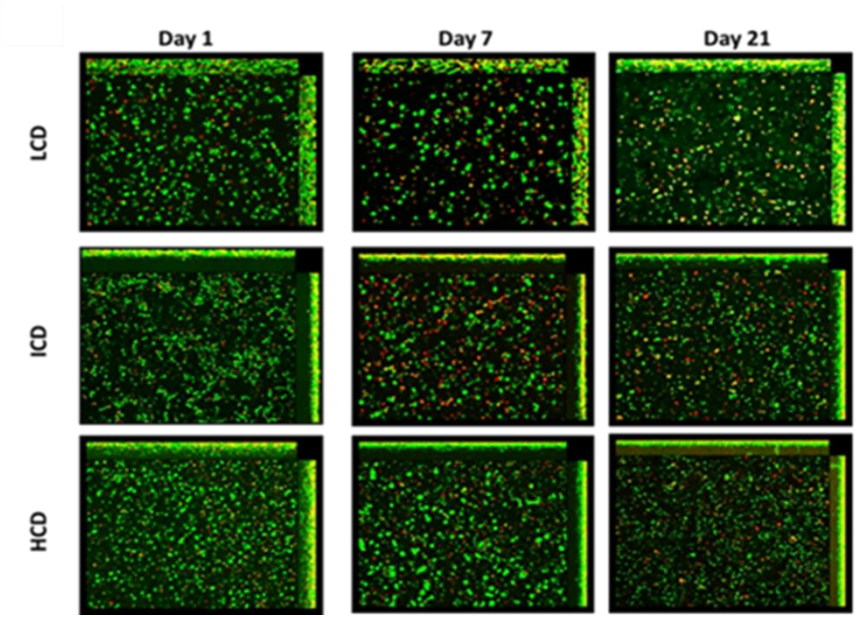

Fig. 5.1: Representative maximum intensity projection images of viability stains of encapsulated IPCs at low (LCD), intermediate (ICD) and high (HCD) cell densities using a LIVE/DEAD® Viability/Cytotoxicity Kit for mammalian cells (Invitrogen, Molecular Probes, Eugene, OR). Stains of encapsulated ISCs were taken on day 1, day 7 and day 21. Dead cells appear red and live cells appear green.

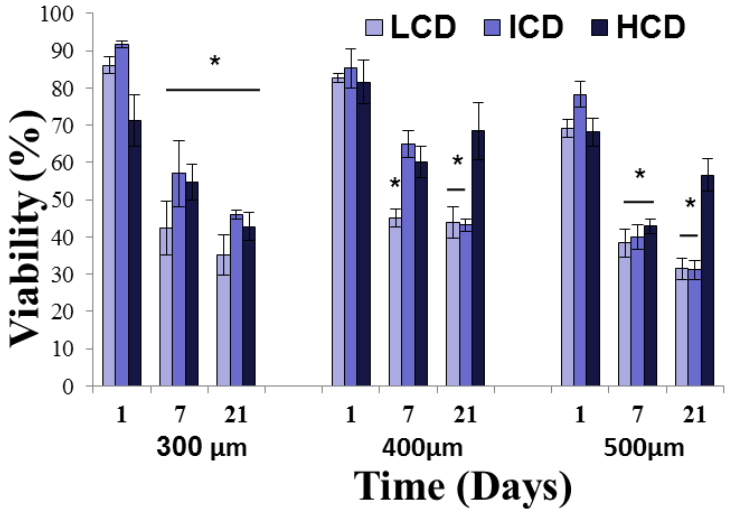

Fig. 5.2: Percentage viability curve of encapsulated IPCs at low (LCD), intermediate (ICD) and high (HCD) cell densities over time. Error bars show standard error of mean. Asterisks indicate statistical significance ($p<0.05$) compared to viabilities on day 1.

5.3.2 Glucose Stimulated Insulin Release

The effect of hydrogel geometry on insulin secretion characteristics of IPCs was evaluated by exposing hydrogel encapsulated IPCs to incremental glucose concentrations. The insulin secretory characteristics of sheet-encapsulated IPCs were unchanged and they remained unresponsive to glucose stimulation. Secreted insulin concentrations increased with increasing cell densities within hydrogels. Average insulin secretion levels were 0.45 ng/ml, 1.06 ng/ml, and 1.62 ng/ml in LCD, ICD, and HCD sheets, respectively (Figure 5.3).

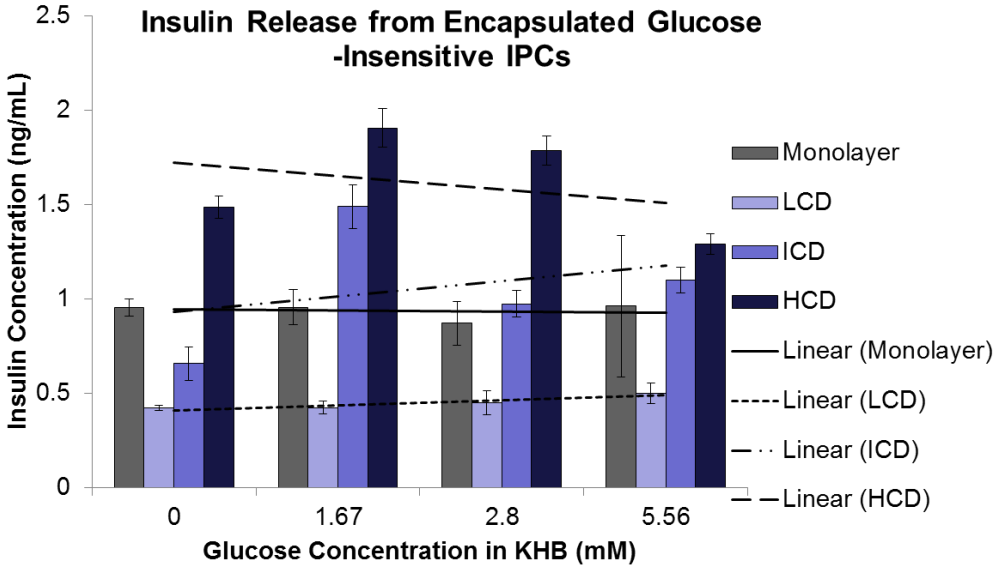

Fig. 5.3: Static glucose stimulation of monolayer and encapsulated IPCs at low (LCD), intermediate (ICD) and high (HCD) cell densities. Trend lines fit to IPCs at all cell densities are relatively flat, indicating no response to glucose stimulation. Asterisks show statistically significant differences ($p < 0.05$) in insulin secretion between incremental glucose concentrations versus control (0 mM). Error bars show standard error of mean.

5.3.3 Insulin Secretion is dependent on cell encapsulation density

A decrease in insulin secretion was observed with increasing cell densities within the hydrogels. Insulin release significantly decreased from 7.8 ± 0.84 ng/mL/10^6cells in LCD hydrogels to 4.7 ± 0.13 ng/mL/10^6cells in ICD and 1.3 ± 0.08 ng/mL/10^6cells in HCD hydrogels when sampled from day 1 cultures (Figure 5.4). However, comparing insulin release between day 1, 7 and 21 demonstrated that insulin secretion from ICD and HCD did not decrease over time and each hydrogel construct maintained its secretion levels; for example insulin secretion from HCD was 1.3 ± 0.08, 1.32 ± 0.07 and 0.8 ± 0.03 ng/mL/10^6cells on day 1, 7 and 21, respectively. Though insulin release from LCD peaked on day 7, no significant differences in insulin levels were observed between day 1 and day 21 secretion levels.

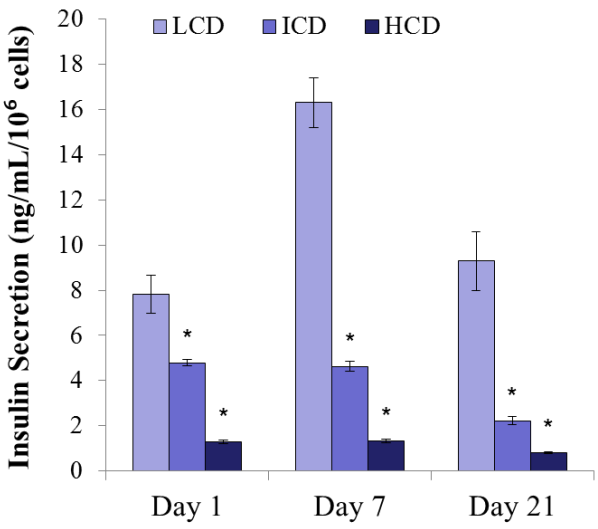

Fig. 5.4: Concentration of insulin in insulin-conditioned media sampled from encapsulated IPCs at low (LCD), intermediate (ICD) and high (HCD) cell densities. Asterisks indicate statistically significant differences (p<0.05) compared to LCD on respective days. No significant decrease in insulin secretion was observed at any encapsulation cell density until at least day 21. Error bars show standard error of mean.

5.4 DISCUSSION

The viability of encapsulated cells is dependent on the exchange of nutrients, oxygen and waste across the hydrogel sheet thickness. PEGDA hydrogel microspheres have previously been shown to maintain IPC viability and insulin secretion. Glucose independent RIN-m IPCs were encapsulated in 300 μm, 400 μm, and 500 μm thickness PEGDA sheets at LCD (0.5 x 10^6 cells/sheet), ICD (2 x 10^6 cells/sheet), and HCD (5 x 10^6 cells/sheet) to characterize the relationship between sheet thickness and cell viability at multiple encapsulated cell densities. The hydrogel sheet thickness was optimized for cell encapsulations by conducting cell viability and cytotoxicity assays at 300, 400 or 500 μm thick sheets at low, intermediate or high cell densities. In 3D cultures that are too thick, towards the center there tends to be an area where oxygen and nutrients do not reach; cells in this area die. No hypoxic centers of dead cells nor any statistically

significant difference in cell viability were observed in cell-laden PEGDA hydrogels of any sheet thickness or encapsulation density. This confirmed that cells even in the geometric center have access to nutrients and oxygen and waste products are able to diffuse out of the hydrogel. Hydrogels sheets of 400 µm thickness were therefore chosen for subsequent experiments due to their ease of handling and transparency. The opacity of the hydrogel is important for objective gross evaluation of the wound without removal of the hydrogel. Glucose stimulation studies confirmed that the insulin secretion characteristics of IPCs is maintained after the encapsulation procedure and is comparable to monolayer IPCs. The highest insulin secretion was achieved at low cell densities.

5.5 CONCLUSION

In this chapter the cell encapsulation protocol was optimized to achieve 100 % encapsulation efficiency while maintaining cell viability and the secretion profiles of the encapsulated cells. The aim of this entire study is to develop a system that delivers therapeutic products at the wound site in a single application without the need for dressing changes. At the end of this chapter, 400 µm hydrogel sheets were selected because they provide all these desired attributes, and the transparency of the sheets allows objective evaluation of the wound area without removal of the hydrogel or covering membrane and can be applied just like a bioactive bandage on the wound. The next few chapters are aimed at improving and assessing the *in vivo* therapeutic potential of these dressings.

5.6 REFERENCES

1. Pedraza E, Coronel MM, Fraker CA, Ricordi C, Stabler CL. Preventing hypoxia-induced cell death in beta cells and islets via hydrolytically activated, oxygen-generating biomaterials. Proceedings of the National Academy of Sciences of the United States of America. 2012;109(11):4245-4250. doi:10.1073/pnas.1113560109.

CHAPTER 6: COENCAPSULATION OF INSULIN-PRODUCING CELLS AND MESENCHYMAL STEM CELLS IN PEGDA HYDROGELS

Note: Portions of this chapter have been published in: 'A. Aijaz et al., **Hydrogel microencapsulated insulin-secreting cells increase keratinocyte migration, epidermal thickness, collagen fiber density, and wound closure in a diabetic mouse model of wound healing.** Tissue Eng Part A. 2015 Nov;21(21-22):2723-32. doi: 10.1089/ten.TEA.2015.0069', and represent the original work of the candidate.

6.1 INTRODUCTION

In addition to insulin, bone marrow stromal cells or mesenchymal stem cells have been reported to promote healing of chronic wounds by secretion of paracrine growth factors. MSCs have been shown to regulate inflammation by secreting anti-inflammatory cytokines and promoting macrophage migration [1, 2]. Moreover, MSCs secrete pro-wound healing MSC factors such as interleukin-1 receptor antagonist (IL-1RA), TGF-β1, EGF, KGF, bFGF, VEGF and SDF-1, all of which have been reported to increase vascularity and reduce wound size [3-5]. Additionally, MSCs induce differentiation of fibroblasts to myofibroblasts, which express α-smooth muscle actin (α-SMA) thereby contracting the wound, while VEGF secretion by MSCs stimulates angiogenesis [3]. However, MSCs applied as a cell suspension tend to migrate away from the wound site or do not remain viable in the protease-rich chronic wound environment. MSCs have been embedded in scaffolds made of natural or synthetic polymers; however, natural polymers are themselves immunogenic while hydrolysis products of synthetic polymers reduce growth factor bioactivity over time.

Exogenous insulin [6-10] and MSC administration [11, 12] have separately accelerated wound healing in both diabetic and non-diabetic animals as well as in deep burns, but with the exclusion of this study, these two therapies have never been combined for wound healing. Since topical insulin creams preclude using MSCs, in this chapter, IPCs and MSCs were coencapsulated in

various ratios in PEGDA hydrogels sheets to explore the synergistic potential of insulin and MSCs in accelerating wound healing and to exploit the beneficial properties of MSC-derived trophic factors on insulin secreting cells. Studies have shown that MSCs demonstrate a protective effect on islet (insulin-producing cells) viability, increase their insulin secretory function and result in fewer islets required to achieve efficacy [13].

Another goal of this chapter is to explore the mechanism through which insulin and MSCs promote wound healing. One of the major signaling pathways through which insulin exerts a prowound healing response is the ERK1/2 and PI3K signaling [14]. The PI3K/Akt pathway is activated in an insulin-dependent manner and Akt phosphorylation is stimulated by insulin and factors secreted by MSCs, specifically VEGF and EGF [15]. Insulin also prevents apoptotic cell death induced by inflammatory stimuli by counteracting the dephosphorylation of Akt by TNF-α and promotes angiogenesis by stimulating the expression of VEGF via Akt signaling [16].

The final goal of this chapter was to select IPC and MSC coencapsulation ratio(s) that (1) maximize insulin and MSC factor release and (2) maximize keratinocyte migration and Akt phosphorylation *in vitro*.

6.2 MATERIALS AND METHODS

6.2.1 Cell Culture

The constant insulin producing rat insulinoma beta RIN-m cell line was purchased from American Type Culture Collection (ATCC, Manassas, VA) and propagated in RPMI-1640 medium (ATCC) supplemented with 10% fetal bovine serum (FBS; Sigma), 1% w/v penicillin-streptomycin (pen-strep; Sigma) in a humidified incubator at 37 °C/5% CO_2. Human bone-marrow derived MSCs were purchased from the Institute of Regenerative Medicine at Texas A&M at passage 1 and propagated in alpha-minimal essential medium (α-MEM; Sigma) without deoxyribo- or ribo-nucleotides, supplemented with 10% v/v fetal bovine serum (FBS; Atlanta

Biologicals, Flowery Branch, GA), 1% w/v penicillin-streptomycin, 4 mM L-glutamine (Life Technologies) and 1 ng/ml basic fibroblast growth factor (bFGF; Life Technologies).

6.2.2 Cell Encapsulation

RIN-m cells (IPCs) and human MSCs (hMSCs) were encapsulated within PEGDA hydrogel sheets by photopolymerizing cells suspended in a precursor solution formed by combining 0.1 g/mL 10 kDa PEGDA (10% w/v; Laysan Bio, Inc.) with (1.5% v/v) triethanolamine/ HEPES buffered saline (pH 7.4), 37mM 1-vinyl-2-pyrrolidinone, 0.1mM eosin Y. The cell-prepolymer suspension (1.5×10^4 – $1.5x10^5$ cells/μL) was pipetted into 1 cm^2 custom made molds and exposed to white light for 20 seconds to achieve 400 μm thick cell-laden hydrogel sheets. Thus, IPC-laden hydrogels were encapsulated at low (LCD; 0.5 x 10^6 cells/sheet), intermediate (ICD; 2 x 10^6 cells/sheet) and high (HCD; 5 x 10^6 cells/sheet) cell densities and MSCs encapsulated with IPCs at ratios of 1:1, 1:5, 10:1, 5:1, or 10:1 (IPC:MSC) were formed, with the 1:1 (IPC:MSC) ratio referring to 0.5 x 10^6 IPCs and 0.5 x 10^6 MSCs. Crosslinked hydrogels were gently lifted with blunt forceps and placed in Transwells® (0.4 mm pore polycarbonate membrane Transwell® inserts; Corning, Inc., Lowell, MA) in a 12-well plate with 3 ml culture medium. Hydrogels were maintained in a humidified incubator at 37 °C/5% CO_2. For monolayer comparisons, 1 x 10^6 IPCs or hMSCs were plated on 6-well tissue culture plates.

6.2.3 Concentration of insulin and released MSC factor

IPCs encapsulated alone and ISCs coencapsulated with hMSCs in PEGDA hydrogel sheets were maintained in complete culture medium at 37°C in a humidified, 5% CO2 incubator. CM containing insulin and MSC factors released from the cell-laden hydrogel sheets was collected on day 1, 7 and 21 to assess the synergistic effect of the MSC and ISC secretome. Media were

changed on every second day, such that odd days had 24 hours of MSC factor accumulation. Concentrations of insulin and MSC factors (TGF-β1 and VEGF) in the CM was assessed by ELISA.

6.2.4 Keratinocyte Scratch Assay

Human keratinocytes (HaCaT; Addex Bio, San Diego, CA) were propagated in DMEM (Sigma), supplemented with 10% FBS (Sigma), pen-strep (Sigma) in a humidified incubator at 37 °C/5% CO_2. For scratch assays, 180,000 HaCaT cells/well were seeded onto 24 well plates (Greiner Bio-one; Monroe, NC). Cells were cultured for 48 hours to form a confluent monolayer at which time a single scratch of 415 μm ± 73 μm was produced in the center of the well with a 10 μL pipette tip. The wells were washed twice with Dulbecco's Phosphate Buffered Saline (DPBS; Sigma) to remove cell debris. HaCaT cells were then stimulated with CM containing insulin and/or MSC factors sampled on days 1, 7 and 21 from cell-laden hydrogels. IPCs and MSCs cells were not maintained in monolayers beyond four days since the cells became over-confluent, resulting in cell death too great to collect insulin-conditioned media on days 7 and 21. Media from empty hydrogels was used as negative controls. HaCaT cell migration across the scratch was imaged at 0, 24, 48, 72 and 96 hours using phase contrast microscopy and analyzed on NIH ImageJ software.

6.2.5 AKT phosphorylation

Rat L6 myoblast cells (ATCC) were plated at 112,500 cells/mL in a 96 well plate. L6 myoblasts are known to produce phosphorylated Akt (p-AKT) when stimulated by numerous wound healing moieties. L6 myoblasts were stimulated with CM from release experiments and the levels of p-Akt were compared against the levels of total-Akt (T-Akt) using a Fast Activated Cell-based ELISA kit.

6.3 RESULTS

6.3.1 MSCs Improve Insulin Secretion

Coencapsulation with MSCs improved insulin release from IPCs. Insulin secretion levels from LCD hydrogels were 7.8 ± 2.1, 16.3 ± 2.7 and 9.3 ± 3.2 ng/mL/10^6 cells on day 1, 7 and 21, respectively, and increased to 12.9 ± 3.9, 20.9 ± 2.2 and 27.5 ± 13.1 ng/mL/10^6 cells on day 1, 7 and 21, respectively in IPC:MSC (1:1) (Figure 6.1). This corresponds to fold increases of 1.7 on day 1 and 3.0 on day 21 in insulin secretion between LCD and IPC:MSC (1:1), which are hydrogel constructs with equivalent numbers of IPCs (0.5 x 10^6 cells). IPC:MSC (1:1), followed by LCD, provided the most significant per cell increases in insulin secretion which were maintained for at least 21 days.

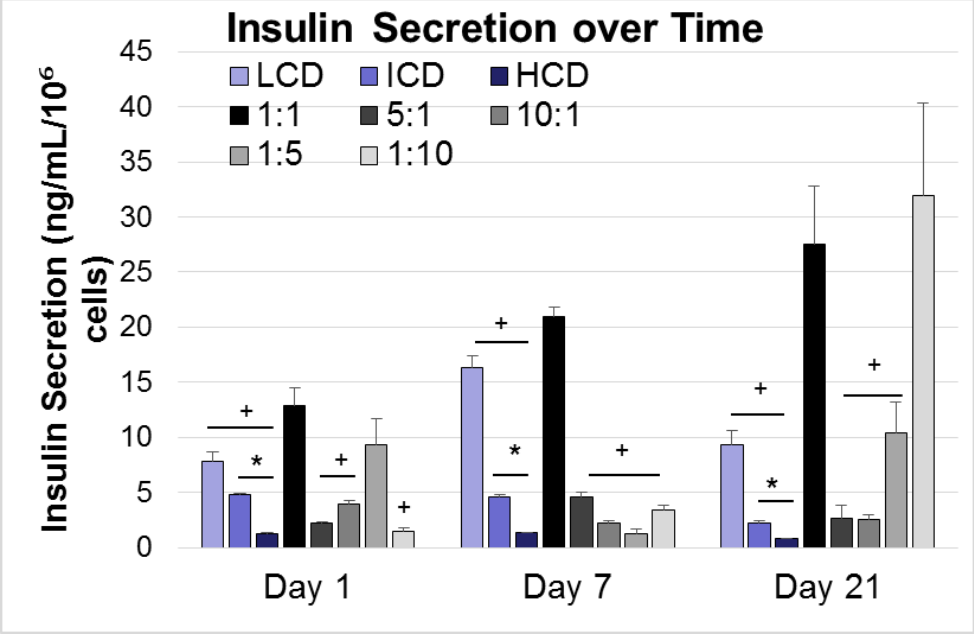

Fig. 6.1: Concentration of insulin in insulin-conditioned media sampled from encapsulated IPCs at low (LCD), intermediate (ICD) and high (HCD) cell densities and IPC:MSC coencapsulations 1:1, 5:1, 10:1, 1:5 and 1:10 ratios. Asterisks indicate statistically significant differences (p<0.05) compared to LCD on respective days. Plus signs indicate statistically significant differences (p<0.05) compared to 1:1 coencapsulations on respective days. No significant decrease in insulin secretion was observed at any encapsulation cell density until at least day 21. Error bars show

standard error of mean.

6.3.2 MSC Factor Release

An increase in TGF-β1 secretion from MSCs was seen in hydrogels with a higher ratio of IPCs compared to when MSCs were cultured alone, whether in monolayers or encapsulated in hydrogels. This increase in TGF-β1 secretion continued for at least 21 days. TGF-β1 concentration secreted on day 1 from monolayer MSCs, MSC-alone hydrogels, and IPC:MSC coencapsulation hydrogels at 1:1, 5:1, and 10:1 ratios were 161.6 ± 102.3, 347.1 ± 48.2, 610.4 ± 70.1, 414.3 ± 91.2 and 493.7 ± 133.2 pg/mL/10^6 cells, respectively (Figure 6.2). A fold increase of 1.8 was observed in TGF-β1 between day 7 and day 21 in IPC:MSC (1:1) hydrogels.

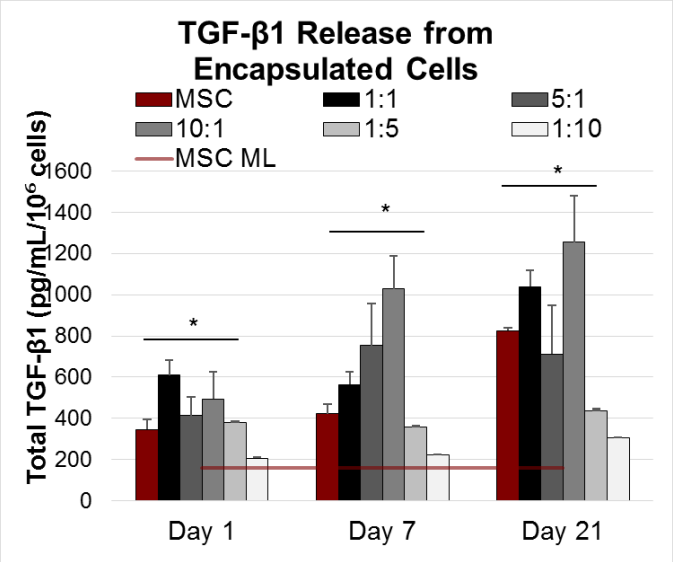

Fig. 6.2: Concentration of TGF-β1 in CM. MSC ML = MSC monolayers, MSC = MSCs encapsulated in hydrogel sheets, ratios are IPC to MSC coencapsulations at 1:1, 5:1, 10:1, 1:5 and 1:10. Asterisks indicate statistically significant differences (p<0.05) compared to MSCs in hydrogels on respective days. No significant decreases were observed at any encapsulation cell density until at least day 21. Error bars show standard error of mean.

VEGF release was not detected in MSC monolayers, but was in IPC:MSC hydrogels. MSCs are known to secrete VEGF to promote islet vascularization. The highest levels of VEGF were achieved in high IPC ratio coencapsulations with concentrations of 562.2 ± 216.0, 353.8 ± 204.4, 470.6 ± 139.9 pg/mL/10^6 cells from 1:1, 5:1 and 10:1 ratios, respectively, while secretion from MSC-alone hydrogels was 23.6 ± 5.1 pg/mL/10^6 cells (Figure 6.3).

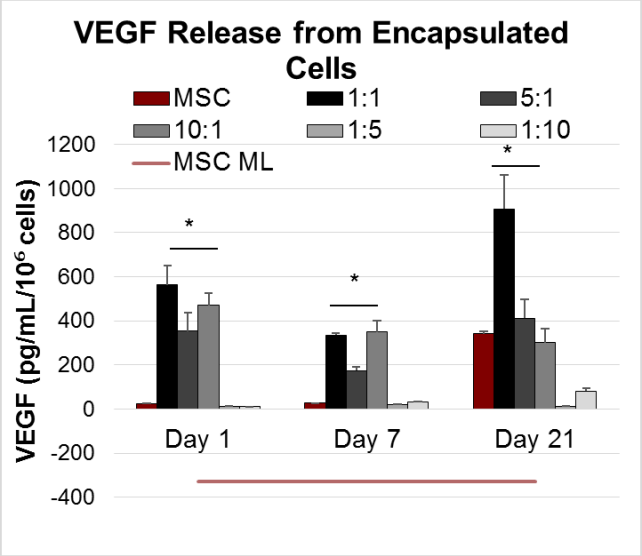

Fig. 6.3: Concentration of VEGF in CM. MSC ML = MSC monolayers, MSC = MSCs encapsulated in hydrogel sheets, ratios are IPC to MSC coencapsulations at 1:1, 5:1, 10:1, 1:5 and 1:10. Asterisks indicate statistically significant differences (p<0.05) compared to MSC on respective days. No significant decreases were observed at any encapsulation cell density until at least day 21. Error bars show standard error of mean.

6.3.3 Presence of insulin and MSC factors promote in vitro keratinocyte migration

Significant increases in scratch closure rates were observed when scratches in keratinocyte monolayers were treated with insulin and/or MSC factor CM sampled on days 1, 7 and 21 compared to unstimulated conditions (Figure 6.4). Closure rates achieved when scratches were stimulated with CM from single-cell hydrogels were analyzed. CM from LCD hydrogels

promoted significant keratinocyte migration compared to CM from ICD or HCD hydrogels on days 1, 7 and 21. No significant differences were observed between closure rates from ICD and HCD hydrogel CM. Scratch closure rates were 75.1 ± 18.7, 16.0 ± 2.9 and 7.6 ± 1.9 μm/h/10^6 cells from CM from LCD, ICD and HCD hydrogels, respectively. Scratch closure rates induced by day 1 MSC and LCD hydrogels were statistically similar.

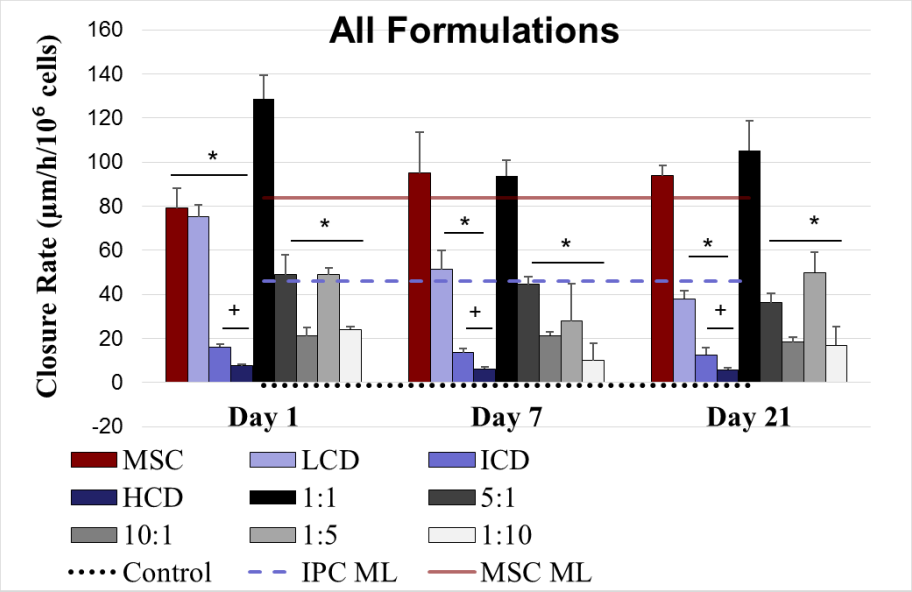

Fig. 6.4: Quantification of keratinocyte scratch assays demonstrating insulin/MSC bioactivity. Scratch closure rates following stimulation with media from empty hydrogels (control), insulin-containing CM sampled from: low (LCD), intermediate (ICD), and high (HCD) cell density hydrogels, and IPC to MSC coencapsulations at 1:1, 5:1, 10:1, 1:5 and 1:10. Asterisks indicate statistically significant differences (p<0.05) compared to 1:1 hydrogels. Plus signs indicate statistically significant differences (p<0.05) compared to LCD hydrogels. All cell-laden hydrogels promoted significant keratinocyte migration compared to controls. Error bars show standard error of mean.

Scratch closures stimulated by CM collected on day 1 from IPC:MSC (1:1), LCD and MSC hydrogels were 128.6 ± 10.53, 75.1 ± 6.61, 79.02 ± 8.9 μm/hr/10^6 cells, respectively, while controls demonstrated a rate of -1.2 ± 1.7 μm/hr. Closure rates in keratinocytes stimulated by CM collected on day 1 from IPC:MSC (1:1) hydrogels were significantly higher than those achieved with CM collected from MSC-alone hydrogels or IPC-alone hydrogels. Specifically, no significant difference was observed in closure rates from MSC and LCD hydrogels. LCD hydrogels showed decreasing insulin bioactivity over time; conversely, the bioactivity of MSC trophic factors remained steady. Closure rates induced by CM sampled from IPC:MSC (1:1) on day 7 and day 21 were 93.6 ± 13.9, 105.0 ± 23.8 μm/hr/10^6 cells, respectively. Thus, no significant differences were observed between the bioactivity of CM from IPC:MSC (1:1) hydrogels sampled on day 1 and day 21. Closure rates from 1:1 and MSC hydrogels were statistically similar. The fastest closure rates were observed with IPC:MSC (1:1) hydrogels, followed by MSC, LCD and IPC:MSC (5:1) hydrogels.

6.3.4 Akt Phosphorylation is stimulated by both insulin and MSC factors

Akt phosphorylation is stimulated in an insulin dependent manner and provides a confirmation of insulin bioactivity *in vitro*. All cell-laden hydrogels stimulated significant Akt phosphorylation compared to controls. Similar to keratinocyte migration assays, LCD elicited significantly higher Akt phosphorylation levels compared to ICD and HCD hydrogels (Figure 6.5). ICD and HCD hydrogels were statistically similar in inducing levels of p-Akt. No significant decrease in bioactivity of CM sampled from LCD, ICD, HCD or MSC hydrogels was observed for at least 21 days as measured via Akt phosphorylation assay. P-AKt levels were 243.5 ± 81.5, 49.7 ± 9.5, 28.7 ± 12.9 and 255.1 ± 20.6 % p-Akt/total Akt/10^6 cells for LCD, ICD, HCD and MSC-alone hydrogels, respectively. No difference was observed in the bioactivity of factors released from monolayer and encapsulated MSCs. A slight decrease was observed in Akt phosphorylation achieved from LCD hydrogels compared to monolayer IPCs; however, the phosphorylation levels

did not diminish when the same number of IPCs were coencapsulated with MSCs at the IPC:MSC (1:1) ratio.

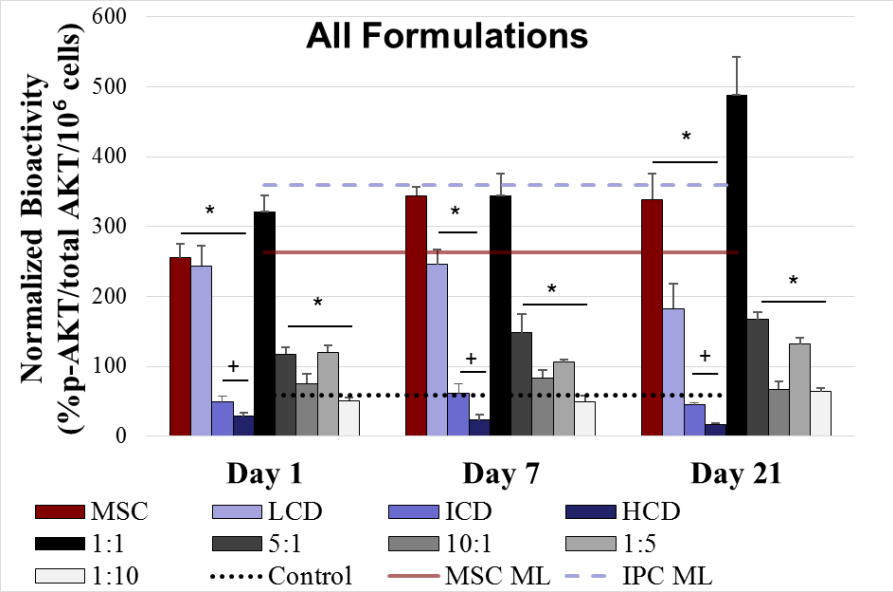

Fig. 6.5: Quantification of Akt phosphorylation and insulin/MSC bioactivity. P-Akt following stimulation by media from empty hydrogels (control), insulin CM sampled from: low (LCD), intermediate (ICD) and high (HCD) cell density hydrogels, and IPC:MSC coencapsulations at 1:1, 5:1, 10:1, 1:5 and 1:10 ratios. Asterisks indicate statistically significant differences (p<0.05) compared to IPC:MSC (1:1) hydrogels. Plus signs indicate statistically significant differences (p<0.05) compared to LCD hydrogels. All cell-laden hydrogels promoted significant Akt phosphorylation compared to controls. Error bars show standard error of mean.

The bioactivity of insulin and MSC factors from CM collected on day 1 in stimulating Akt phosphorylation were 321.4 ± 23.4, 243.5 ± 28.8, 255.1 ± 20.6 and 59.2 ± 5.9 % p-Akt/total Akt/10^6 cells for IPC:MSC (1:1), LCD, MSC alone and control hydrogels, respectively. Phosphorylated Akt achieved from IPC:MSC (1:1) was significantly higher for at least 21 days compared to all other hydrogel constructs, with the exception of CM sampled on day 7 from MSC hydrogels, which was equal to IPC:MSC(1:1).

6.4 DISCUSSION

Insulin has been shown to accelerate wound healing by recruiting keratinocytes, endothelial cells and fibroblasts via the PI3-Akt pathway [1], while MSCs have been demonstrated to improve IPC viability and function [2], regulate inflammation, and secrete pro-wound healing factors [3]. The goal of this chapter was to achieve IPC and MSC coencapsulations with superior insulin and MSC factor release, keratinocyte migration, and Akt phosphorylation compared to single-cell hydrogels. MSCs improved insulin secretion by as much as 3 fold compared to IPCs encapsulated alone, and the insulin concentration in the media increased until at least day 21. This increase in insulin release over time might be attributed to the ability of MSCs to sustain IPC viability and improve their insulin secretion function. TGF-β1 secretion increased with increasing IPC density. TGF-β1 is known to preserve and prolong survival of islets. Increases in TGF-β1 release between day 7 and day 21 suggest that MSCs increase TGF-β1 secretion to improve IPC survival in later days. VEGF release was not detected in MSC monolayers, but was in IPC:MSC hydrogels; MSCs are known to secrete VEGF to promote islet vascularization. This "rescue phenomenon" was particularly evident when considering that conditions that caused insulin secretion to drop simultaneously caused MSC factor release to increase. When comparing insulin secretion from higher IPC density coencapsultion (5:1 and 10:1) to TGF- β1 and VEGF release from MSCs, insulin levels from IPC:MSC (5:1) and IPC:MSC (10:1) were significantly lower while TGF- β1 and VEGF from these hydrogels was considerably higher. This suggests that MSCs increased their factor release in response to apoptosing IPCs, which are known to underdo hypoxic cell death at high cell densities. In addition to protecting IPCs, both TGF-β1 and VEGF play a critical role in wound healing.

Results from both single-cell and dual-cell hydrogels were assessed. LCD provided the maximum stimulation of keratinocyte migration compared to ICD and HCD, and 0.5 x 10^6 cells were sufficient to achieve this effect. LCD hydrogels showed decreasing insulin bioactivity over time

and this drop in insulin bioactivity was also observed in IPC:MSC (1:1) hydrogels, which initially demonstrated a slight decrease in closure rate from day 1 and day 7 CM, but the bioactivity was regained in day 21 CM possibly due the presence of MSCs. *In vitro* analysis of scratch assay closure rates and insulin bioactivity suggested that IPC:MSC (1:1) hydrogels might outperform MSC hydrogels, particularly when considering day 21 results. However, *in vitro* results do not fully predict the profound differences in wound healing responses *in vivo* and demonstrate the continued need to evaluate *in vitro* models in concert with *in vivo* models. Taking keratinocyte migration assay results together, a 100 μm wide scratch wound closed in 46.6, 75.9 and 79.8 minutes when treated with CM containing both insulin and MSC factors, only MSC factors or only insulin, respectively.

Results also revealed the role of the Akt pathway in the accelerated healing achieved by the hydrogels. Protein kinase B or Akt is a downstream signaling target of the ERK1/2 and PI3K pathways that plays a vital role in multiple cellular processes such as glucose metabolism, apoptosis, cell proliferation and cell migration [21]. Both insulin and MSCs factors, specifically, VEGF and EGF induce Akt phosphorylation. The released insulin and MSC factors stimulated Akt phosphorylation with the most significant effect achieved on day 21 with IPC:MSC (1:1) with fold increases of 2.7 and 1.4 over LCD and MSC hydrogels, respectively.

6.5 CONCLUSIONS

Experiments conducted in this chapter led to the understanding that IPCs and MSCs have a cooperative effect on each other; MSCs improve insulin secretion from IPCs, conversely IPCs induce growth factor, particularly TGF-β1 and VEGF release from MSCs. The *in vitro* bioactivity demonstrated the synergistic effect of insulin and MSC growth factors on keratinocyte migration and Akt phosphorylation both of which are pro-wound healing responses. *In vitro* bioactivity assays confirmed the superior performance of IPC:MSC (1:1), LCD, and MSC hydrogels, thus

these hydrogels were chosen to move forward with for *in vivo* studies. The increased TGF-β1 and VEGF secretion from IPC:MSC hydrogels was expected to have implications during *in vivo* wound healing by inducing granulation tissue formation, collagen maturation, reepithelialization and neovascularization in the wound bed.

An analogy can thus far be derived here: achieving the right stoichiometry is critical. That is to say, finding the critical cell number of IPCs and MSCs for coencapsulation in order to maximize insulin and MSC factor release will provide the desired therapeutic benefit.

6.6 REFERENCES

1. Chen L, Tredget EE, Wu PYG, Wu Y. Paracrine factors of mesenchymal stem cells recruit macrophages and endothelial lineage cells and enhance wound healing. PLoS One. 2008 Apr 2;3(4):e1886. PMID:18382669.
2. Lee EY, Xia Y, Kim W, Kim MH, Kim TH, Kim KJ, Park B, Sung J. Hypoxia-enhanced wound-healing function of adipose-derived stem cells: Increase in stem cell proliferation and up-regulation of VEGF and bFGF. Wound Repair Regen. 2009 Jul-Aug;17(4):540-547. PMID:19614919.
3. Faulknor RA, Olekson MA, Nativ NI, Ghodbane M, Gray AJ, Berthiaume F. Mesenchymal stromal cells reverse hypoxia-mediated suppression of α-smooth muscle actin expression in human dermal fibroblasts. Biochem Biophys Res Commun. 2015
4. Vojtassak J, Danisovic L, Kubes M, Bakos D, Jarabek L, Ulicna M, Blasko M. Autologous biograft and mesenchymal stem cells in treatment of the diabetic foot. Neuro Endocrinol Lett. 27(Suppl 2), 134, 2006
5. Han SK, Yoon TH, Lee DG, Lee MA, Kim WK. Potential of human bone marrow stromal cells to accelerate wound healing in vitro. Ann Plast Surg. 55(4):414, 2005.
6. Greenway, S.E., Filler, L.E., and Greenway, F.L. Topical insulin in wound healing: a randomised, double-blind, placebo-controlled trial. J Wound Care 8, 526, 1999.
7. Madibally, S.V., Solomon, V., Mitchell, R.N., Van De Water, L., Yarmush, M.L., and Toner, M. Influence of insulin therapy on burn wound healing in rats. J Surg Res 109, 92, 2003.
8. Rezvani, O., Shabbak, E., Aslani, A., Bidar, R., Jafari, M., and Safarnezhad, S. A randomized, double-blind, placebo controlled trial to determine the effects of topical insulin on wound healing. Ostomy Wound Manage 55, 22, 2009.
9. Sen, C.K., Gordillo, G.M., Roy, S., Kirsner, R., Lambert, L., Hunt, T.K., Gottrup, F., Gurtner, G.C., and Longaker, M.T. Human skin wounds: a major and snowballing threat to public health and the economy. Wound Repair Regen 17, 763, 2009.
10. Procha´zka, V., Gumulec, J., Jaluvka, F., Salounova´, D., Jonszta, T., Czerny, D., Krajca, J., Urbanec, R., Klement, P., and Martinek, J. Cell therapy, a new standard in management of chronic critical limb ischemia and foot ulcer. Cell Transplant 19, 1413, 2010.
11. Liu D, Xiong H, Ning P, Chen J, Lan W. Amniotic membrane loaded with bone marrow mesenchymal stem cells facilitates the healing of deep burn wound. Biomedical Engineering and Informatics (BMEI), 2010 3rd International Conference on. 2010 4:1633-1635.

12. Yoshikawa T, Mitsuno H, Nonaka I, Sen Y, Kawanishi K, Inada Y, Takakura Y, Okuchi K, Nonomura A. Wound therapy by marrow mesenchymal cell transplantation. Plast Reconstr Surg. 2008 Mar;121(3):860-877. PMID:18317135.
13. Kerby A, Jones ES, Jones PM, King AJ. Co-transplantation of islets with mesenchymal stem cells in microcapsules demonstrates graft outcome can be improved in an isolated-graft model of islet transplantation in mice. Cytotherapy. 15(2), 192, 2013.
14. Shanley, L.J., McCaig, C.D., Forrester, J.V., and Zhao, M. Insulin, not leptin, promotes in vitro cell migration to heal monolayer wounds in human corneal epithelium. Invest Ophthalmol Vis Sci 45, 1088, 2004.
15. Joshua D. Ochocki and M. Celeste Simon. Nutrient-sensing pathways and metabolic regulation in stem cells. J Cell Biol. 203(1), 23, 2013.
16. Hermann, C., Assmus, B., Urbich, C., Zeiher, A.M., and Dimmeler, S. Insulin-mediated stimulation of protein kinase Akt: a potent survival signaling cascade for endothelial cells. Arterioscler Thromb Vasc Biol 20, 402, 2000.
17. Liu, Y., Petreaca, M., Yao, M., and Martins-Green, M. Cell and molecular mechanisms of keratinocyte function stimulated by insulin during wound healing. BMC Cell Biol 10, 1, 2009.
18. Lee EY, Xia Y, Kim W, Kim MH, Kim TH, Kim KJ, Park B, Sung J. Hypoxia-enhanced wound-healing function of adipose-derived stem cells: Increase in stem cell proliferation and up-regulation of VEGF and bFGF. Wound Repair Regen. 2009 Jul-Aug;17(4):540-547. PMID:19614919
19. Kerby A, Jones ES, Jones PM, King AJ. Co-transplantation of islets with mesenchymal stem cells in microcapsules demonstrates graft outcome can be improved in an isolated-graft model of islet transplantation in mice. Cytotherapy. 15(2), 192, 2013.
20. Aijaz, A., Faulknor, R., Berthiaume, F., and Olabisi, R. M. (2015). Hydrogel microencapsulated insulin-secreting cells increase keratinocyte migration, epidermal thickness, collagen fiber density, and wound closure in a diabetic mouse model of wound healing. Tissue Eng Part A. 21(21-22):2723-32. doi: 10.1089/ten.TEA.2015.0069.
21. Brendan D. Manning and Lewis C. Cantley. AKT/PKB Signaling: Navigating Downstream. Cell. 2007 Jun 29; 129(7): 1261–1274. doi: 10.1016/j.cell.2007.06.009.

CHAPTER 7: INSULIN-PRODUCING CELLS AND MESENCHYMAL STEM CELLS COENCAPSULATED INTO PEGDA HYDROGELS ACCELERATE WOUND CLOSURE AND REDUCES SCAR AND SCAB FORMATION IN A DIABETIC MOUSE MODEL OF WOUND HEALING

Note: Portions of this chapter have been published in: 'A. Aijaz et al., **Hydrogel microencapsulated insulin-secreting cells increase keratinocyte migration, epidermal thickness, collagen fiber density, and wound closure in a diabetic mouse model of wound healing.** Tissue Eng Part A. 2015 Nov;21(21-22):2723-32. doi: 10.1089/ten.TEA.2015.0069', and represent the original work of the candidate.

7.1 INTRODUCTION

Cytokines play an important role as mediators of host-injury responses and regulate subsequent repair. A skewed cytokine milieu of the wound bed leads to abnormal wound healing responses. Cytokines are predominantly secreted by immune cells and act both locally at the site of injury and systemically to initiate reparative responses. Chronic wounds are characterized by an increased presence of wound macrophages and an imbalance of pro and anti-inflammatory cytokines, resulting in a prolonged inflammatory phase. This persistence of wound inflammation alters the expression of growth factors and inhibits the normal transition to the proliferation and remodeling phase that would repair the cutaneous injury and restore the epidermal barrier. Topical growth factor treatments have been explored to address the altered cytokine milieu of chronic wounds; however, the presence of high concentrations of proteases in the inflammatory wound environment results in the degradation and loss of growth factors. MSC growth factors play critical roles in orchestrating a multitude of effects; they act as mitogens and chemoattractants to neutrophils and macrophages and as stimulants of fibroblast, keratinocyte and

endothelial cell proliferation, thereby regulating extracellular matrix production, wound contraction, reepithelialization and angiogenesis.

In this chapter, the potential of combined insulin and MSC factors to synergistically accelerate wound healing was explored. Results from the previous chapter demonstrated that each cell type has a stimulating effect on pro-wound healing factor secretion from the other cell type, i.e MSCs promote insulin secretion from IPCs and IPCs promote MSC growth factor secretion. Therefore, the rationale of the current chapter is that the increased pro-wound healing factors from coencapsulated cells will accelerate wound healing faster than reduced levels released by singly encapsulated cells.

7.2 MATERIALS AND METHODS

7.2.1 Cell Culture

The constant insulin producing rat insulinoma beta RIN-m cell line was purchased from American Type Culture Collection (ATCC, Manassas, VA) and propagated in RPMI-1640 medium (ATCC) supplemented with 10% fetal bovine serum (FBS; Sigma) and 1% w/v penicillin-streptomycin (pen-strep; Sigma) in a humidified incubator at 37 °C/5% CO_2. Human bone-marrow derived MSCs were purchased from the Institute of Regenerative Medicine at Texas A&M at passage 1 and propagated in alpha-minimal essential medium (α-MEM; Sigma) without deoxyribo- or ribo-nucleotides, supplemented with 10% v/v fetal bovine serum (FBS; Atlanta Biologicals, Flowery Branch, GA), 1% w/v penicillin-streptomycin, 4 mM L-glutamine (Life Technologies) and 1 ng/ml basic fibroblast growth factor (bFGF; Life Technologies).

7.2.2 Cell Encapsulation

RIN-m cells (IPCs) and/or human MSCs were encapsulated within PEGDA hydrogel sheets by photopolymerizing cells suspended in a precursor solution formed by combining 0.1 g/mL 10 kDa PEGDA (10% w/v; Laysan Bio, Inc.) with (1.5% v/v) triethanolamine/ HEPES buffered

saline (pH 7.4), 37mM 1-vinyl-2-pyrrolidinone, 0.1mM eosin-Y. The cell-prepolymer suspension containing 1 x 10^4 IPCs and/or MSCs was pipetted into 1 cm^2 custom made molds and exposed to white light for 20 seconds to achieve 400 μm thick cell-laden hydrogel sheets. Crosslinked hydrogels were gently lifted with blunt forceps and placed in Transwells (0.4 mm pore polycarbonate membrane Transwell inserts; Corning, Inc., Lowell, MA) in a 12-well plate with 3 ml culture medium. Hydrogels were maintained in a humidified incubator at 37 °C/5% CO_2. IPCs or hMSCs were plated on 6-well tissue culture plates for monolayer comparisons.

7.2.3 Animal Studies

Animal studies were performed to quantify wound healing responses in vivo. All procedures were performed in accordance with protocols approved by the Rutgers University IACUC. A 1 cm x 1 cm full thickness excisional wound was created on the dorsa of genetically diabetic male mice (BKS.Cg-m +/+ Leprdb/J; 10 weeks old, N=24; Jackson Laboratories, Bar Harbor, ME). Hydrogels laden with LCD (n=6), MSCs alone (n=6), or IPC:MSC (1:1) (n=6) were applied to wounds, which were then covered with Tegaderm™ and photographed at postoperative days (POD) 3, 7, 14, 18, 21, and 28 for gross appearance. Phosphate buffered saline (PBS) at 50 μL was applied to control animals (n=6). Wound area was measured by tracing the wound margins using ImageJ. Wound closure was calculated as percent area of original wound. Animals were sacrificed by CO_2 inhalation on PODs 14 (N=12; n=3 per group) and 28 (N=12; n=3 per group) and wound tissue was collected for histology.

7.2.4 Histological Analysis

Wound tissue was excised for histological analysis after sacrifice by cutting around the edges of the wounded area. Tissue sections were stained with H & E for morphological analysis, PASR stain for collagen fiber density, Ki67 for cell proliferation and α-SMA for wound contraction. Wound tissues were fixed in 10 % formalin for 24 hours at room temperature and then stored in 70 % ethanol at 4^{o}C until serial sectioning (5 μm thick) and staining with H & E PASR at the

Digital Imaging and Histology Core, Rutgers-NJMS Cancer Center. Histological images were analyzed on ImageJ software to find epidermal and dermal thickness and collagen density. H & E-stained sections were analyzed in ImageJ to measure the thickness of epidermis and dermis using the Line Selection Tool. Lines were created across the thickness of the epidermal or dermal boundaries at five random locations in each H & E section and lengths were averaged. RGB images of PASR-stained sections were converted to gray scale by splitting the images into red, green and blue channels. For accurate visual determination of image threshold for collagen-stained areas, the red and green channels were selected as it yielded the best contrast between the stain and the background. The thresholded images were analyzed to measure percent area of collagen density [4].

7.2.5 Statistical Analysis

All data were taken in triplicate and reported as mean ± standard deviation. Different treatment groups were compared using a one-way analysis of variance (ANOVA). Pairwise comparisons were made between groups using Fisher's Least Significant Difference (LSD) post-hoc test. *P*-values less than 0.05 were considered significant. All analyses were performed using KaleidaGraph statistical software version 4.1.0, Synergy Software (Reading, PA).

7.3 RESULTS

7.3.1 In vivo Wound Healing Response

No difference in wound closures was observed between the treatments and the controls until POD 7. Compared to controls, IPC:MSC (1:1) and IPC treated wounds demonstrated significant differences in wound closures by POD 14, while MSC treated wounds showed improvement on POD 18. At each time point until POD 28, IPC:MSC(1:1) treated wounds were superior in wound closure compared to IPC or MSC treated wounds. No scab formation was observed in any of the IPC:MSC (1:1) treated animals. Wounds in these animals were soft to the touch, while control

animals had either open wounds or had a hard scab formed on the wounds. Some of the wounds treated with IPC or MSC had an initial scab formation which was weakly attached to the underlying tissue. IPC:MSC (1:1) demonstrated remarkable increase in wound closure by POD 14, with 5 of 6 animals' wounds completely healed. Complete closure was achieved on POD 18 in all animals treated with IPC: MSC (1:1), a significant difference compared to all other groups, which were still open on POD 28. Percent wound closure on POD 18 were 100 ± 0 %, 65.6 ± 15.2 %, 62.9 ± 16.2 % and -10.44 ± 9.65 % in IPC:MSC (1:1), MSC, IPC and control animals, respectively (Figure 7.1). No significant difference was observed in healing rates between IPC and MSC treated wounds. Controls did not show any difference in wound closure dynamics between successive time points until at least POD 28.

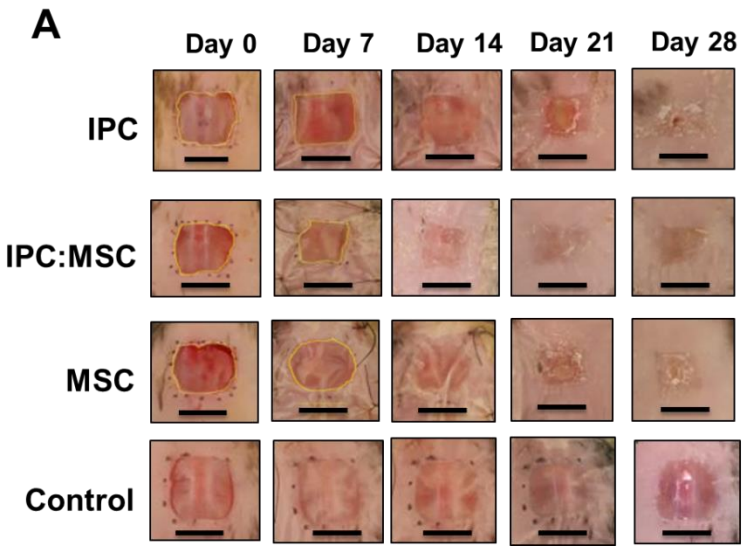

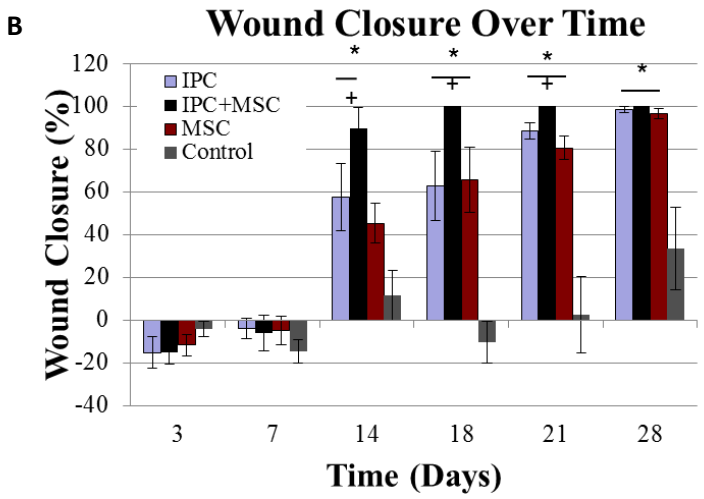

Fig. 7.1: Representative images and quantification of wound closure over time. (A) Gross appearance and (B) Percent wound closure. Asterisks indicate statistically significant differences ($p < 0.05$) between hydrogel encapsulated cells versus control. Plus signs indicate statistically significant differences ($p < 0.05$) between IPC:MSC(1:1) versus other groups. Error bars show standard error of mean.

7.3.2 Histological Analysis

IPC:MSC (1:1) treated wounds demonstrated accelerated wound closure and H & E sections showed distinct epidermis, dermis and hypodermis. Distinct layers of epidermis were visible in histological sections of IPC+MSC treated wounds, namely: stratum corneum, stratum lucidum, stratum granulosum and stratum basale (Figure 7.2). The stratum corneum was noticeable as 15-20 layers of flattened terminally differentiated keratinocytes or corneocytes and containing a dense network of keratin with the underlying stratum lucidum. The stratum granulosum could be identified as a layer consisting of migrating keratinocytes containing keratohyalin granules. A single layer of proliferating keratinocytes comprising the stratum basale was clearly identifiable as the deepest layer of epidermis in histological sections of wounds treated with IPC:MSC (1:1). In addition, H & E sections of IPC:MSC (1:1) treated wounds demonstrated a clear dermal and hypodermal layer. Similar features were identified in wounds treated with IPC or MSC-laden

hydrogels; however the hypodermal layer was not visible in wound tissue sections of either group. Keratinocytes in IPC or MSC treated wounds were longer and flatter, representative of migrating keratinocytes Histological sections of PBS treated control wounds lacked the structural organization of healthy skin and only a thin membrane-like tissue had formed. A scab composed of dead cells was visible in the histological sections.

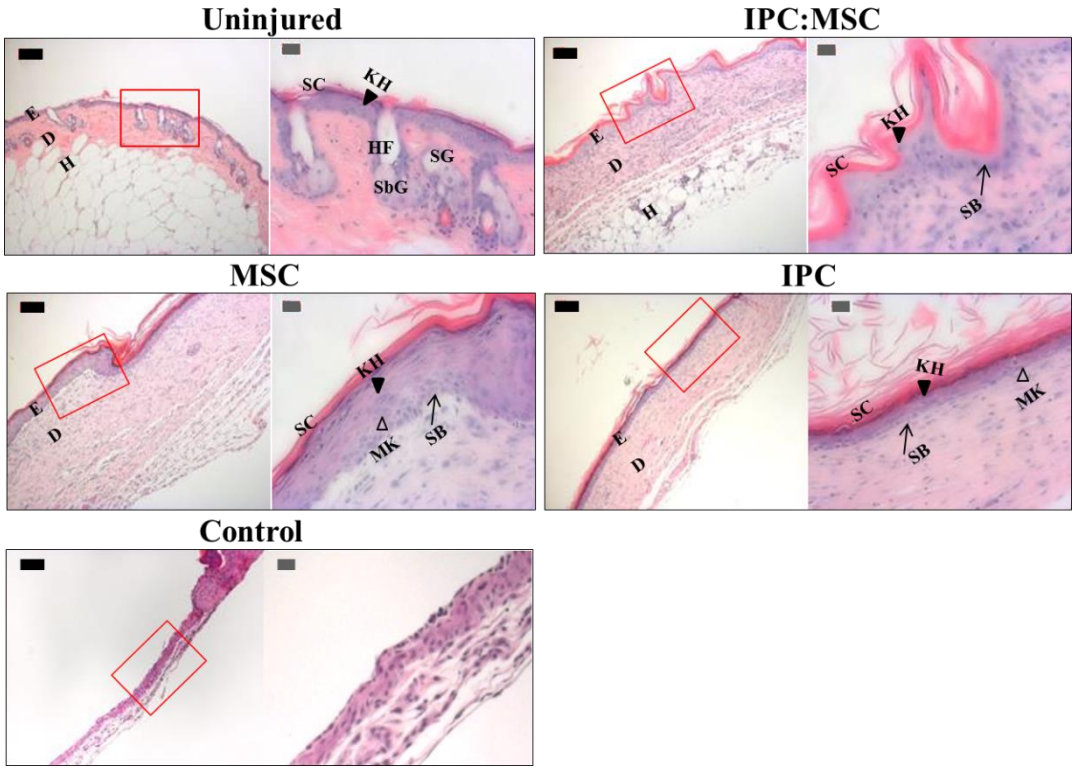

Fig. 7.2: Images of H & E stained histological sections of wound explants. E: epidermis, D: dermis, H: hypodermis, SC: stratum corneum, KH: keratohyalin granules in stratum granulosum, MK: migrating keratinocytes, SB: stratum basale, HF: hair follicle, SG: sweat gland, SbG: sebaceous gland. Only IPC:MSC and uninjured explants show the presence of a hypodermis. Neither show evidence of migrating keratinocytes. Control explants had not healed, and thus show no structural features of skin. Black scale bars = 100 μm, grey scale bars = 20 μm.

PASR-stained histological sections were first analyzed under bright-field microscopy. IPC:MSC (1:1) and uninjured skin demonstrated intense red collagen fibers, while IPC and MSC had a

slightly lighter and diffuse red staining of the collagen fibers. In the areas where a scab was present, collagen fibers were aligned perpendicular to the epidermis compared to completely closed wound areas where the collagen fibers aligned either parallel to the epidermis or in a basket-weave like pattern (later remodeling phase) (Figure 7.3).

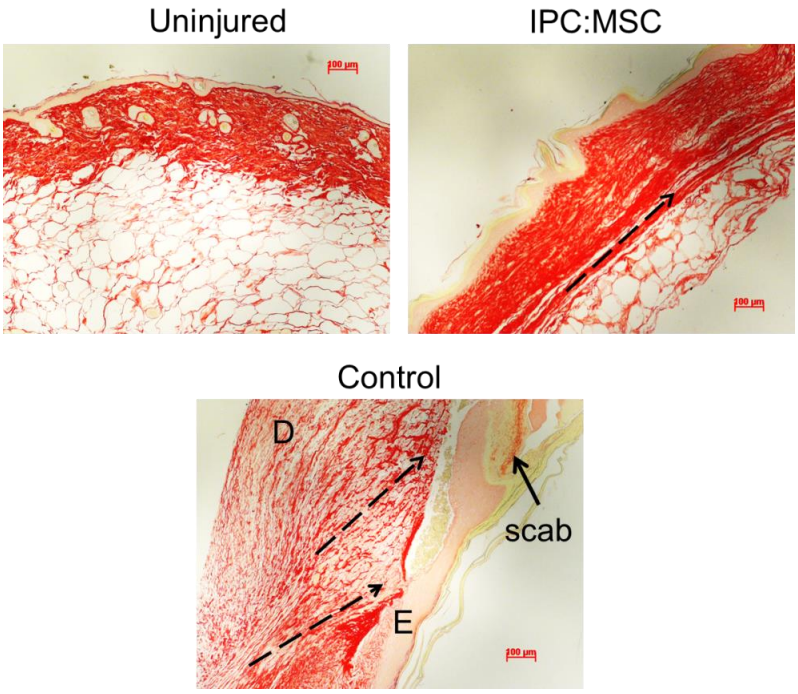

Fig. 7.3: The PASR-stained histological sections imaged under bright field. Solid arrow points to yellow-staining scab, dashed arrows represent alignment of collagen fibers. E: epidermis, D: dermis. Collagen fibers in IPC:MSC are beginning to attain the basket-weave alignment similar to the uninjured skin.

The PASR-stained histological sections were analyzed under cross-polarized light to quantify collagen type I and collagen type III content in the wound sections (Figure 7.4). Collagen type I was 57.03 ± 2.67 %, 56.73 ± 1.91 %, 51.26 ± 12.11 %, 46.94 ± 7.30 % and 31.02 ± 10.26 % in uninjured skin, IPC:MSC (1:1), MSC, IPC and control wounds, respectively, while collagen type III was present at 42.96± 2.67 %, 43.26 ± 1.91 %, 48.73 ± 12.11 %, 53.06 ± 7.30 % and 68.9 ± 10.26 % respectively (Figure 7.5A). This corresponds to collagen type I to type III (I:III) ratios of

1.33:1, 1.31:1, 1.14:1, 0.90:1 and 0.47:1 in uninjured skin, IPC:MSC (1:1), MSC, IPC and control wounds, respectively (Figure 7.5 B). Type I:III ratios in IPC:MSC (1:1), MSC and IPC treated wounds were significantly higher than controls and not statistically different than uninjured skin.

A basket-weave like collagen alignment was observed in uninjured skin and IPC:MSC (1:1) treated wound sections demonstrated a trend towards this basket-weave like alignment. A similar basket-weave trend was observed in MSC treated wound sections; however, the fibers were thinner and immature, while IPC:MSC collagen fibers were thicker and closer in size to uninjured collagen fibers. The basket-weave was absent in other groups. Thin immature collagen fibers in IPC treated wounds were aligned parallel to the epidermis and control wounds were composed of nascent and immature collagen identified as blue to green fibers under cross-polarized light.

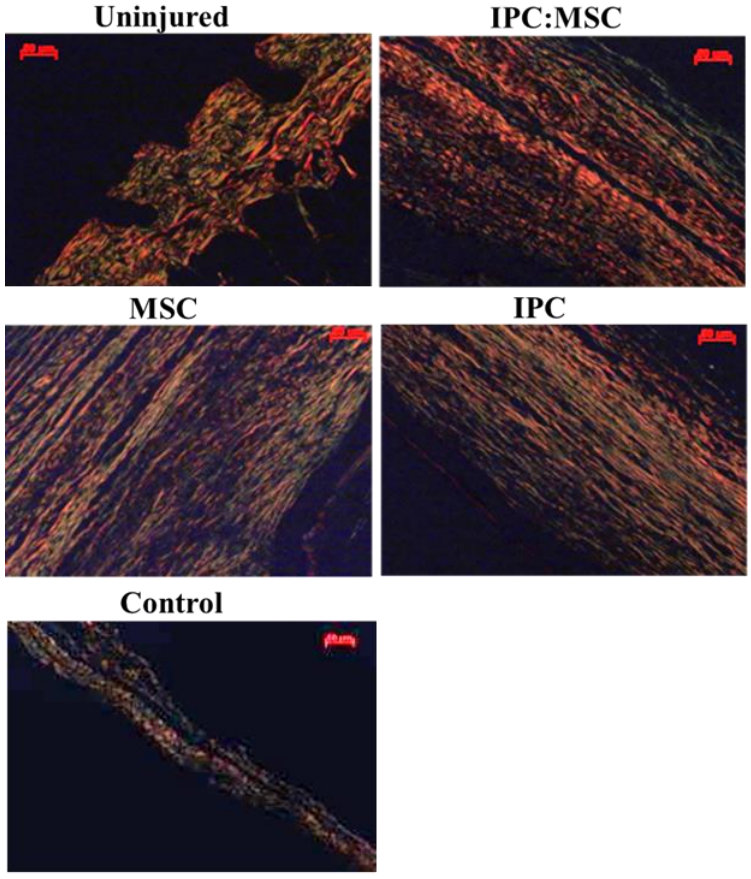

Figure 7.4: Images of picric acid sirius red stain histological sections of wounds taken under cross-polars. Orange represents type I collagen, green represents type III collagen.

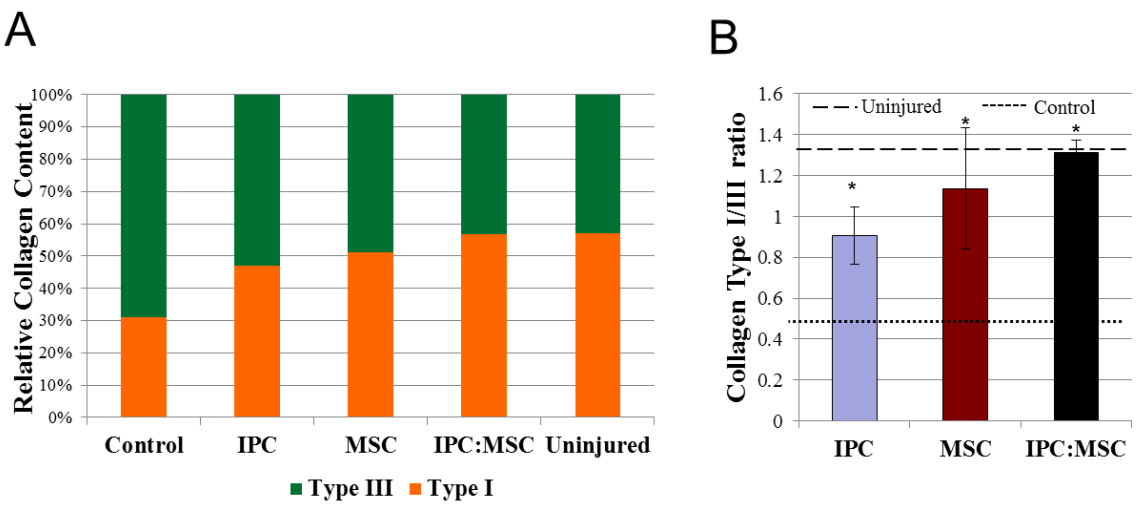

Fig. 7.5: (A) Quanitfication of relative content of collagen type I and III in PASR-stained histological sections of wound tissue. (B) Collagen type I to III ratio. Histological sections were imaged under cross-polars. Dashed line: type I/III ratio in uninjured skin, dotted line: type I/III ratio in control wounds, asterisks: significance vs. control.

Analyzing Ki67 stained wound tissue sections revealed a highly proliferative basal keratinocyte layer which was 2-3 cells thick at the wound edges just bordering the uninjured skin in all groups except control wounds, which lacked the presence of proliferating keratinocytes at the wound edges and throughout the wounded tissue (Figure 7.6) [1]. The basal layer of migrating keratinocytes [2] became one-cell thick towards the center of the healed wound in IPC:MSC (1:1) treated animals, while it was multiple cells thick in IPC or MSC treated wounds. In IPC:MSC (1:1) sections the Ki67 positively stained cells were mostly localized in the stratum basale with only a few positively stained cells present in the dermis. In comparison, Ki67 positive cells were present in both the stratum basale and dermal layer of IPC and MSC treated wounds. The number of Ki67 positive cells in MSC, IPC, IPC:MSC and uninjured skin were 179.86 ± 44.36, 213.30 ± 41.64, 237.69 ± 48.35 and 262 ± 32.4, respectively. The number of Ki67 positive cells were significantly lower in controls (48.7 ± 41.8) compared to MSC, IPC, IPC:MSC and uninjured skin.

Proliferating keratinocytes were seen in the basal layer of uninjured skin tissue sections with most proliferating cells concentrated near the hair follicles.

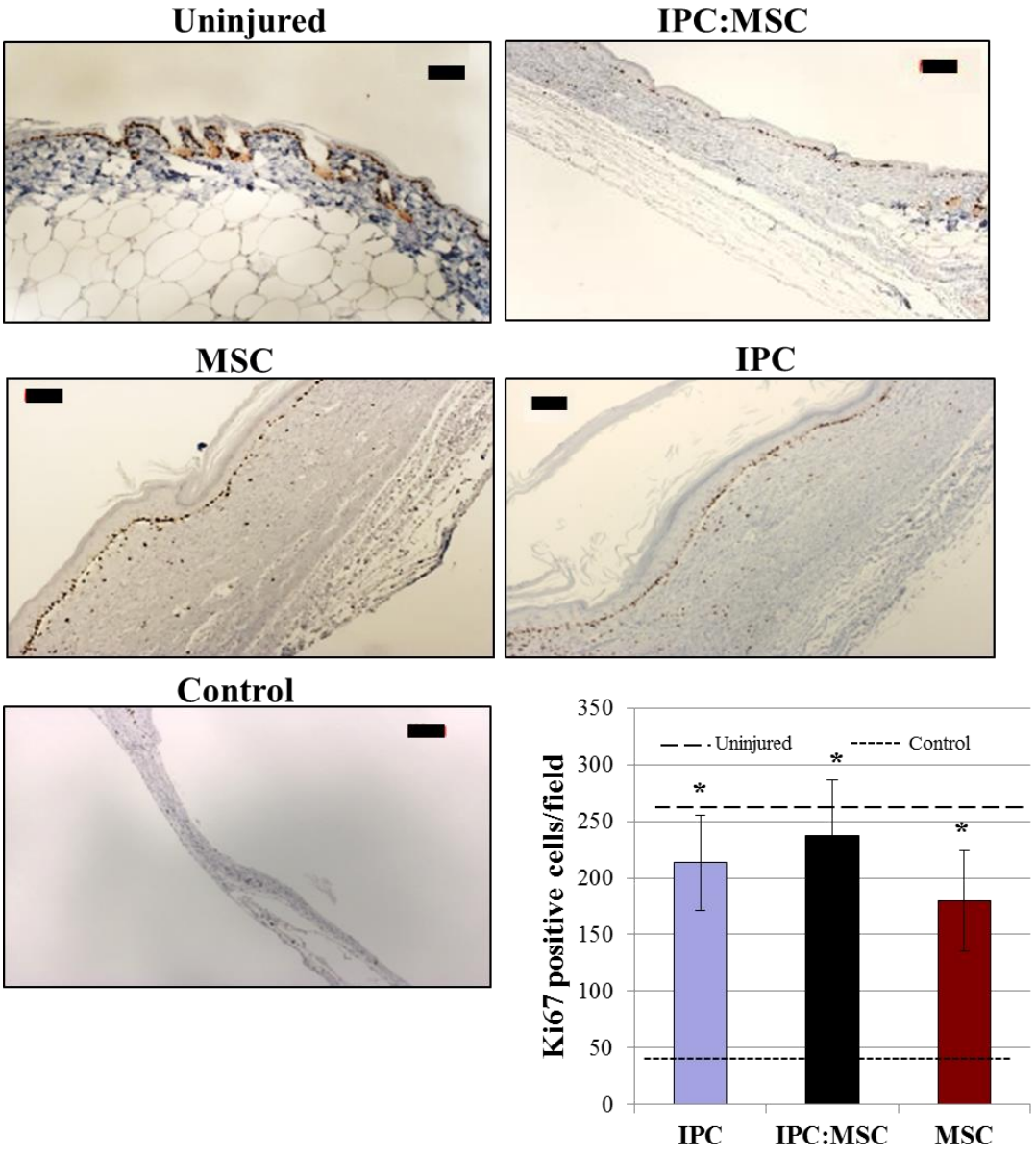

Figure 7.6: Images and quantification of Ki67 immunohistochemical staining of wounds. Dashed line: number of Ki67 positive cells in uninjured skin, dotted line: number of Ki67 positive cells in control wounds. Asterisks: significance vs. control.

Positive α-SMA stain present throughout tissue sections of wounds treated with IPC:MSC (1:1), IPC and MSC hydrogels indicating wound contraction (Figure 7.7). Diffuse α-SMA was visible in control wounds. Positive α-SMA stain was only seen around vessel lumen and some around sebaceous and sweat glands in uninjured tissue sections. Positive α-SMA staining was also around vessel lumen with visible blood cells (not stained); IPC:MSC (1:1) treated wounds represented bigger mature endothelia. Many tiny endothelia were seen in IPC or MSC treated wounds, representative of neovascularization and vascular proliferation in the granulation tissue. This was confirmed by staining for CD31, which specifically stained the developing endothelia Figure (7.8). The number of blood vessels was quantified in each histological image field and 12.74, 8.93, 2.31, 0.389 and 0.16 blood vessels/field could be seen in IPC, MSC, IPC:MSC(1:1), uninjured and control wounds, respectively.

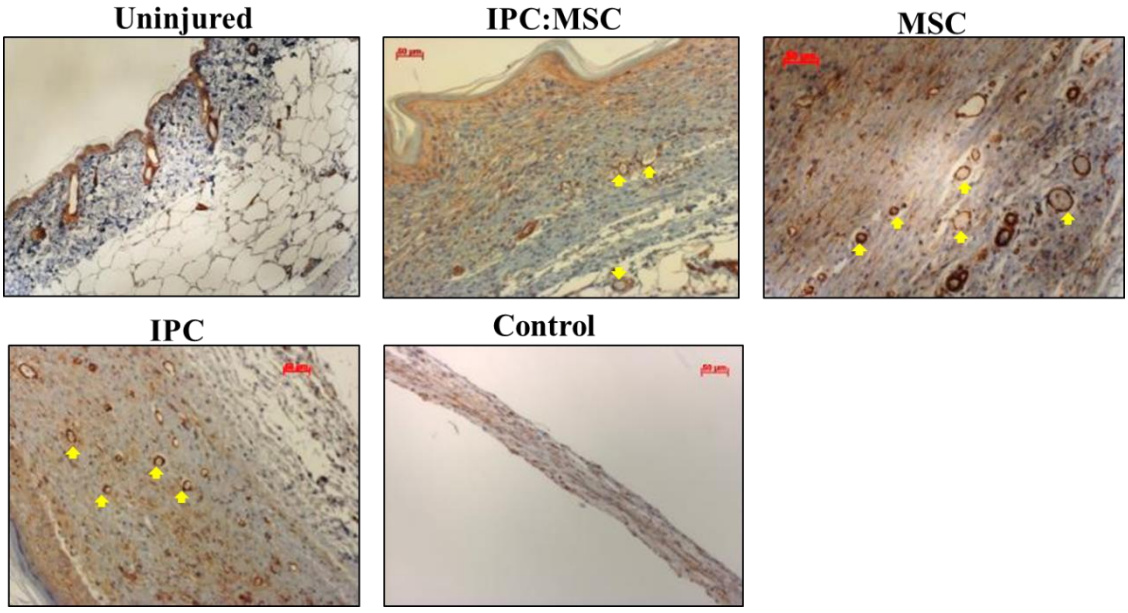

Figure 7.7: Images of α-SMA immunohistochemical staining of wounds. Yellow arrows point to blood vessels (BV).

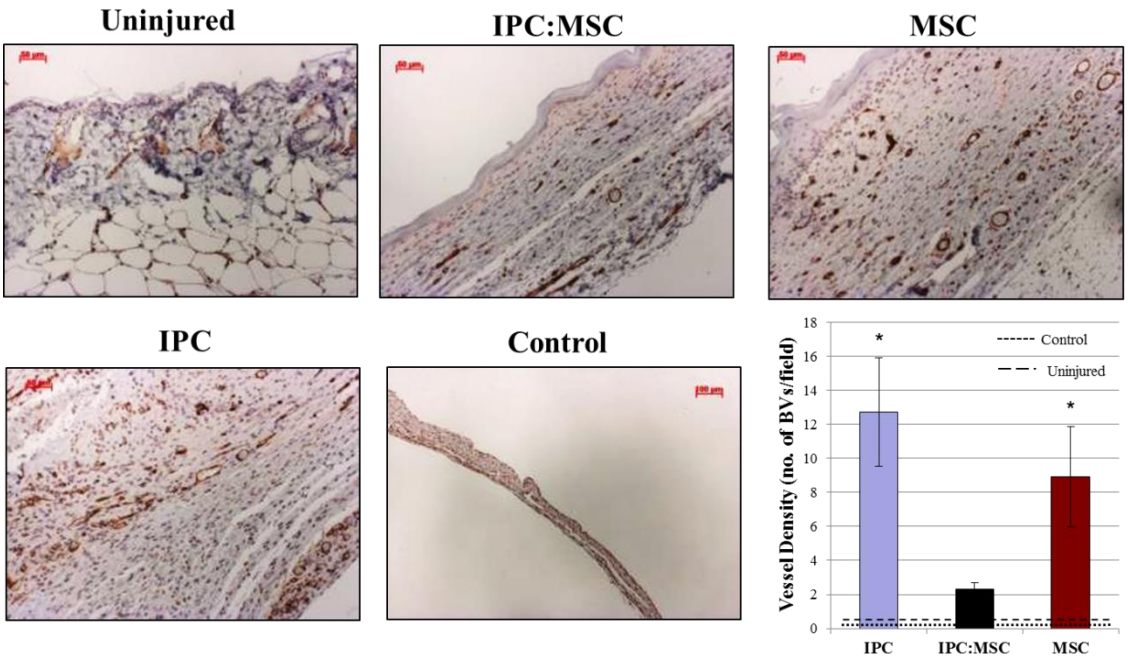

Figure 7.8: Images of CD31 immunohistochemical staining of wounds. Quantification of blood vessels (BVs) per field in a histological section. Dashed line: number. of BVs/field in uninjured skin, dotted line: no. of BVs/field in control wounds. Asterisks: significance vs. control.

DISCUSSION

In the previous chapters it was reported that IPCs encapsulated within PEGDA hydrogel microspheres stimulated *in vitro* keratinocyte migration, promoted significant wound closure, and increased epidermal thickness and collagen fiber density in a diabetic mouse model. It was demonstrated that the PEGDA encapsulated IPCs remain viable and secrete bioactive insulin at the wound site for a therapeutic effect. Herein, a bioactive hydrogel dressing was presented that combined IPCs and MSCs to synergistically accelerate wound closure through sustained secretion of insulin and MSC factors at the wound site.

PEGDA hydrogels absorbed wound exudate when the wound was open, and dried and sloughed off the wound and stuck to the Tegaderm™ when the wound was closed and dry. This suggests that PEGDA helps in wound closure by absorbing excess wound fluid; this can be reinforced

from our finding that wounds treated with empty PEGDA hydrogel microspheres demonstrated 73 % wound closure compared to PBS treated wounds that were only 33 % closed on POD 28. The PEGDA hydrogel that encapsulated the cells cools the underlying wound and thus decreases pain.

TGF-β1 plays a critical role in the wound healing process by affecting granulation tissue formation [6, 7], fibroblast differentiation to myofibroblasts [8] and re-epithelialization [9]. In the previous chapters it was demonstrated that TGF-β1 secretion from MSCs is increased in the presence of IPCs. Given this knowledge, it was unsurprising to observe superior wound tissue in IPC:MSC (1:1) treated wounds. The results presented thus far suggest that IPC:MSC (1:1) induced advanced fibroblast chemotaxis, ECM production and α-SMA expression (characteristic of myofibroblast transformation). The higher content of type I collagen in these wound sections further corroborates this finding and reinforces the role of TGF- β1 in collagen maturation.

The presence of elongated and flattened keratinocytes in the epidermis of IPC:MSC (1:1) treated wounds and their absence in other treatment groups suggests that wounds treated with either IPC or MSC containing hydrogels were still undergoing reepithialization and wound closure while the IPC:MSC (1:1) wounds had completely reepithelialized. Moreover, in IPC:MSC treated wounds, the Ki67 positive cells were mostly concentrated in the stratum basale while in IPC and MSC treated wounds, positive staining was visible in both the stratum basale and the dermis. The *in vitro* results showed that VEGF secretion from MSCs was stimulated by insulin; thus, it follows that this phenomenon also occurred *in vivo.* In normally healing wounds, there is a localized increase in vascularity within the healing tissue. It was expected that the exogenous VEGF would promote localized neovascularization in IPC, MSC and IPC:MSC treated wounds. This localized vascularity recedes as the wound closes and matures. Taking these results together, the presence of multiple tiny blood vessels (angioplasia) and Ki67 positive cells in the dermal layer (fibroplasia) in IPC and MSC treated wounds suggests that these wounds are in the proliferative phase [3]. In comparison, IPC:MSC (1:1) treated wound sections had fewer blood vessels,

demonstrating a transition to the maturation phase [3]. This can be confirmed from wound closure dynamics which demonstrate that IPC:MSC (1:1) treated wound had completed closed by POD 18 while IPC or MSC treated wound demonstrated wound closure around POD 28. Control wounds were stagnant in the healing process as demonstrated by insignificant differences in wound closure dynamics. Moreover, control wounds healed by scab formation, which makes it difficult for keratinocytes, fibroblasts and endothelial cells to migrate. Once a scab is formed, cells have to dissolve the clot, debris and damaged ECM before they can migrate, which delays wound healing and in indolent wounds cells do not secrete factors that help to dissolve the clot. In contrast to controls, IPC and MSC treated wounds healing with minimal scab formation while no scab formation occurred in IPC:MSC (1:1) treated wounds. This may also suggest that the IPC:MSC (1:1) reduce scar formation. Type I and III collagens play a critical role in scar formation; though necessary for wound healing, an excess deposition of collagen can result in scarring [10, 11]. Therefore, a critical balance of type I and III collagen is required for scar-free healing [12]. Results presented here demonstrate that the type I and III collagen content in IPC:MSC (1:1) treated wounds is similar to uninjured skin. Compared to healed wounds, the uninjured skin has a much thinner epidermis and dermis, which is expected since the wound tissues were excised on POD 28 and remodeling is not complete until much later when healed tissue regains the morphology of uninjured skin.

CONCLUSION

The rationale of this chapter was that the combination of IPCs and MSCs would accelerate wound closure faster than when either IPCs or MSCs are applied to wounds alone. In this chapter, results demonstrate that IPC and MSC coencapsulation significantly accelerated wound closure by POD 14 with a standard error of only 9.7 %. This standard error stems from one of the six IPC:MSC (1:1) hydrogel treated animals which demonstrated 41 % wound closure compared to all others, which were 100 % closed. Moreover, it was observed that the PEDGA hydrogel sheets provide a

moist environment which promotes moist healing through the formation of granulation tissue and reepithelialization while absorbing wound exudate. Our results confirm that IPC:MSC (1:1) reduce scab formation, will potentially reduce scar tissue, and histology of the healed tissue signify a mature tissue in the remodeling phase while wounds treated with IPC or MSC-alone hydrogels remain in the proliferative phase, and control wounds are in the inflammatory phase. It is worthy to note that once the wound reepithelialized, the cell-laden hydrogel sloughed off, which prevents hyper-proliferation of keratinocytes and fibroblasts, and limits excessive collagen deposition, thus limiting hyperplastic scar formation.

REFERENCES

1. Antsiferova M1, Klatte JE, Bodó E, Paus R, Jorcano JL, Matzuk MM, Werner S, Kögel H. Keratinocyte-derived follistatin regulates epidermal homeostasis and wound repair. Lab Invest. 2009 Feb;89(2):131-41. doi: 10.1038/labinvest.2008.120. Epub 2008 Dec 15.
2. Pastar I, Stojadinovic O, Yin NC, et al. Epithelialization in Wound Healing: A Comprehensive Review. Advances in Wound Care. 2014;3(7):445-464. doi:10.1089/wound.2013.0473.
3. Tanaka Y, Matsuo K, Yuzuriha S. Long-term histological comparison between near-infrared irradiated skin and scar tissues. Clinical, cosmetic and investigational dermatology : CCID. 2010;3:143-149. doi:10.2147/CCID.S15729.
4. Hunter, J.M., Kwan, J., Malek-Ahmadi, M., Maarouf, C.L., Kokjohn, T.A., Belden, C., Sabbagh, M.N., Beach, T.G., and Roher, A.E. Morphological and pathological evolution of the brain microcirculation in aging and Alzheimer's disease. PLoS One 7, e36893, 2012.
5. Lillian Rich and Peter Whittaker. Collagen and picrosirius red staining: a polarized light assessment of fibrillar hue and spatial distribution. Braz. J. morphol. Sci. (2005) 22(2), 97-104.
6. Zimmerman, K. A., Graham, L. V., Pallero, M. A. & Murphy-Ullrich, J. E. Calreticulin Regulates Transforming Growth Factor-β -stimulated Extracellular Matrix Production. J Biol Chem 288, 14584–14598 (2013).
7. Munger, J. S. & Sheppard, D. Cross talk among TGF-beta signaling pathways, integrins, and the extracellular matrix. Csh Perspect Biol 3, a005017, doi: 10.1101/cshperspect.a005017 (2011).
8. Vaughan, M. B., Howard, E. W. & Tomasek, J. J. Transforming Growth Factor-β 1 Promotes the Morphological and Functional Differentiation of the Myofibroblast. Exp Cell Res 257, 180–189, doi: http://dx.doi.org/10.1006/excr.2000.4869 (2000).
9. Reynolds, L. et al. Accelerated re-epithelialization in β 3-integrin-deficient-mice is associated with enhanced TGF-β 1 signaling. Nat Med 11, 167–174 (2005).
10. Verhaegen PD, Marle JV, Kuehne A, Schouten HJ, Gaffney EA, et al. (2012) Collagen bundle morphometry in skin and scar tissue: a novel distance mapping method provides superior measurements compared to Fourier analysis. J Microsc 245: 82–89.

11. Verhaegen PD, Schouten HJ, Tigchelaar-Gutter W, van Marle J, van Noorden CJ, et al. (2012) Adaptation of the dermal collagen structure of human skin and scar tissue in response to stretch: An experimental study. Wound Repair Regen 20: 658–666.
12. Oliveira GV, Hawkins HK, Chinkes D, Burke A, Tavares AL, Ramos-e-Silva M, Albrecht TB, Kitten GT, Herndon DN. Hypertrophic versus non hypertrophic scars compared by immunohistochemistry and laser confocal microscopy: type I and III collagens.

CHAPTER 8: CONCLUSIONS

In this thesis, I presented a novel dual-cell therapy that delivers sustained release of insulin and MSC factors to the wound area by encapsulating insulin-secreting cells and mesenchymal stem cells in non-immunogenic PEGDA hydrogels. With the increasing economic and emotional burden associated with chronic wounds in terms of treatment costs and amputations, it is critical to develop strategies that accelerate wound healing in at risk populations; one such method is to optimize the delivery of growth factors to maximize their therapeutic efficacy. Molecular genetic approaches are also being explored to transduce cells within the wound for a prolonged therapeutic effect. This thesis describes the development of a dual-cell dressing that can potentially reduce the duration of hospital stays associated with chronic wounds, thereby reducing surgical healthcare costs. To date, the work presented here is the first cell therapy to combine IPCs with MSCs to improve wound healing.

8.1 KEY FINDINGS

8.1.1 Microencapsulation of IPCs in PEGDA hydrogel microspheres maintains cell viability and insulin secretion

Cell viability and insulin secretory characteristics of microencapsulated cells were evaluated. Cytotoxicity analysis confirmed that cell viability was not affected by the encapsulation procedure. Glucose stimulation studies verified free diffusion of glucose and insulin through the microspheres and the IPCs continued to demonstrate their secretion characteristics; RIN-m maintained a constant insulin secretion profile and AtT-20ins demonstrated increased insulin secretion in response to incremental glucose concentrations.

8.1.2 RIN-m IPCs demonstrate superior in vitro keratinocyte migration and in vivo wound closure

Scratch assays demonstrated accelerated keratinocyte migration *in vitro* when treated with microencapsulated cells. In excisional wounds on the dorsa of diabetic mice, microencapsulated RIN-m cells demonstrated significant difference in wound closure by POD 7 compared to AtT-20ins treated and control groups. The results suggest that microencapsulation enables insulin-secreting cells to persist long enough at the wound site for a therapeutic effect and thereby functions as an effective delivery vehicle to accelerate wound healing. It was also concluded that the presence of insulin is sufficient to circumvent the hyperglycemic wound environment and insulin release from IPCs need not to be tailored to the changing glucose levels in the wound bed.

8.1.3 Coencapsulation has a cooperative effect on IPCs and MSCs

The combination of IPCs and MSCs demonstrated increased insulin, TGF-β1 and VEGF secretion which further promoted *in vitro* keratinocyte migration and Akt phosphorylation compared to when these cells were encapsulated alone. Moreover, the coencapsulations resulted in fewer cells required to achieve the effects. Achieving an effective stoichiometry of IPC and MSC ratio not only had a beneficial effect on the encapsulated cells' viability and secretome but also on the downstream wound healing pathways' recruitment and hallmarks of proliferation, migration and collagen metabolism.

8.1.4 IPC and MSC combination improves wound healing in diabetic mice by promoting accelerated transition through the wound healing phases

The combination of IPCs and MSCs (IPC:MSC) demonstrated the most significant effect on healing performing at least 35 % better than IPC or MSC hydrogels and 87 % better than controls as early as POD 14. Remarkably, IPC:MSC hydrogels promoted complete wound closure by POD 14 and histology analysis revealed a mature wound tissue. This results stems from insulin's

ability to regulate the initial inflammatory wound environment present in diabetic subjects, the concerted effort of insulin to stimulate keratinocyte and fibroblast proliferation, the increased release of TGF-β1 and VEGF from MSCs when coencapsulated with IPCs, the role of TGF-β1 to regulate collagen metabolism and induce myofibroblast transformation required for wound contraction, and the facilitation of neovascularization by VEGF. It is worthy to note that the IPC:MSC hydrogels did not induce excessive reepithelialization, collagen synthesis or blood vessel formation that leads to scar formation but promoted efficient transition through the wound healing phases as was evident from morphological and immunohistochemical analysis. This has profound clinical implications since most growth factor therapies like PDGF and bFGF have been associated with risk of cancer and tumor angiogenesis due to hyperproliferation. This ability of the IPC and MSC combination to promote accelerated healing while avoiding excessive healing may prove beneficial in the treatment of other wound healing complications such as hypertrophic scars and keloids.

8.2 POTENTIAL MECHANISMS

From *in vitro* studies it was demonstrated that the coencapsulation of MSCs with IPCs increased the release of both insulin and MSC factors from these cells. Increasing the amount of singly encapsulated MSCs did not increase MSC factor release as much as coencapsulating the cells with an equal number of IPCs. Similarly, increasing the number of singly encapsulated IPCs did not increase insulin release as much as coencapsulating the cells with an equal number of MSCs. MSC factor release increased the most when coencapsulated with increasing IPC densities while the highest insulin release was achieved from IPC:MSC (1:1). Consequently, the highest stimulation of keratinocyte migration and Akt phosphorylation was also achieved from IPC:MSC (1:1). Both the increased keratinocyte migration and Akt phosphorylation suggest that the presence of high levels of insulin in concert with MSC factors is required for significant increases in keratinocyte migration, Akt phosphorylation and *in vivo* wound healing.

Since MSCs are known to increase their factor release in the presence of IPCs, it is possible that the enhanced wound healing effects are due to the increased release of MSC factors triggered by the presence of IPCs. Although this is possible, it is unlikely. If the role of IPCs in this enhanced response is merely to stimulate MSC factor release and the effect of insulin during the wound healing is trivial, the most significant increases in MSC factor release and in *in vitro* keratinocyte migration would be expected when more MSCs were present. However, this was not the case. Counterintuitively, the greatest TGF-β1 release happened when *more* IPCs than MSCs were present, as in the IPC:MSC (10:1) hydrogels. The greatest VEGF release happened when the ratio was equal, as in the IPC:MSC (1:1) hydrogels, but in Days 1 and 7, IPC:MSC (1:1) hydrogel VEGF levels were not statistically different than IPC:MSC (10:1) levels. Thus, if the increased MSC factors were solely responsible for this enhanced wound healing effect, it would be expected that faster keratinocyte migration would be induced by the IPC:MSC (10:1) hydrogels.

Alternatively, if the importance of the MSCs was merely to support the IPCs and the presence of MSC factors had a lesser role in this wound healing than insulin, certain observations would be expected. Increased insulin release, keratinocyte migration, and Akt phosphorylation would be expected in hydrogels with a higher IPC ratio (IPC:MSC (5:1) and IPC:MSC (10:1)). On the contrary, the IPCs encapsulated alone (LCD) had faster keratinocyte migration and higher Akt phosphorylation levels than all coencapsulations with MSCs with the exception of the IPC:MSC (1:1). Further, on Days 1 and 7, the release of insulin from IPC-only LCD hydrogels was second only to IPC:MSC (1:1) levels. On Day 21, IPC:MSC (1:10) released the highest insulin. If the presence of MSCs were merely to support IPCs, it would be expected that on all days, all ratios of coencapsulations would improve insulin release from the IPCs, keratinocyte migration, and Akt phosphorylation. The 1:1 ratio of cells shows improvements over the other ratios and the single encapsulations that is not easily explained by increased insulin or by increased MSC factors. This strongly suggests that both insulin and MSC factors are equally responsible for promoting the observed enhanced wound healing.

Insulin and insulin-like growth factor (IGF) promote DNA synthesis in various cells [10-12].. However, the addition of both insulin and IGF to skin fibroblasts cultures does not result in additive increases in DNA synthesis, while the addition of insulin and serum does result in additive effects in DNA synthesis, suggesting that the growth factors present in serum somehow complement or reinforce the action of insulin [12]. It has also been shown that MSC factors, particularly EGF and PDGF, act synergistically with insulin in promoting DNA synthesis, and insulin may further be required to elicit the action of these and other growth factors [14-16]. For example, insulin is required for the action of nerve growth factor (NGF) for induction of neurite formation [17]. Given these results, it can be hypothesized that the acceleration of keratinocyte migration, Akt phosphorylation, and wound healing with IPC:MSC hydrogels were also additive effects that resulted from the presence of both insulin and MSC factors at the wound site.

Thus, it is possible that the IPC:MSC hydrogels elicit accelerated wound healing through: (1) a synergistic effect of insulin and MSC factors, and/or (2) insulin eliciting the action of MSC factors. If true, would MSC-alone hydrogels plus exogenous insulin provide the same accelerated wound healing as IPC:MSC hydrogels? How long would the exposure of exogenous insulin need to be for an identical effect? Regardless of the answers, a detailed study should be conducted to underpin the signaling mechanisms of IPCs and MSCs in the accelerated wound healing that was achieved in this thesis.

8.3 LIMITATIONS

The goal of this thesis was to develop a sustained-release dressing that accelerates wound repair. Significant acceleration was achieved by combining IPCs and MSCs in a hydrogel sheet. One future direction of this study is to investigate the mechanism of the synergistic effect; however, one limitation with the current hydrogel coencapsulation system is that the key source of stimulation of signaling molecules was not precisely defined, i.e whether IPCs, MSCs, or the combination of the two are the source.. For instance, if it were possible to stimulate MSCs to

overproduce VEGF and TGF-β1 without using IPCs, could the same result be achieved? Alternatively, if insulin and MSCs could be applied exogenously without the use of IPCs, would this achieve the same result? Is it simply insulin plus MSCs, or is it IPCs plus MSCs that are necessary? In this study non-degradable PEGDA was utilized; it would be difficult to release cells from the nondegradable polymerized PEGDA mesh in order to study intracellular signaling moieties. However, in future work, cells can be entrapped in degradable PEG hydrogels and some of these questions can be addressed.

The mouse model employed in this study was a diabetic chronic wound model. We were able to elucidate the effect of our cell-laden hydrogel dressing in a diabetic wound environment. However, this model lacks the ischemic component in human chronic wounds. Moreover, mice do not identically mimic human wound healing and large animal models such as pig or nonhuman primate models are required. Pig skin has an architecture with many anatomic similarities to human skin. Pig epidermis is thick like human epidermis and the epidermal-dermal interface has rete ridges and papillary projections, similar to human skin and in contrast to animals that rely on vigorously shaking their bodies as a rapid method to dry off [1-5]. These animals have evolved loose skin that enables increased rotational speeds and thus high centripetal forces necessary to propel water from their fur [4]. Such animals have loose dermal structures compared to humans, including many laboratory animals (e.g. mice, rats, dogs, rabbits). Additionally, pig and human skin heals at the same rate (27-30 days) and both heal primarily through reepithelialization while the skin of animals with loose skin heals predominantly through contraction [2, 6, 7]. Nevertheless, mouse models are cost effective and allow for the evaluation of multiple treatment strategies prior to the investment in a large animal model.

8.4 FUTURE DIRECTIONS

This thesis demonstrated that the coencapsulation of IPCs and MSCs promotes accelerated wound healing compared to when either cell is encapsulated alone. However, further study must be conducted to probe the underlying mechanisms and signaling molecules involved in achieving this effect. Conducting western blot analysis of phosphor-proteins in the POD 14 tissue lysate is one step towards underpinning the mechanism of the accelerated wound healing achieved. Specifically, phospho-proteins of the insulin signaling pathway, particularly p-ERK, p-GSK, e-NOS and IRS, can provide evidence that the accelerated wound healing was through stimulation of the insulin signaling pathway. The role of insulin in this accelerated wound healing can further be examined by repeating the studies while using insulin inhibitors to prevent the IPCs from secreting insulin. This way it is possible to detect the action of any unknown factors secreted by the IPCs that may be playing a role in wound healing.

Insulin release from IPCs can be inhibited by using ATP sensitive potassium (K(ATP)) channel diazoxide and potassium channel opener compound, NN414 [8, 9]. If following the inhibition of insulin release MSC factor release decreases and time to complete wound healing increases, it would suggest that the presence of the insulin is necessary for accelerated wound healing from IPC:MSC hydrogels. If after inhibiting insulin release, MSCs continue to secrete high levels of MSC factors and the coencapsulated hydrogels provide the same acceleration of wound healing, it would suggest that the presence of IPCs stimulates MSCs to secrete higher levels of MSC factors and insulin is not required to achieve this effect. Then new questions would arise. If the IPCs with no insulin could still produce this enhanced wound healing, are the IPCs in particular shedding something that the MSCs respond to, or would any cell suffice? Would a different cell type such as fibroblast provide the same advantage if coencapsulated with MSCs?

Additionally, the mechanism of wound healing acceleration by IPC:MSC hydrogels can be further probed by DNA microarray analysis. In this approach wounds treated with IPC:MSC hydrogels can be harvested at multiple time points, the total RNA can be extracted and the

differential gene expression can be studied. This would allow predicting a mechanism of wound acceleration by underpinning distinct components of the signaling pathway such as ligands, receptors, adaptor proteins and transcription factors involved in downstream responses such as cell proliferation, cell migration, inflammatory responses or regulation of cell growth. This would also enable the study of the changes as wound healing phases transition from the inflammatory to the proliferative to the remodeling phase.

Though current results point towards reduction in scar formation in IPC:MSC treated wounds, a longer animal study with an end-point in the remodeling phase is required to confirm these findings. If true, future studies to explore the systems efficacy in models of hypertrophic scarring would be warranted. Moreover, it will be interesting to determine whether the IPC:MSC hydrogels also promote regeneration of skin appendages such as hair follicles, sweat and sebaceous glands.

Cell viability analysis performed on hydrogels that had sloughed off of healed wounds revealed that all the cells within the hydrogel were dead. It will be interesting to remove the cell-laden hydrogels at an earlier point such as day 5 or day 7 and conduct western blot and polymerase chain reaction (PCR) analysis to investigate any difference in the expression of cells. Culturing cell-laden hydrogels in wound exudate *in vitro* may also be an alternative in determining the fate of these cells.

In addition to chronic wounds, there are a variety of wounds that are difficult to treat, including chemical, thermal and radiation burns. In future, this bioactive hydrogel dressing will be tested in pig and nonhuman primate models of chronic wounds and burns to evaluate a model more similar to human wound healing. The success of the system as reported in this thesis could lead to a transformative new treatment for intransigent wounds, and thus further studies are necessary to ensure the result extends beyond rodents.

8.5 REFERENCES

1. Velander, P., Theopold, C., Hirsch, T., Bleiziffer, O., Zuhaili, B., Fossum, M., Hoeller, D., Gheerardyn, R., Chen, M., Visovatti, S. and Svensson, H. Impaired wound healing in an acute diabetic pig model and the effects of local hyperglycemia. Wound Repair and Regeneration 16(2):288-293, 2008.
2. Sadeghipour, H., Torabi, R., Gottschall, J., Lujan-Hernandez, J., Sachs, D.H., Moore Jr, F.D. and Cetrulo Jr, C.L. Blockade of IgM-Mediated Inflammation Alters Wound Progression in a Swine Model of Partial-Thickness Burn. Journal of Burn Care & Research 2017.
3. Shilo, S., Roth, S., Amzel, T., Harel-Adar, T., Tamir, E., Grynspan, F. and Shoseyov, O. Cutaneous wound healing after treatment with plant-derived human recombinant collagen flowable gel. Tissue Engineering Part A 19(13-14): 1519-1526, 2013.
4. Liu, Y., Chen, J. Y., Shang, H. T., Liu, C. E., Wang, Y., Niu, R., Wu, J. and Wei, H. Light microscopic, electron microscopic, and immunohistochemical comparison of Bama minipig (Sus scrofa domestica) and human skin. Comparative Medicine 60(2): 142, 2010.
5. Swindle, M. M., Makin, A., Herron, A. J., Clubb, F. J. and Frazier, K. S. Swine as models in biomedical research and toxicology testing. Veterinary Pathology Online 49(2): 344-356, 2012.
6. Dickerson, A. K., Mills, Z. G. and Hu, D. L. Wet mammals shake at tuned frequencies to dry. Journal of the Royal Society Interface 9(77): 3208-3218, 2012.
7. Summerfield, A., Meurens, F. and Ricklin, M. E. The immunology of the porcine skin and its value as a model for human skin. Molecular immunology 66(1): 14-21, 2015.
8. Hansen JB, Arkhammar PO, Bodvarsdottir TB, Wahl P. Inhibition of insulin secretion as a new drug target in the treatment of metabolic disorders. Curr Med Chem. 2004 Jun;11(12):1595-615.
9. Carr RD, Brand CL, Bodvarsdottir TB, Hansen JB, Sturis J.NN414, a SUR1/Kir6.2-selective potassium channel opener, reduces blood glucose and improves glucose tolerance in the VDF Zucker rat. Diabetes. 2003 Oct;52(10):2513-8.
10. Girbau M, Gomez JA, Lesniak MA and de Pablo F. Insulin and insulin-like growth factor I both stimulate metabolism, growth and differentiation in the postneurula chick embryo. Endocrinology, 121, 1477, 1987.
11. Lockwood DH, Voytovich AE, Stockdale FE, Topper YJ. Insulin-dependent DNA polymerase and DNA synthesis in mammary epithelial cells in vitro. Proceedings of the National Academy of Sciences of the United States of America. 1967;58(2):658-664.
12. Matthew M. Rechler, Judy M. Podskalny, Ira D. Goldfine, Charles A. Wells; DNA Synthesis in Human Fibroblasts: Stimulation by Insulin and by Nonsuppressible Insulin-like Activity (NSILA-S). J Clin Endocrinol Metab 1974; 39 (3): 512-521. doi: 10.1210/jcem-39-3-512.
13. Petrides, P. E. and Böhlen, P. (1980) The mitogenic activity of insulin: An intrinsic property of the molecule. Biochem. Biophys. Res. Comm. 95, 1138–1144.
14. O'Keefe, E. J. and Pledger, W. J., A model of cell cycle control: sequential events regulated by growth factors, Mol. Cell. Endocrinol.. 31. 167, 1983. 36.
15. Shipley GD, Childs CB, Volkenant ME, Moses HL. Differential effects of epidermal growth factor, transforming growth factor, and insulin on DNA and protein synthesis and morphology in serum-free cultures of AKR-2B cells. Cancer Res. 1984 Feb;44(2):710-6.
16. Sand, T.-E. and Christoffersen, T. (1987), Temporal requirement for epidermal growth factor and insulin in the stimulation of hepatocyte DNA synthesis. J. Cell. Physiol., 131: 141–148. doi:10.1002/jcp.1041310202
17. Recio-Pinto E, Lang FF, Ishii DN. Insulin and insulin-like growth factor II permit nerve growth factor binding and the neurite formation response in cultured human neuroblastoma

cells. Proceedings of the National Academy of Sciences of the United States of America. 1984;81(8):2562-2566.